



New insights on flocculation in lager yeast

Luís Miguel Santos Sousa

Thesis to obtain the Master of Science Degree in

Biotechnology

Supervisors:

Doctor Ir Niels Gerard Adriaan Kuijpers

Professora Doutora Isabel Maria de Sá Correia Leite de Almeida

Examination committee

Chairperson: Professor Doutor Nuno Gonçalo Pereira Mira

Supervisor: Professora Doutora Isabel Maria de Sá Correia Leite de Almeida

Members of the committee: Doutora Margarida Isabel Rosa Bento Palma

November 2019

Preface

The work presented in this thesis was performed at the HEINEKEN Supply Chain, Global Innovation and Research Department (Zoeterwoude, The Netherlands), during the period March-September 2019, under the supervision of Dr. Ir Niels Kuijpers. The thesis was co-supervised at Instituto Superior Técnico by Prof. Isabel Sá Correia.

Declaração

Declaro que o presente documento é um trabalho original da minha autoria e que cumpre todos os requisitos do Código de Conduta e Boas Práticas da Universidade de Lisboa.

Declaration

I declare that this document is an original work of my own authorship and that it fulfils all the requirements of the Code of Conduct and Good Practices of the Universidade de Lisboa.

Acknowledgements

I want to thank Heineken Supply Chain B.V., Global Innovation and Research Department for receiving me at the facilities and giving me the opportunity of improving my scientific skills and knowledge. To Dr. Niels Kuijpers, my supervisor, thank you for your constant availability and patience, and Dr. Tom Elink Schuurman, which was also my supervisor, just not in the paper. To all laboratory and micro facilities technicians and GIR team. I also want to thank Prof. Isabel Sá Correia, for supporting this internship abroad and helping with all bureaucratic issues.

Now, off the record: Niels, thank you for the opportunity. Hope you enjoyed working with me. I guarantee you that it was really a pleasure and honour to take part on this project and team. Tom, the same goes to you. Hope you did not get home late too many times, because of my endless questions. At least, I'm already an expert in counting scratches on a glass. August, as in jazz there's trumpets and guitars and allegro and double swing, in science we have ions and genes and proteins and pH. Thank you for teaching me how beautiful it is to know that we do not know nothing. To Tadgh and Petra, for your friendship and sympathy every day of this internship. My colleagues: Sebastián, Luuk and Victor, besides work and science, life has more colour with people to laugh and talk and think. Thank you for your friendship, it helped me through these weeks in the low countries!

Para a Doutora Maria José, obrigado por me ajudar a agarrar esta oportunidade de ir além-fronteiras e fazer parte de uma equipa de luxo. Muito obrigado.

A todos os meus amigos e colegas de faculdade, que me acompanharam neste processo de crescimento. Sem mencionar nomes, acho quem ler sabe a quem me dirijo, e sabe o que significam para mim. A faculdade não volta, mas fica guardada num espacinho muito especial. Obrigado BCM e turma 2014/2015.

À gente da minha terra, amigos, que cresceram comigo, conviveram comigo, me viram ir e voltar, e aos que ficaram, um imenso obrigado.

Ciência, Investigação, Trabalho: na estrada da vida, começo a gatinhar, e na estrada da escola, começo por aprender a ler e a pensar. Professora Albertina e Professora Conceição Baptista: $1+1=2$ é tão óbvio como o ADN ter quatro bases diferentes. Também é óbvio que vos devo o primeiro lancil nesta escada académica, que começou com vocês a segurar-me. Esta tese é também fruto do vosso trabalho. Obrigado.

Porque a escola é importante, mas não é tudo, Mestre Ricardo e Padrinho Luís Santos: para contar, basta uma calculadora, para escrever um teclado, para pescar uma cana. Para viver, basta ser. Obrigado por me ajudarem na construção do meu ser, no fundamento da humildade, perseverança, resiliência, cultura e sabedoria.

Por fim, família: papá e mamã, ainda vos hei de pagar a fortuna que gastaram. No entanto, não posso pagar o pilar que representam. Com isso, contentem-se com o meu obrigado profundo. Tios e tias, padrinho e madrinha, primos/as – fazem parte de mim. Gosto muito de todos vocês. Obrigado por tudo.

Abstract

Lager beer is one of the most consumed beverages worldwide, which relies on a standardized and solid process workflow. The demand for innovative products, as the use of alternative wort compositions instead of malted barley, obligates for the research of different raw materials, which might influence the stability of the product or the metabolism of the used fermenting microorganism.

Yeast flocculation is a widely applied method in the brewing industry for the separation of the yeast slurry from the fermented wort. Its influencing parameters, being them biological, chemical or physical, are still of great debate. However, it is assured that the use of different fermentation conditions or wort types might influence the yeast flocculation characteristics.

In this work, three strains were tested for their flocculation phenotype in different wort compositions. Different conditions were applied, as alternative temperature setups, pH ranges and nitrogen sources. A flocculation “fingerprint” of each strain was pursued, in order to unravel the influence of different conditions in each of the tested strains. This was achieved by a new flocculation measurement method, which gave a different perspective of the flocculation influencing parameters.

Finally, in order to know the influence of different wort compositions and genetic background on the flocculation characteristics, a transcriptomic analysis of the most relevant genes for flocculation was performed, with the three strains. RNA seq was the chosen method for the transcriptomic profiling, with the aid of already sequenced reference genomes of the tested strains.

Keywords: flocculation; lager; *FLO* genes; transcription; measurement

Resumo

Cerveja lager é uma das bebidas mais consumidas mundialmente, cujo processo de produção está já altamente padronizado. No entanto, a demanda por produtos inovadores, como o uso de mostos alternativos à cevada maltada, obriga à investigação de diferentes matérias primas, que podem implicar efeitos na estabilidade do produto final ou no metabolismo do microrganismo usado para fermentação.

A floculação natural da levedura é um método há muito aplicado pela indústria cervejeira, para separação da biomassa do mosto fermentado. Os parâmetros influenciadores deste fenómeno, sejam químicos, físicos ou biológicos, são ainda matéria de debate. Sabe-se, no entanto, que a aplicação de diferentes condições de fermentação ou mostos alternativos poderão influenciar as características de floculação da levedura utilizada.

Neste trabalho, três estirpes foram testadas para o seu fenótipo de floculação em diferentes mostos. Diferentes condições foram utilizadas, como perfis de temperatura alternativos, pH e concentrações iniciais de substratos. Um perfil de floculação para cada estirpe foi investigado, para entender a influência de diferentes condições nas estirpes testadas. Tal foi possível com um novo método de medição da floculação, dando novas perspetivas acerca de como as diferentes condições influenciam este fenómeno, em cada estirpe.

De modo a entender como o diferente genoma de cada estirpe influencia este processo, uma análise transcritômica dos genes relevantes foi conduzida nas três estirpes testadas. Para tal, o método de RNA-seq foi utilizado, com recurso aos genomas de referência das três estirpes, já sequenciados.

Palavras-chave: floculação; lager; genes *FLO*; transcrição; medição

Table of contents

| | |
|---|------|
| Preface..... | i |
| Acknowledgements | iii |
| Abstract | iv |
| Resumo..... | v |
| List of figures | viii |
| List of tables | x |
| List of Abbreviations..... | xi |
| 1. Introduction..... | 1 |
| 1.1. Cells are particles – colloids science vs flocculation..... | 3 |
| 1.2. Cell Surface Charge and Cell Surface Hydrophobicity | 8 |
| 1.3. Physiological environment implications in flocculation | 9 |
| 1.3.1. The different flocculation phenotypes and sugars impact on flocculation..... | 9 |
| 1.3.2. Chemical/physical environment impact on flocculation..... | 10 |
| 1.4. Flocculation genetics: from gene to protein | 12 |
| 1.4.1. <i>Saccharomyces pastorianus</i> : the hybrid genome | 12 |
| 1.4.2. The FLO genes and their phenotypes..... | 14 |
| 1.4.3. Yeast Flocculins: structure and interactions | 16 |
| 1.4.4. <i>FLO</i> genes regulation | 20 |
| 2. Aim and approach of work | 22 |
| 3. Materials and Methods | 23 |
| 3.1. Yeast strains and media..... | 23 |
| 3.2. Fermentation setups | 23 |
| 3.3. RNA sequencing analysis | 26 |
| 3.4. Cell Surface Hydrophobicity analysis..... | 27 |
| 3.5. Quality Analysis | 27 |
| 4. Results | 29 |
| 4.1. Flocculation Measurement Method..... | 29 |
| 4.1.1. Non-volume changed fermentations: the proof of concept | 29 |
| 4.2. – Temperature impact on flocculation..... | 31 |
| 4.3. – Full malt wort vs Adjunct wort: different media impact on flocculation | 31 |
| 4.4. – Adjunct wort pH-controlled fermentations..... | 37 |
| 4.5. Adjunct-wort fermentations with higher initial nitrogen content | 42 |
| 4.6. Cell Surface Hydrophobicity evolution during the fermentations | 46 |
| 4.7. RNA-seq data results | 47 |

| | |
|---|----|
| 4.7.1. Quality assessment of the RNA samples | 47 |
| 4.7.2. Evolution of the transcript levels among the different strains | 49 |
| 4.7.3. The gene structure of the Y1 homologues | 49 |
| 5. Discussion | 51 |
| 6. Conclusions and future perspectives | 54 |
| 7. References | 55 |
| Supplemental material | 62 |

List of figures

| | |
|---|----|
| Figure 1 - Schematic representation of the lectin-like theory of flocculation (Miki et al. 1982). | 2 |
| Figure 2 - Interaction between two negative charged particles suspended in low (a) or high (b) ionic strength solutions (Gregory 1993). | 4 |
| Figure 3 - Electrical repulsion (VE), van der Waals (VA) and total energy (VT) of interaction between two equal spheres, as a function of the separation distance (Gregory 1993). | 5 |
| Figure 4 - Schematic representation of steric repulsion between particles (a) and bridging flocculation (b) (Gregory 1993). | 7 |
| Figure 5 - Logarithmic scale plots of mass against size of the aggregate (Gregory 1993). | 8 |
| Figure 6 - Domain organization of <i>Saccharomyces cerevisiae</i> adhesins (flocculins) (Brückner and Mösch 2012). | 16 |
| Figure 7 - Ligand binding by adhesins (Brückner and Mösch 2012). | 17 |
| Figure 8 - Flo5A/PA14 domain of <i>Saccharomyces cerevisiae</i> . (Brückner and Mösch 2012).. | 18 |
| Figure 9 - N-terminal domain of Flo1p in <i>Saccharomyces cerevisiae</i> (Willaert 2018). | 20 |
| Figure 10 - Raw data points representative of the flocculation strength parameter, for the fermentation carried with strain C in Full malt wort without volume change (F19J series). | 29 |
| Figure 11 - Flocculation strength for the two tested strains B and C in Full malt wort composition. | 30 |
| Figure 12 - Flocculation Behaviour graph for the non-volume change runs (F19J series). In the graph are represented strains B and C in Full malt wort. | 30 |
| Figure 13 - OD growth curves of the tested B (a) and C (b) strains in Full malt wort, for the temperature changed fermentations (F19L series). | 32 |
| Figure 14 - Flocculation strength graph for the three tested strains – C, B and A – in the two different wort compositions – Full malt wort and 50% Adjunct wort (F19F, F19G, F19H and F19I series). | 33 |
| Figure 15 - Flocculation Behaviour of strains C (a) and B (b) in each fermentation media, Full malt wort and 50% Adjunct wort (F19F, F19G, F19H and F19I series). | 34 |
| Figure 16 - Sugars (glucose, fructose, sucrose, maltose, maltotriose and total fermentable sugars) consumption trends correspondent to the Full malt and 50% Adjunct wort fermentations (F19F, F19G, F19H and F19I series). | 36 |
| Figure 17 - pH evolution and alcohol production trends in Full malt and 50% Adjunct wort fermentations (F19F, F19G, F19H and F19I fermentations). | 37 |
| Figure 18 - OD growth curves of the tested strains in Full malt and 50% Adjunct wort fermentations (F19F, F19G, F19H and F19I fermentations). | 38 |
| Figure 19 - Flocculation strength graphs for strains C and B in 50% Adjunct wort and 50% Adjunct wort pH corrected. | 38 |
| Figure 20 - Flocculation Behaviour graphs for B (a) and C (b) strains in 50% Adjunct wort (F19G and F19I series) and 50% Adjunct wort pH corrected (F19K1 series). | 40 |
| Figure 21 - OD curves for both C and B strains in normal Adjunct wort (F19G and F19I fermentations) and in Adjunct wort pH corrected (F19K1 fermentations). | 41 |
| Figure 22 - pH profiles comparison for the Heinken wort (F19F and F19H series), 50% Adjunct wort (F19G and F19I series) and 50% Adjunct wort pH controlled (F19K1 series) for the strains C and B. | 42 |

| | |
|--|----|
| Figure 23 - Flocculation strength graphs of C and B strains for the normal Adjunct wort fermentations (F19G and F19I series) and nitrogen supplemented Adjunct wort fermentations (F19K2 series). | 43 |
| Figure 24 - Sugars (maltose, maltotriose and total fermentable sugars) consumption, ethanol production and pH profiles on normal Adjunct wort (F19G and F19I series) and nitrogen supplemented Adjunct wort (F19K2 series) for B and C strains. | 45 |
| Figure 25 - OD growth curves for C and B strains. Fermentations in normal Adjunct wort (F19G and F19I fermentations) and nitrogen supplemented Adjunct wort (F19K2 fermentations) are represented. | 46 |
| Figure 26 - Cell Surface Hydrophobicity evolution during the fermentations in Full malt and 50% Adjunct wort, for all the three tested strains A, B and C (F19F, F19G, F19H and F19I fermentations). | 47 |
| Figure 27 - PCA analysis of the 48 analysed RNA samples. | 48 |
| Figure 28 - Protein level comparison of the Y1 homologue for each of the studied strains C (fig. a)), A (fig. b)) and B (fig. c)), with the sequence of each strain's homologue represented in grey. | 50 |

List of tables

| | |
|---|----|
| Table 1 - RNA seq fermentations overview | 25 |
| Table 2 - Volume impact fermentations overview. | 25 |
| Table 3 - pH impact fermentations overview. | 25 |
| Table 4 - Nitrogen impact fermentations overview. | 26 |
| Table 5 - Temperature impact fermentations overview. | 26 |

List of Abbreviations

AE – Apparent Extract

COMPASS – Complex proteins associated with Set1

CSC – Cell Surface Charge

CSH – Cell Surface Hydrophobicity

DHAP – Di-Hydrogen Ammonium Phosphate

ECD – Electron Capture Detector

EDL – Electrical Double Layer

FID – Flame Ionisation Detector

GC – Gas Chromatography

MATH – Microbial Adhesion to Hydrocarbons

OD – Optical Density

OG – Original Gravity

PCA – Principal Component Analysis

PI – Propidium Iodide

RE – Real Extract

RS interval – Reduced Stirring Interval

UPLC – Ultra performance Liquid Chromatography

V_A – Potential Energy of attraction

VDKs – Vicinal Diketones

V_R – Potential Energy of repulsion

V_T – Total potential energy

1. Introduction

“*Quand on l’agite dans l’eau, elle retombe tout de suite au fond, comme ferait un précipité caillebotté, et l’eau surnageant est à peine trouble par quelques globules en suspension.*” The previous sentence is part of the 1876 book of Louis Pasteur, *Études sur la Bière* (Pasteur Louis ML 1876), which is the first known description of yeast flocculation. In the sentence it is said that after agitation of the liquid, the yeast sediments to the bottom, forming a curdled precipitate while the supernatant is barely cloudy, except for some globules in suspension. Besides the fact that the “flocculation” terminology is not used as such, the phenomena observed by Pasteur is the process by which yeast cells form flocs in the media and sediment. But what is, in fact, flocculation?

Flocculation is described as the asexual, reversible, calcium-dependent and homotypic (between the same type of cells, in this case, flocculent) process by which yeast cells aggregate into clumps composed of thousands/millions of cells that quickly sediment from the bulk medium where they are suspended (Soares 2011). Aggregation of yeast cells might refer, however, to many other different processes, apart from flocculation. Therefore, flocculation should not be confused with sexual aggregation (fusion of haploid cells of complementary mating types) (Chen et al. 2007); co-flocculation (heterotypic interaction between a flocculent and a non-flocculent strain) or chain formation (younger buds that don’t separate from the mother cell during division, giving rise to cell aggregates) (Stewart 2009). Moreover, other types of yeast cell aggregates may even include biofilms (communities of microorganisms attached to a surface) (Monds and O’Toole 2009) or pseudohyphal growth (chains of attached and elongated cells formed from each other by budding) (Gimeno et al. 1992).

In the brewing context, the *curriculum vitae* of a yeast strain must include not only the ability to flocculate, but as well the perfect timing to do so. Specifically, at the end of beer fermentation, when all fermentable sugars are converted into ethanol and CO₂, yeast flocculation should occur, allowing for its sedimentation to the bottom of the fermenter (in the case of bottom-fermenting yeast) or its flotation to the surface of the fermentation vessel (top-fermenting yeast) (Van Mulders et al. 2010). The capacity for yeast cells to flocculate at the end of the fermentation imposes a considerable advantage to the process, since it represents a cost-free and effective way to separate yeast cells from the fermented beer, enabling its re-pitching in subsequent fermentations (Verstrepen et al. 2003). Regarding the timing at which flocculation takes place, two undesired scenarios might be possible: weak or non-existent flocculation, or premature yeast flocculation, resulting in high concentrations of residual sugars and unsatisfactory flavour profiles (Stratford 1992). Yeast flocculation is the recurrent (and traditional) way by which brewers separate the biomass from the fermented beer; however, its application to other industries it’s also reported (Bauer et al. 2010). In depth studies include the application of flocculent yeast strains in ethanol production to improve productivity during continuous ethanol fermentations (Jones et al. 1984) or its application in bioremediation processes, in which flocculent yeast is able to remove metal ions from solution (Machado et al. 2010).

The mechanisms by which yeast cells flocculate and how the process is initiated is not completely understood. However, the more consented hypothesis takes as assumption the lectin-like theory of

flocculation (Miki et al. 1982). According to this theory, specific proteins present on the yeast cell wall named lectins (or flocculins) interact with oligosaccharide receptors that decorate the cell wall of an adjacent cell, in the presence of calcium (Bony et al. 1997) (fig. 1). The oligosaccharide receptors consist of mannan side-branches, with the length of two to three mannose residues. These are present in flocculent or non-flocculent cells, contrarily to flocculins, which are only expressed by flocculent strains. Flocculin-encoding genes belong to the *FLO* gene family (Van Mulders et al. 2009), whose presence has a great impact on the observed phenotype by each specific strain. The way that yeast flocculates is highly strain-dependent, with the genetic background as major influence on that characteristic (Vidgren and Londesborough 2011). Moreover, a previous work conducted using several different strains of ale and lager yeast (Van Mulders et al. 2010) proved that the study of *FLO* genes is rather ambiguous and imprecise, being that adhesion encoding gene sequences are highly variable from strain to strain, making it even more difficult to assign a single flocculation profile to different strains.

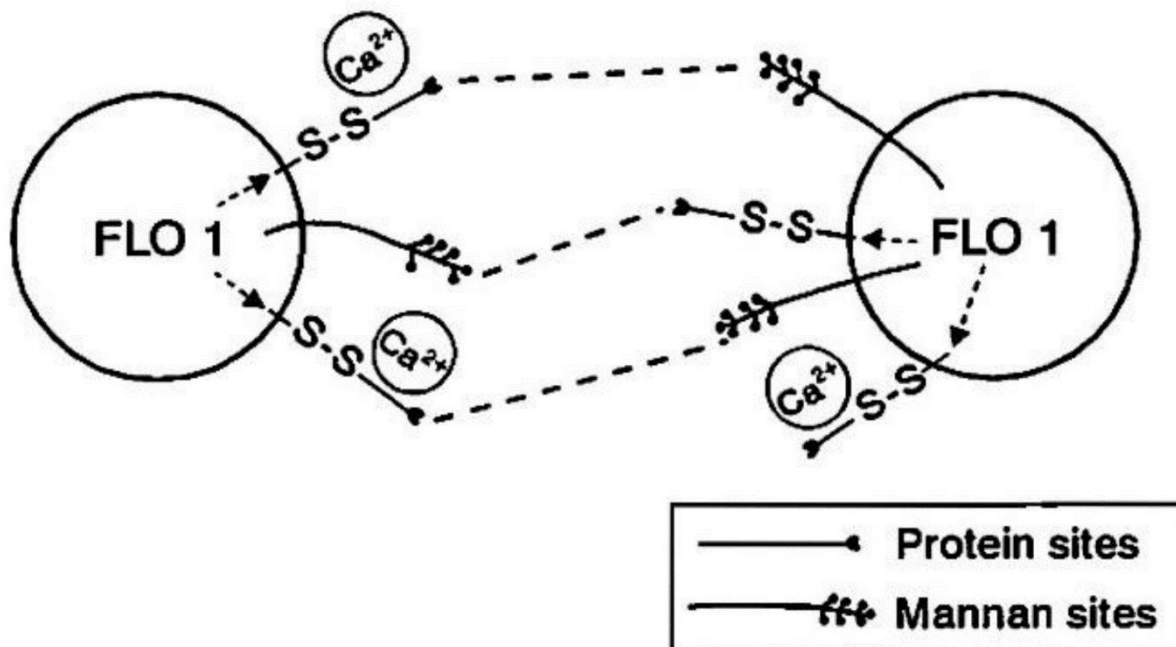


Figure 1 - Schematic representation of the lectin-like theory of flocculation. Lectins expressed on flocculent cell walls interact with carbohydrate receptors present on neighbour cells, in the presence of calcium (Miki et al. 1982).

Besides the impact of the genetic background on the flocculation phenotype of yeast cells, the physiological and physical environment are also preponderant factors affecting the flocculation characteristics of cells (Stewart 2018). Physiological factors include pH, nutrient and metal ions availability (Stewart et al. 1975), oxygen availability (Lorenz and Parks 1991) and temperature (Jin and Speers 2000). The physical environment plays a role by the hydrodynamic characteristics in which cells are inserted, as well their physical properties itself, like their intrinsic hydrophobicity or surface charge (Stewart 2018). The complexity of this phenomena is increased due to the different levels at which the same parameter may act as a flocculation determinant, i.e., sugars interact directly with the protein lectins on the cell wall, but may also induce changes at a genetic level, by altering the expression of determinant genes in flocculation (Soares 2011).

The present introduction aims cover the flocculation thematic in different perspectives. Insights regarding the physical properties of flocculating cells are addressed. A broad perspective of the chemical/physical properties of cells – particles – is given. Aiming its correlation between the biology (genetics) and physics of flocculation phenomena, the most studied physiological parameters affecting flocculation are also approached. Finally, the impact of the genome, gene expression and protein structure on the phenomena takes place. In the end, this introduction has the goal of giving the reader a broad perspective of yeast flocculation, taking in mind that many/different factors are in place, and that biology alone cannot give a complete answer to the problem.

1.1. Cells are particles – colloids science vs flocculation

The study of yeast flocculation may take different directions and perspectives. The study of the intervenient proteins on the mechanism or the genes that confer the referred ability and their regulation (transcriptional or post-transcriptional), is undoubtedly of considerable importance. A beer fermentation is a complex mixture of water, yeast, organic and inorganic compounds, which all physically and chemically interact with each other. Clumping and sedimentation of yeast cells is, in a more archaic meaning, the aggregation and deposition of solid particles (yeast) from an aqueous solution (green beer). Moreover, the beer fermentation is no more than a suspension of yeast in a complex liquid mixture. The study of particle – particle interactions in suspensions is of great importance in many different industry sectors (Elimelech 1995). The rules and forces applying to their aggregation and deposition depend in a long range to their size, being that particles can be divided in suspended and colloidal particles. A direct distinction between particle characteristics is not available: rule of thumb says that a colloidal particle needs to have at least one dimension with a size inferior to 1 μm ; in other way, colloidal particles remain in suspension for rather longer times than a suspended particle, which settle out relatively fast due to gravitational forces (Elimelech 1995). Considering these distinctions, yeast cells (and so, yeast flocs) remain at the interface of colloidal and suspended particles. The type of interactions happening between colloidal particles maybe extrapolated to yeast cells – the average diameter of a *Saccharomyces cerevisiae* cell is around 5 μm (Phillips et al. 2012).

Despite the rationale behind the applicability of the colloidal science to the flocculation phenomena, little research has been developed in that thematic (Speers et al. 1992), comparing with the preponderant research regarding the biochemical and microbiological perspectives of the theme. Since yeast flocculation can be considered a solid-liquid separation, the knowledge of the types of forces involved might be useful to better understand the process (Gregory 1993). Colloidal science may help in the understanding of the phenomena in two different points of view: predicting the energy of interaction between two approaching yeast cells, by knowing interaction mechanisms in colloidal particles; and predicting the rate at which yeast cells flocculate, by applying colloid kinetic theories (Speers et al. 1992).

One of the most important theories regarding the science of colloids is the DLVO theory of aggregation, developed by Boris Derjaguin and Lev Landau followed by Evert Verwey and Theodoor Overbeek (Elimelech 1995). The theory states that the forces intervenient in the interaction between colloidal particles are a sum of the van der Waals forces of attraction plus the electrostatic forces of repulsion (Elimelech 1995). In one side, van der Waals forces are referred as the omnipresent forces that act

upon all molecules and atoms, and are always of the attractive type (between surfaces of the same material). (Walstra 2003). The applicability of the van der Waals forces to the interaction energies between surfaces was afterwards developed (Hamaker 1937). According to Hamaker, the intensity of the van der Waals forces between two spheres is given as a function of the diameters of the spheres and their separation distance (geometrical part of the formula) plus the addition of a constant A, the Hamaker constant, which accounts for the chemical properties of the interacting particles and medium in which they are suspended. In this way, the potential energy of attraction can be computed as:

$$\text{Equation 1: } V_A = -A f(h, T) r/12h$$

in which A.f(h,T) is a function of the Hamaker constant, which depends on the separation of the particles (h) and the temperature (T), and r represents the radius of the interacting particles (Hamaker 1937; Speers et al. 1992). On the other side, the electrostatic repulsion forces have its basis on the electrical double layer (EDL) theory. This theory states that a negative charged particle in an electrolyte suspension will attract positive charged ions to its surface, forming a diffusive layer of cations (or counterions) around it. The concentration of positive charged particles in suspension will determine the length of this diffusive layer around the negative particle (fig. 2) – the higher the concentration of counterions, the more adsorbed the positive particles will be towards the negative particle, and the thinner will be the diffusive layer. When two negative charged particles are approaching each other, the repulsion between them will be higher (and act at higher separations) as longer is the cations diffusive layer around them (Elimelech 1995). In this way, for large particles with small double layers, separated at a distance superior to 2nm, the potential energy of repulsion can be computed as:

$$\text{Equation 2: } V_R = 2\pi \epsilon \epsilon_0 r \psi^2 \ln(1 + e^{-kh})$$

Where ϵ is the dielectric constant of the medium, ϵ_0 is the permittivity of free space, r is the radius of the particles, ψ is the surface potential (or zeta potential), k is the inverse of the double layer thickness and h the distance between both particles (Speers et al. 1992).

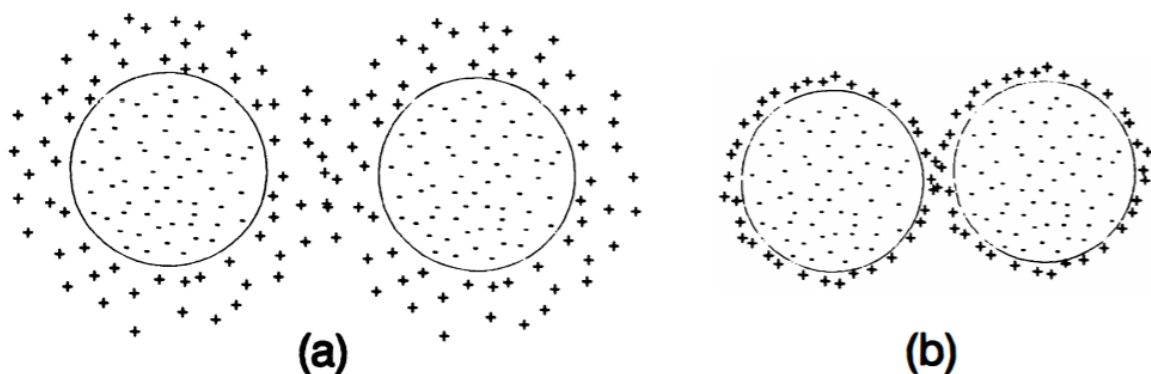


Figure 2 - Interaction between two negative charged particles suspended in low (a) or high (b) ionic strength solutions. The higher is the concentrations of counterions in solution, the thinner is the diffusive layer of positive ions around it (Gregory 1993).

Taking the two previous concepts in consideration, the DLVO theory is computed as the sum of the van der Waals attraction forces and EDL repulsion forces. In fig. 3 is depicted the profile of the potential

energy plotted against the separation distance between particles (DLVO curve). According to this curve, a primary minimum exists at extremely small separations (potential of attraction is maximum), directly followed by a primary maximum, in which repulsive forces predominate. At higher separations, a secondary minimum with much lower amplitude than the first is developed, at which some attraction occurs (Gregory 1993). The understanding of this mechanism makes it possible the extrapolation of these curves to yeast cells (Speers et al. 1992). However, by answering the question of what kind of forces are in place, another question remains: how to predict the rate of collisions and associations between interacting yeast cells?

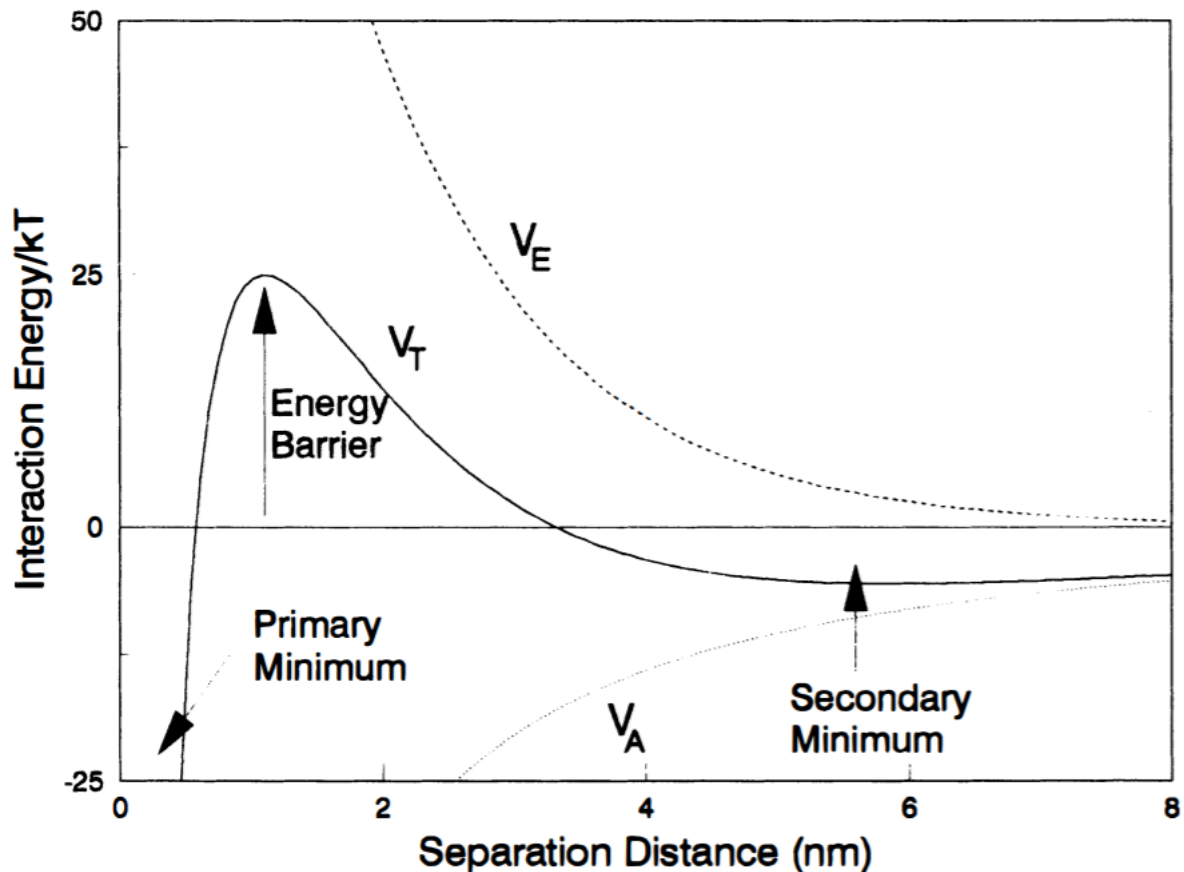


Figure 3 - Electrical repulsion (V_E), van der Waals (V_A) and total energy (V_T) of interaction between two equal spheres, as a function of the separation distance. Particles diameter: 1nm; zeta potentials: 20 mV; Hamaker constant: 8.1×10^{-21} J (Gregory 1993).

Three major mechanisms explain the kinetic association of particles: perikinetic aggregation, which is dependent on Brownian motion; orthokinetic aggregation, which is dependent on fluid motion; and differential settling, dependent on the collisions of particles during their settling from a suspension (Elimelech 1995). Since yeast cells are too big to be transported by Brownian motion, it's fair to say that orthokinetic and differential settling are the mechanisms which can explain the yeast flocculation phenomena (Speers et al. 1992). Regarding the orthokinetic aggregation mechanism, a mathematical expression is derived, describing the flocculation rate of perfect spheres in laminar shear flow (van de Ven and Mason 1977):

$$\text{Equation 3: } \frac{N_t}{N_0} = e^{-\left(\frac{\alpha_0 \dot{\gamma} \varphi_0}{\pi}\right)t}$$

where N_t is the concentration of particles/flocs at time t , N_0 is the initial concentration of particles, α_0 corresponds to the orthokinetic capture coefficient, φ_0 corresponds to the initial volume fraction of particles and $\dot{\gamma}$ is the shear rate. In the above-mentioned equation, the capture coefficient takes a clear importance to the expression, since it comprises all the forces involved in cell collisions plus the probability of colliding cells/flocs forming a doublet.

The gathering of both interaction forces and kinetic behaviour in yeast flocculation was investigated (Speers et al. 1993; Hsu et al. 2001; Speers et al. 2006). In work conducted using flocculent and non-flocculent yeast strains (ale and lager), the orthokinetic flocculation rate was measured, at different shear rates (Speers et al. 1993). The results showed that the concentration of yeast flocs in suspension decreased, as the shearing time was increased. Regarding the impact of the DLVO interactions between yeast cells in flocs formation, theoretical values for the orthokinetic capture coefficient were derived, taking into consideration aspects as cell size, cell surface potential, shear rate, Hamaker constant of cell membrane constituents and composition of the medium (Duszyk and Doroszewski 1986). However, experimental values measured afterwards (Speers et al. 1993) proved that the theoretical values predicted were far lower than the experimental values obtained, proving that the DLVO theory alone cannot explain the flocculation phenomena of yeast cells, and that other interactions take part in the mechanism.

Besides DLVO interactions, other types of interactions are likely to happen among yeast cells in aggregation processes, which include hydrophobic interactions, polymer bridging and steric interactions (Speers et al. 1992). Water is a highly organized structure, due to the hydrogen bonds forming between molecules, which form large transient clusters (Gregory 1993). However, when in contact with a hydrophobic surface, water clusters cannot grow, since they cannot bind the hydrophobic surface. In this way, molecules entrapped between two hydrophobic surfaces will tend to migrate from the gap to the bulk medium, resulting in attraction between the two hydrophobic surfaces (or particles). The forces arising from this type of interaction are rather stronger and of larger ranges than a van der Waals type of interaction (Claesson and Christenson 1988). The phenomena of polymer bridging and steric interaction are interconnected, and directly correlated with the lectin-like theory of flocculation (fig. 4) (Miki et al. 1982). Depending on how much of a given polymer is adsorbed to a particle, the result is either attraction or repulsion between the particles. In one hand, at high concentrations of polymer, the polymer chains of two different particles may extend their ends towards the surface of the particle, preventing attachment due to impossibility of contact (fig. 4a) – steric hindrance. However, the inverse may happen as well: at lower concentrations of a determined polymer, the chains may interact with the adjacent particle, thereby forming a bridge, which maintain the particles bound to each other (fig.4b) – which corresponds to the process by which lectins bind carbohydrate residues of adjacent cells (Miki et al. 1982; Gregory 1993).

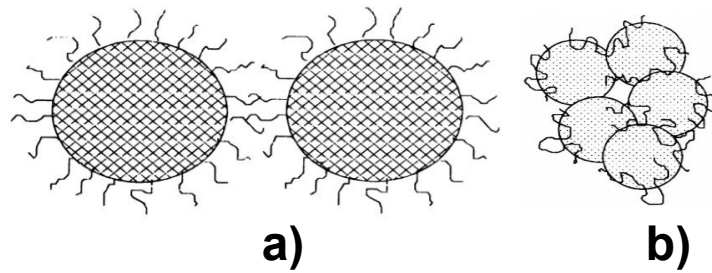


Figure 4 - Schematic representation of steric repulsion between particles (a) and bridging flocculation (b) (Gregory 1993).

In a paper published in the later 1900s, a computational model was developed to describe the mechanism of formation of cell doublets associated by receptor-ligand bonds (Long et al. 1999). Besides this study took place in medical research field, the authors stated that an extrapolation to other receptor-ligand systems could be a possibility. So on, the applicability of the model to yeast flocculation was investigated (Hsu et al. 2001). In this posterior paper, two *S. cerevisiae* strains were tested for flocculation behaviour in laminar flow fields. Orthokinetic capture coefficients were measured experimentally at different shear rates and temperatures, and then compared with theoretical coefficients predicted by the model. It was concluded that the capture coefficient increases with increasing temperature and decreasing shear rate. Moreover, a comparison was made with pronase treated cells (which would digest the lectins in the cell wall). Results showed that capture coefficients were decreased but not abolished, suggesting that other type of non-specific interactions might be involved in cell flocculation, being electrostatic (DLVO) or hydrophobic forces.

The last topic to be discussed regarding the physical aspects of flocculation regards the form of aggregates. The concept of fractality is of extreme importance, in order to understand the idea of formation of flocs. When two cells collide, the form of the aggregate is simple to predict – something like a dumbbell. However, as a third or fourth particle collide with the previous one, the aggregate may have several different forms. In this way, it becomes complex the exact form of the aggregate. Consensus came that aggregates are recognized as fractal objects (Meakin 1987). Fractal object is defined as structure which presents self-similarity, so that its macroscopic form and structure is a mirror of the small clusters that associated together to form it (fig. S1). The consequence of this structure formed from clusters of clusters is that, as its size increases, its density decreases. In this way, if the mass of the object is plotted against its size (in a logarithmic scale), the result is a linear slope, which is called the *fractal dimension* – the smaller the slope, the less dense is the macroscopic aggregate (fig. 5) (Elimelech 1995).

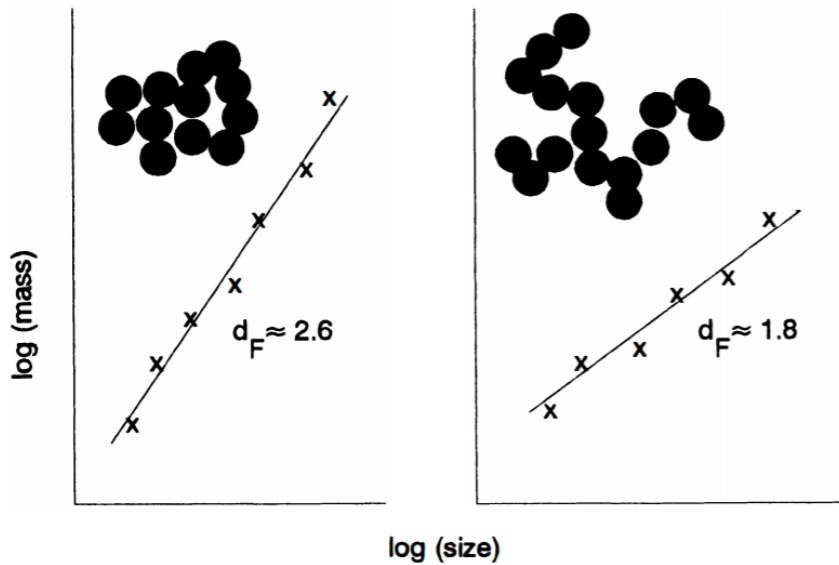


Figure 5 - Logarithmic scale plots of mass against size of the aggregate. The slope of the resultant curve gives the fractal dimension of the aggregate (Gregory 1993).

When this concept is translated to flocculent yeast cells, the flocs may be considered as fractal objects. When cell flocs begin to form, single cells collide with single cells, doublets with doublets, quadruplets with quadruplets, and so on (Stratford 1992). There is a tendency of particles binding other particles of similar size. Binding of particles of different sizes is a rarer phenomenon, due to the sweeping effect – large structures falling under gravity will sweep aside smaller structures. Such evidence come out from the observation that floc particles sizes undergo a bimodal distribution in solution or, in other words, there is existence of high number of large flocs and single cells, but there is very low concentration of medium sized flocs in suspension (Davis and Hunt 1986). Moreover, studies carried out in single strains point to the fact that the larger the floc size, the lower is its correspondent density, since there is an increased proportion of empty space inside them, and they're more loosely packed (Davis and Hunt 1986). Consequently, the higher the bond strength between cells, the lower is the possibility of cell relocation within the cell floc, resulting in a less closely packed structure (fig. S2). A lower bond strength will mean that cells may not totally attach at a first contact, enabling single particles to “search” for a better location, in which less empty space is left between them, resulting in more dense structures (Stratford 1992).

1.2. Cell Surface Charge and Cell Surface Hydrophobicity

Considering the previous chapter, it's clear that the analysis of cell surface charge and hydrophobicity are essential to understand the mechanism of flocculation. The role of those cell properties is described in literature, but some controversy exists with respect to the impact of cell wall physics on flocculation phenomena and which kind of mechanism lead to their change.

Several papers report that increase in cell surface hydrophobicity correlates with flocculation onset (Amory and Rouxhet 1988; Straver et al. 1993; Jin et al. 2001; Speers et al. 2006; Van Holle et al. 2012). In a study conducted with top and bottom fermenting strains, analysis of surface phosphate, ammonium and potassium showed a correlation between a higher ammonium to phosphate ratio and increase in

hydrophobicity (Amory and Rouxhet 1988), but with a highly strain dependent variation. Moreover, cell surface hydrophobicity (CSH) appears to be rather low during the exponential phase and rapidly increases as the cell population reaches the stationary phase of growth (Speers et al. 2006). The lower CSH during exponential growth could be correlated with the higher proportion of young cells to old cells, which are proved to be either less hydrophobic and less flocculent (Powell et al. 2003). Regarding the conditions that leads to the CSH increase, reports point to increased CSH with higher pitching rates and ethanol concentrations (Jin et al. 2001). Ethanol may play a role in exposing hydrophobic sites of the cell wall, thereby increasing the action of the flocculins. However, other studies point out that the increase in CSH is a consequence of the expression of flocculins in the cell wall, since degradation of cell wall proteins leads to decrease in CSH (Van Holle et al. 2012) and the increase in CSH is dependent on the expression of flocculins on the cell wall (Van Mulders et al. 2009). Another interesting phenomenon is the production of 3-OH oxylipins by yeast cells, which is thought to be correlated with increased hydrophobicity of the cells, and thereby increased flocculence. The repression of the production of these components leads to significant decrease in flocculation (Kock et al. 2000; Strauss et al. 2005). In close relation to CSH is the Cell surface charge (CSC). A decrease in cell surface charge would promote flocculation, since electrostatic repulsion between cells would be reduced, but no clear relationship is found between CSC and flocculation onset (Smit et al. 1992).

An important final consideration regarding this aspect is the difference between ale and lager yeast. Ale strains are often reported to be less negatively charged and more hydrophobic than lager strains (Amory and Rouxhet 1988). This feature, of course important for flocculation behaviour, may explain as well the reason why ale strains rise to the top of the fermenter in traditional beer fermentations: their relative high hydrophobicity in comparison to lager yeasts results in higher affinity to CO₂ bubbles, culminating in floc flotation at the top of the fermenter (Dengis et al. 1995). Such behaviour for ale yeast does not occur in cylindroconical vessels, due to the higher hydrostatic pressure that restricts the size of the bubbles, detaching them from the flocs (Vidgren and Londesborough 2011).

1.3. Physiological environment implications in flocculation

It's evident how the physical and chemical properties of yeast cells impact their flocculation behaviour. The last two chapters described how physical interactions rule out the aggregation process of yeast. However, the environment in which they are inserted should be noted as well, and how that environment affects flocculation and cell wall properties. Moreover, the physiological parameters have different implications in flocculation, depending on the expressed flocculation phenotype of the tested strain. Specially, the sugar composition of the environment dictates the flocculation onset of the cell population, which is intimately related to the phenotype of the correspondent yeast population.

1.3.1. The different flocculation phenotypes and sugars impact on flocculation

Currently, three distinct sub-phenotypes of flocculation are described, based on the free carbohydrates that competitively inhibit cell aggregation: (i) mannose sensitive or Flo1 phenotype, in which aggregation is inhibited only by mannose residues in solution; (ii) the NewFlo phenotype, in which glucose, sucrose, maltose, maltotriose and mannose are able to inhibit the aggregation process (Stratford and Assinder 1991; Sato et al. 2001) and (iii) a flocculation phenotype in which flocculation is not inhibited by any

sugar in solution (Masy et al. 2010). Most brewer's yeast strains, ale and lager types, possess the NewFlo phenotype. For that reason, those strains are the most suitable for the brewing process, since the onset of flocculation is delayed until most of the sugars in wort are mostly consumed (Stratford and Assinder 1991).

1.3.2. Chemical/physical environment impact on flocculation

pH: The pH of the medium in which cells are inserted has obvious implications, regarding the physical state of the cell wall. The isoelectric point of yeast cells is stated as being 3. In this way, above this pH value, yeast cell surface has a negative charge, and below this pH yeast cell surface is positively charged (Mercier-Bonin et al. 2004). In this way, it can be stated that the higher the pH of the medium, the higher will be the negative charge of the cell, and the higher the electrostatic repulsions will be. Besides, variations in pH may also impart conformational changes in the cell wall flocculins, by ionization of side groups of their aminoacids skeleton (Jin and Speers 2000). The influence of pH on flocculation ability turns to be a highly strain dependent parameter. In this study (Jin and Speers 2000), two strains expressing two different flocculation phenotypes (NewFlo and Flo1) appear to have opposite behaviours regarding the pH value: for the Flo1 phenotype strain, the pH value did not seem to impart a relevant effect on flocculation ability; on the opposite, the tested NewFlo phenotype strain showed a massive decline in flocculation ability, as the media was more acidic (below 4.45). This unexpected trend may prove that the difference from NewFlo to Flo1 strains could be explained by different characteristics of the binding sites of the zymolectins of each strain (Jin et al. 2001). Upon this, NewFlo strains are also more affected by the buffering capacity of the surrounding media and on the initial pH of the culture at the beginning of growth – too low pH initial ranges lead to inhibition of flocculation on such strains (Soares et al. 1994). The same tendency was found in other tested NewFlo ale strains, which showed not to flocculate in more acidic pH. Interestingly, one of the three tested strains showed stable flocculation ability for the higher tested pH ranges, contrarily to the other two tested strains, which stopped to flocculate above pH of 5.2 (Stratford 1996). Differences are also found among top and bottom fermenting strains: lager yeast shows to flocculate within a range of 3.5-6, with the best performance at 4-4.5, whereas ale yeast from 3-4.5 (Dengis et al. 1995). Another important aspect of the pH value of the media is its influence on the solubility of calcium ions in solution. Since only the free calcium in solution is suitable for flocculation induction, it must be considered the fraction of calcium that is free or complexed. In general, the fraction of free Ca²⁺ increases with pH decrease (Soares and Seynaeve 2000).

Temperature: The way by which temperature affects flocculation seems also to be strain specific. Regarding the yeast metabolism, the arresting of population growth plus temperature decrease will lead to lower metabolism rate, coincident with a reduced CO₂ production rate. Consequently, the turbulence inside the fermentation vessel will reduce, which has implications on flocs stability – which can be another factor favouring the flocculation onset at the beginning of the stationary phase of yeast growth, when the shear rate in the fermenter is lower (fig. S3) (Speers et al. 2006). It seems that, generally, NewFlo strains are more sensitive to temperature alterations than Flo1 strains, with respect to the flocculation capacity (Jin and Speers 2000; Soares et al. 2004). In the study from Jin and Speers (Jin

and Speers 2000), NewFlo and Flo1 strains were tested for flocculation ability for temperatures ranging from 5-25°C. The NewFlo strain showed to be sensitive to the temperature of the surrounding medium, with higher flocculation ability at 25°C. Contrary, the Flo1 phenotype strain did not show great temperature dependency. In another study, a tested NewFlo strain showed to be sensitive to the applied growth temperature, losing flocculation ability in growth temperatures above 30 degrees (Soares et al. 2004). Rule of thumb states that lager yeast strains show reduced flocculation at higher temperatures (Jin and Speers 2000). However, the way by which temperature impacts flocculation is quite specific, since NewFlo strains at the exponential phase did not show induced flocculation in response to applied heat stress (mild heat or brief heat shock) (Claro et al. 2007).

Ethanol: There is no consensus on the effect of ethanol on flocculation ability. D'Hautcourt et al. (D'Hautcourt and Smart 1999) performed flocculation measurements in different yeast strains, concluding that the effect of ethanol on flocculation intensity couldn't be generalised to each strain phenotype (bottom/top fermenting or NewFlo/Flo1 phenotype strains). Ethanol is known to be a stress inducer agent, and flocculent cells show a two-fold higher resistance to ethanol than non-flocculent cells (Smukalla et al. 2008). So on, it would be expected that increasing ethanol concentrations would induce flocculence on stressed cells, however, addition of ethanol to exponential growth cells did not induce earlier flocculation (Claro et al. 2007). As an organic solvent, ethanol would associate with cell wall proteins via hydrophobic interactions, reducing the dielectric constant of the cell surrounding medium and therefore decreasing the electrostatic repulsions between cells and exposing their hydrophobic binding sites, enhancing cell-cell interactions (VOLKIN and V. 1989). Indeed, it is reported that ethanol has an increasing effect on CSH (Jin et al. 2001). Flocculation ability is increased in NewFlo phenotype expressing strains, but no effect is observed in Flo1 strains (Jin and Speers 2000). Regarding differences among top and bottom fermenting strains, lager strains did not show flocculation inducement with increased ethanol concentrations, whereas top fermenting did show it (upon concomitant addition of calcium). Interestingly, it is also reported that higher concentrations of ethanol increases the pH range at which cells flocculate (Dengis et al. 1995).

Oxygen: Oxygen seems to have an indirect impact on the flocculation capacity of yeast cells. In fact, oxygen plays an important role in the production of sterols and unsaturated fatty acids (Andreasen and Stier 1953), which apparently connects with cell-cell interactions. A work developed by Straver et al. (Straver et al. 1993) in a flocculent lager yeast showed that the absence of oxygen in the pitching wort resulted in poorer and earlier flocculation, as well in lower final CSH and cell number of the resultant population. Enrichment of oxygen-depleted and oxygen-saturated wort with ergosterol and tween 80 induced a higher flocculation capacity, cell density and CSH, in comparison with wort non-supplemented with both substances. This behaviour seems to be strain dependent. In another study, two lager yeast strains were tested for fermentations either in aerobic or anaerobic conditions, showing distinct behaviours in relation to anaerobiosis. One of the strains clearly shows decreased flocculation capacity in anaerobiosis, but the other strain becomes slightly more flocculent in the same conditions (Lawrence and Smart 2007).

Cations: Among all the cations, calcium seems to play the most important role in flocculation induction (Taylor and Orton 1975; Miki et al. 1982; Nishihara et al. 1982; Stratford 1989; Soares and Seynaeve 2000; Soares et al. 2002). The concentration of calcium needed to induce flocculation is strain dependent: some authors report concentrations of 10^{-8} M (Taylor and Orton 1975), others report higher concentrations as $5 * 10^{-4}$ M (Soares and Seynaeve 2000). Calcium is required for the correct binding between the flocculins and carbohydrate residues (Miki et al. 1982), and it appears that flocculent cells bind more calcium than non-flocculent cells, supporting this hypothesis (Stewart et al. 1975). Besides Ca^{2+} , stated as a specific inducer of flocculation, other ions are reported as flocculation inducers: Mg^{2+} , Mn^{2+} , Sn^{4+} , Cu^{2+} , Ni^{2+} , Zn^{2+} , and Cd^{2+} , which work as non-specific inducers, at determined conditions and to lower extents than calcium (Miki et al. 1982; Nishihara et al. 1982; Stratford 1989; Soares et al. 2002). Mg^{2+} is reported to induce flocculation, but only at neutral pH (Stratford 1989) and its presence is reported to increase the CSH (Smit et al. 1992). Sn^{4+} can induce flocculation in flocculent and non-flocculent cell walls (Nishihara et al. 1982). Both Sn^{4+} and Mg^{2+} appear to interact with cell walls in a non-specific manner. Ions correlated with flocculation inhibition include Pb^{2+} , Sr^{2+} and Ba^{2+} (Nishihara et al. 1982; Gouveia and Soares 2004). Particularly, it was concluded that Pb^{2+} competitively inhibits flocculation, by association with cell wall lectins, but without the capacity of inducing their correct conformation for the lectin-carbohydrate binding (Gouveia and Soares 2004). Other ions, like K^{+} and Na^{+} are shown to induce flocculation at low concentrations, apparently by stimulating the leakage of intracellular calcium (Nishihara et al. 1982; Stratford 1989). At higher concentrations they antagonize the calcium induced flocculation (Stratford 1992). The presence of metal-chelating agents as EDTA inhibits flocculation, by reducing the amount of free calcium in suspension. This observation supports the importance of calcium in the flocculation phenomena (Nishihara et al. 1982; Stratford 1989).

Nitrogen: Nitrogen also appears to have a preponderant effect on yeast flocculation. It's action is more clarified for pseudohyphal growth (Fichtner et al. 2007), but some articles also report its impact on brewer's yeast flocculation. A study carried by Smit et al. (Smit et al. 1992) showed that flocculation onset could be correlated with nitrogen limitation, coinciding as well with the arrest of cell growth. Same was observed later (Sampermans et al. 2005) in an ale-brewing yeast strain, which was also observed to have its flocculation onset in agreement with the shortage of nitrogen nutrients. Other authors showed that the supplementation of the fermenting wort with certain amino acids did not had any impact on flocculation onset (Straver et al. 1993), showing that the connection between nitrogen starvation and flocculation onset seems to be specific for a certain type of nitrogen source.

1.4. Flocculation genetics: from gene to protein

1.4.1. *Saccharomyces pastorianus*: the hybrid genome

In the past, beer brewing was mainly performed using ale yeast species, which belong to *S. cerevisiae* strains species (Meussdoerffer 2009). However, lager beer emerged in the 15th century, which brewing yeast organisms belong to the interspecific hybrid *Saccharomyces pastorianus* (Vidgren and Londesborough 2011).

Saccharomyces pastorianus is the lager brewing yeast, resultant from the hybridization event occurred between *S. cerevisiae* and *S. eubayanus*. The discussion regarding the parentage of *S. pastorianus* was apparently solved with the discovery of a free-living diploid specie of *S. eubayanus* in South America. This newly discovered organism shared high similarity with the non-*Saccharomyces cerevisiae* sub genome of *S. pastorianus*. The suggested scenario for the emergence of *S. pastorianus* includes an initial hybridization event between the parental strains, which formed an allotetraploid yeast. Afterwards, extensive genome reorganization by mitotic recombination followed, which imparted the loss of heterozygosity and the formation of recombinant chimeric chromosomes (Libkind et al. 2011). As a result, *Saccharomyces pastorianus* characteristics include the strong fermentative ability of *S. cerevisiae* and the cold tolerance of *S. eubayanus*. With those characteristics, the hybrid would have attained a competitive advantage over both parental strains, and a rapid population growth lead to its emergence (Gibson and Liti 2015).

The *S. pastorianus* group encompasses two known distinct lineages, lager group 1 yeasts or Saaz group and lager group 2 yeasts or Frohberg group, which presents differences at the ploidy level and genome sequence (Gibson and Liti 2015). These two groups differ in some characteristics: while the Saaz group of yeasts presents a higher flocculation capacity and less sugar utilization ability, the Frohberg group is less flocculent but more fermentative (Guilliermond 1920). Both types are very distinguishable due to the almost complete absence of *S. eubayanus* rDNA in Frohberg strains group (Nakao et al. 2009; Pham et al. 2011). Moreover, the optimal growth temperature of Saaz group yeasts is lower than Frohberg yeasts (Gibson and Liti 2015), with the later having a faster fermentation performance due to the faster and more complete utilization of maltose, plus the ability of fermenting maltotriose – an absent characteristic in Saaz yeast group (Gibson et al. 2013). The differences at genomic level in both groups were for a long time thought to had arisen independently (Liti et al. 2005; Dunn and Sherlock 2008); however, recent studies point to a single hybridization event followed by different patterns of loss of heterozygosity, culminating in the formation of two independent groups (Salazar et al. 2019).

Due to an intricated genomic background, *S. pastorianus* hybrids has received little attention regarding its gene expression regulation (Gibson and Liti 2015). Natural yeast flocculation is a since ever applied method by brewer's to separate yeast biomass from the fermented wort, at the end of the fermentation process (Verstrepen et al. 2003). Besides its relevance, little is still known about its genetic regulation and preponderant environmental effectors. Most of the flocculation-related research is carried with *Saccharomyces cerevisiae* strains, like the laboratory strain S288C (Van Mulders et al. 2009). The inter-specific hydride *Saccharomyces pastorianus* has received less attention. The difficulty in solving DNA sequences for the sub telomeric located *FLO* genes and the added complexity of *S. pastorianus* hydride genomes makes this topic even more complex, in the lager brewing context. However, the availability of high-quality genome sequences of Heineken yeast strains opens the possibility for an in-depth study of *FLO* genes expression and regulation.

1.4.2. The FLO genes and their phenotypes

Yeast flocculins are encoded by the *FLO* genes family. There are at least nine genes described, that belong to this family: *FLO1*, *FLO5*, *FLO9*, *FLO10*, *FLO11* (*MUC1*), *Lg-FLO1*, *FLONS*, *FLONL* and *FLO8*, all of them part of *S. cerevisiae* and *S. pastorianus* genomes (Vidgren and Londesborough 2011).

The FLO genes: *FLO1* is the better described gene of the family, composed by a 4.6kb open reading frame, which codifies for a 1,537 aminoacids protein (Watari et al. 1994). The *FLO1* gene is located in a sub telomeric region at the right arm of chromosome I of *S. cerevisiae* genome, 24kb from its end (Teunissen et al. 1993), and is associated with the Flo1 phenotype (Kobayashi et al. 1998). *FLO5*, *FLO9* and *FLO10* share high sequence homology with *FLO1*: 96%, 94% and 58% respectively (Teunissen and Steensma 1995). Similarly to *FLO1*; *FLO5*, *FLO9* and *FLO10* are also located at sub telomeric regions of their respective chromosomes (Guo et al. 2000). *FLO11* (*MUC1*) is a more distant gene, which gene product shares 37% of similarity with *FLO1*. This gene comprises a 4.1kb open reading frame present in the centromeric region of chromosome IX of *S. cerevisiae* chromosome (Lo and Dranginis 1996).

Although the genes have a high degree of similarity, they produce different phenotypes. Studies were carried out in order to understand precisely the role of each *FLO* gene in the observable phenotypes. Govender et al. (Govender et al. 2008) presented a work in which the native promoters of the genes *FLO1*, *FLO5* and *FLO11* were replaced by the inducible promoters *ADH2* and *HSP30*. Both *FLO1* and *FLO5* showed flocculation inhibition by mannose and the cells expressing *FLO1* presented a stronger flocculation than *FLO5*, with no detectable flocculation presented by the cells expressing *FLO11*. Conversely, *FLO11* over expressing strains showed higher ability for cell adhesion and flor formation and the higher cell surface hydrophobicity induction of all the tested genes. A similar work was performed by Van Mulders et al. (Van Mulders et al. 2009). In the non-flocculent laboratory strain S288C, *FLO* genes were individually expressed, in order to characterize each gene, according to the correspondent phenotype. Results showed that *FLO1*, *FLO5*, *FLO9* and *FLO10* induced flocculation, but with different strengths: by order of strength, *FLO1*>*FLO9*>*FLO5*>*FLO10*, with *FLO10* showing a rather low force of binding between cells. Considering the sugar sensitiveness, *FLO10* revealed high flocculation inhibition in the presence of maltose, sucrose, mannose and glucose, and *FLO9* for maltose and glucose. *FLO1* and *FLO5* showed the lower sensitiveness towards sugars. *FLO11* proved to be a crucial gene regarding the capacity for adhesive and invasive growth and presented as well the higher CSH, in comparison with the other genes. The results regarding the *FLO11* gene are in accordance with other previous works (Lo WS and Dranginis AM 1998; Guo et al. 2000). The reason why the laboratory strain *S. cerevisiae* S288C is non-flocculent is linked to the nonsense mutation present on its *FLO8* gene, which encodes for a transcriptional activator (Liu et al. 1996). The flocculation ability of S288C can be restored by the insertion of a wild type *FLO8* (Fichtner et al. 2007). *FLO8* is reported to be a transcriptional activator of *FLO1*, *FLO11* and *STA1*, which encodes for a glucoamylase (Kobayashi et al. 1996; Kobayashi et al. 1999).

The instability of the FLO genes family: Sub telomeric regions of DNA possess high number of mosaic repeats in variable copy numbers and have a relatively low density of open reading frames

(Pryde et al. 1997; Pryde and Louis 1997). The sub telomeric located *FLO* genes do not escape from these characteristics and are full of highly variable tandem repeats which makes them more prone to evolution and variation (Verstrepen et al. 2004; Brown et al. 2010). The presence of these unstable repeats along the *FLO* genes makes them a highly variable family, enabling frequent replication errors within and among *FLO* genes and pseudogenes – which, in this way, makes it possible to possess a strain specific “arsenal” of flocculin-encoding genes for each strain (Verstrepen et al. 2004; Verstrepen et al. 2005). Moreover, this characteristic of *FLO* genes increases the difficulty in attributing singular phenotypes to each type of strains, since they are highly variable among different brewing yeast strains (Van Mulders et al. 2010).

As previously stated, tandem repeats are an evolutionary driving force which enable intergenic or intragenic recombinations – and this feature leads to the emergence of new flocculin-encoding genes. The most cited report of an intergenic recombination event among *FLO* genes is the frequently mentioned *Lg-FLO1*, which is thought to be a result of a recombination (translocation) event between *FLO5* on chromosome VIII and a *FLO1* pseudogene located on chromosome I in *S. pastorianus*. Actually, the reported position in a lager-fermenting yeast (*S. pastorianus*) genome corresponds to the *S. cerevisiae* chromosome VIII, coincident with the same position of *FLO5* in the *S. cerevisiae* S288C strain (Kobayashi et al. 1998; Sato et al. 2002; Ogata et al. 2008). *Lg-FLO1* is the *sui generis* of the NewFlo phenotype, associated with most lager brewing strains and absent in laboratory strains (Kobayashi et al. 1998; Liu et al. 2007). Because of the broader sugar sensitiveness of this gene product, flocculation in brewing strains occurs only at the end of the fermentation, when sugars are almost depleted (Verstrepen et al. 2003). As a homologue of *FLO1* gene, it presents 60% similarity at the aminoacid sequence with Flo1p (Kobayashi et al. 1998). Despite the general acceptance of *Lg-FLO1* as an important gene regarding the *S. pastorianus* yeasts genome, a recent paper showed the absence of *Lg-FLO1* sequence in the *S. pastorianus* strain CBS 1483 (Salazar et al. 2019).

Another direct consequence of long tandem repeats in the genome is the occurrence of replication errors in the gene, which lead to expansion or contraction of the gene. This changes at the gene level (intragenic recombinations) may lead to qualitative and quantitative phenotypic changes (Verstrepen et al. 2005; Liu et al. 2007). The two last described genes on this introduction, *FLONS* and *FLONL*, are an example of phenotypic variation due to changes in the gene size. This study reported that both above-mentioned genes are highly similar but lost some internal repeats in their sequence. *FLONL* is shorter than *FLONS*, and this slight variation in the tandem repeats number lead to the phenotype conversion of Flo1 to NewFlo, with sugar inhibition by mannose, glucose, sucrose, maltose, maltotriose and even galactose (Liu et al. 2007; Liu et al. 2009). The variation of tandem repeats number in *FLO* genes is also related with the adhesion strength among cells, being that it is reported that longer number of tandem repeats lead to stronger flocculation phenotype (Verstrepen et al. 2005). However, a recent paper also reported the lack of correlation between *FLO* gene size and flocculation strength (Salazar et al. 2019). Surprisingly, another study reported that the decrease in the number of tandem repeats of *FLO* genes lead to an enhanced conformational stability of *FLO1* gene product under more acidic or alkaline conditions, and higher mannose concentrations necessary to inhibit flocculation. Moreover, it was also reported an increased CSH for the cells expressing the shorter *FLO1* gene (Li et al. 2013).

1.4.3. Yeast Flocculins: structure and interactions

Yeast flocculins are structural proteins found at the cell wall of yeast cells, which belong to a large family of fungal glycosylphosphatidylinositol-linked cell wall glycoproteins (GPI-CWPs) (Verstrepen et al. 2004; Verstrepen and Klis 2006; Dranginis et al. 2007). These proteins family share an overall structure, composed of three subunits (fig. 6): N-terminal domain or A domain, responsible for ligand recognition and binding of molecules *in trans*; middle domain or B domain, highly enriched in serine and threonine residues and highly glycosylated and the C-terminal or C domain, which contains a GPI anchor, responsible for the anchoring of yeast adhesins at the cell wall. The adhesins are targeted to the yeast cell wall via an N-terminal secretory sequence (signal peptide), which is removed as the protein moves from the plasma membrane during the protein secretory pathway (Willaert 2018). Several different types of proteins are described for this family, extending from brewer's yeast to *Candida spp.*, going as well to the bacterial domain.

C-terminal domain (C domain): At the endoplasmic reticulum, the C-terminal domain of yeast flocculins receives the attachment site for the GPI anchor, which makes it possible to be covalently linked to the non-reducing end of β -1,6-glucans present in the yeast cell wall, in this way anchoring the adhesin at the yeast cell surface (Klis et al. 2006; Brückner and Mösch 2012; Willaert 2018).

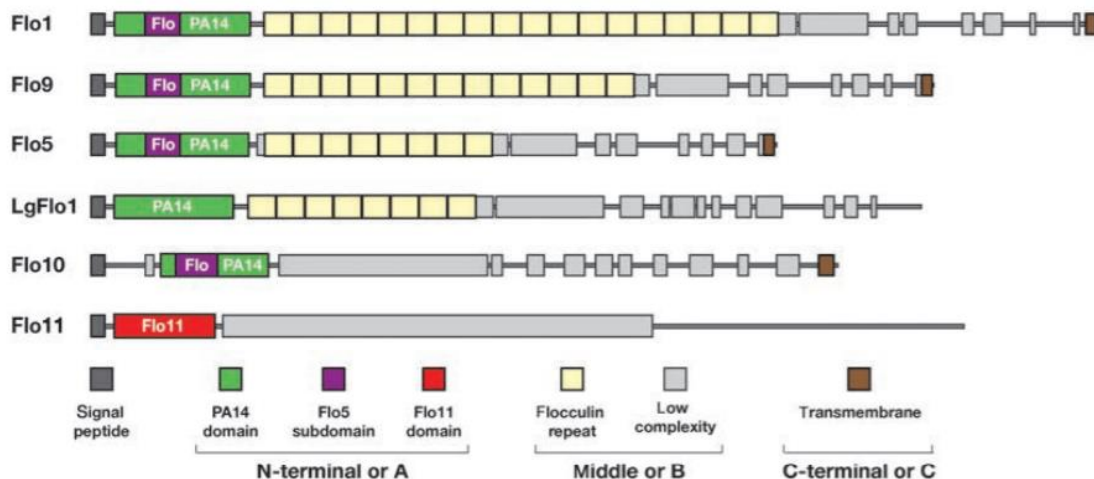


Figure 6 - Domain organization of *Saccharomyces cerevisiae* adhesins (flocculins). Known domains are depicted in different colours, and mainly divided in N-terminal (A), middle (B) and C-terminal (C) domains (Brückner and Mösch 2012).

Middle domains (B domain): The middle domains are highly rich in serine and threonine residues – this characteristic makes them highly prone to *N*- and *O*-linked glycosylation (Lehle et al. 2006; Lommel and Strahl 2009). The high glycosylation profile in the middle domain may have a role in enabling an extended conformation of the flocculin, further stabilized by Ca^{2+} ions (Jentoft 1990). This semi-rigid rod-like structure may be important to project the protein – and, more importantly, the N-terminal recognition domain – towards the outer space of the cell, permitting the efficient interaction of flocculins with their ligands in other cells (Frieman et al. 2002; Verstrepen and Klis 2006). Moreover, adding to the serine and threonine residues, the middle domain repeats also code for proline residues, which also may have some impact in avoiding the central domain from forming a compact structure (Teunissen and Steensma

1995) Additionally, a positive correlation is found between the degree of mannosylation and cell surface hydrophobicity (Masuoka and Hazen 2004), which is also in accordance with the increase in CSH as cell wall flocculins are expressed (Van Mulders et al. 2009).

The tandem repeats that constitute the middle domains of yeast flocculins are also proved to contain sequences for β -branched aliphatic aminoacids. This characteristic, in its way, makes the flocculins highly prone to form β -aggregates and amyloids among each other. Instead of a singular flocculin-ligand configuration, it appears that many flocculins bind in multimers at the middle domains level, which in its way may increase the potential of the N-terminal domains to bind ligands *in trans*, i.e. to bind ligands that are present in other cell wall (fig. 7b) (Ramsook et al. 2010).

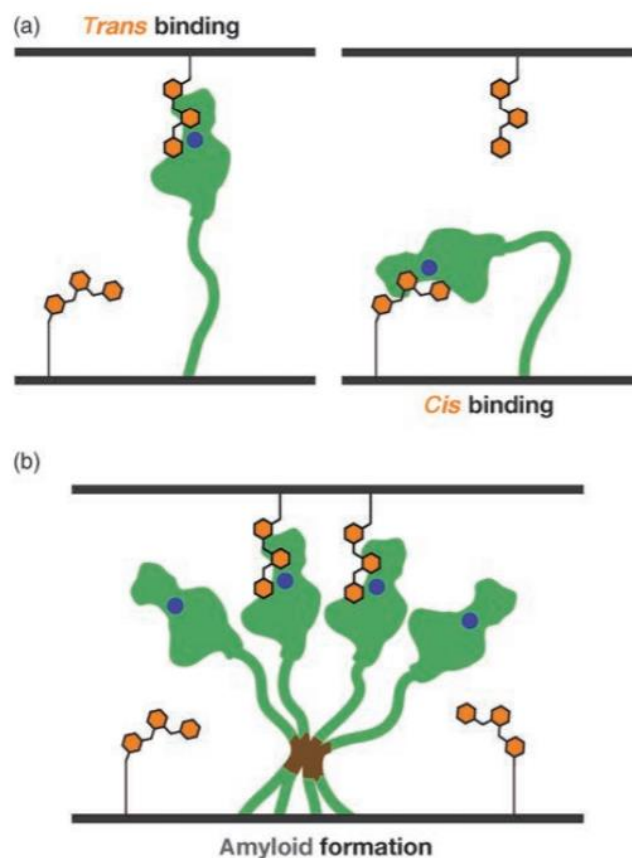


Figure 7 - Ligand binding by adhesins (Brückner and Mösch 2012). In a) is represented the comparison between trans (to other cell) and cis (same cell) binding of the lectins. In b) is represented the multimerization of the lectins by amyloid formation, in which the β -aggregation prone sequences (brown) might favour cell-cell adhesion by directing binding sites towards carbohydrates in neighbour cells. Ca^{2+} in the primary binding site is represented in blue and carbohydrates represented in orange.

N-terminal domain (A domain): The N-terminal region of Flo proteins seems to be the most interesting one, and the unravel of its atomic structure permitted not only the discover of new insights regarding the observed phenotypes in yeast strains but as well the settlement of long standing questions and theories. Yeast flocculins A domain presents the widely characterized PA14 domain, from the anthrax-protective antigen. This specific piece which presents a β -barrel conformation is currently identified as belonging to proteins of the eubacterial and eukaryotic realms, including yeast adhesins,

bacterial toxins, signalling molecules, among others (Rigden 2004). However, the A domain of Flo proteins constitutes a special one of the all kingdom of the PA14 family (Goosens and Willaert 2010).

Flo5A domain: The three-dimensional structure of the N-terminal domain of the Flo5 protein is depicted in figure 8. At the amino acid level, Flo5 subdomain comprises the residues N84-A120 and its 5 β -strands are stabilized by two disulphide bonds (fig. S4). An interesting addition is the location of the N and C-termini regions of the whole Flo5A domain. This sub-region of the protein extends from the core domain as an L-shaped stretch, which is fixed at the main protein by two disulphide bonds to two cysteines located at β -strands 12 and 13 (fig. S5). Apparently, this sub-region plus a second loop located between β 2 and β 3 strands are responsible for sealing the underlying β -sheet from solvent access. The crystalline structure of the mannose/ Ca^{2+} complex of Flo5A shows a C-type lectin-like mode of binding, in which Ca^{2+} mediates the recognition of the 2' and 3' hydroxyl groups of the sugar residue, being that Ca^{2+} is bound between the protein and the sugar. According to the results regarding sugar-binding experiments, there is a preference of the Flo5A domain for mannosides (mannose disaccharides) instead for monosaccharides, which is explained by the interaction of the axial 2' hydroxyl group of the

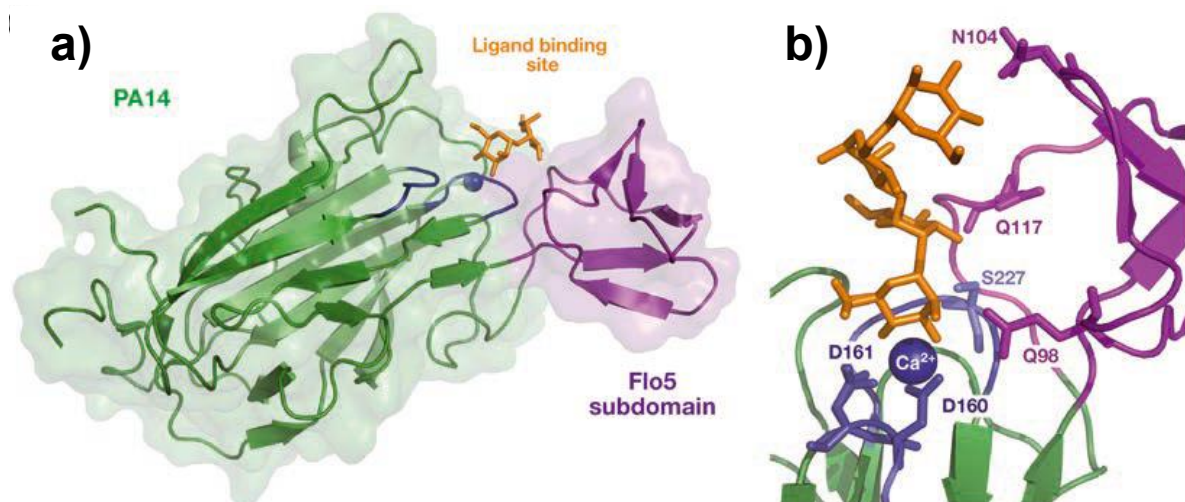


Figure 8 - Flo5A/PA14 domain of *Saccharomyces cerevisiae*. (Brückner and Mösch 2012). In a) is represented the three-dimensional structure of the Flo5A domain, in which is shown PA14 subdomain (green), the Flo5 subdomain (purple), the Ca^{2+} ion (blue sphere) in coordination with the primary binding site and the carbohydrate ligand (orange). The Ca^{2+} -binding loops (CBL) 1 and 2 are represented in blue. In b) is depicted the detailed view of the primary binding site of Flo5A domain. Residues involved in Ca^{2+} binding are depicted in blue (D160, D161 and S227) and residues involved in carbohydrate binding are depicted in purple (N104, Q117 and Q98) (Brückner and Mösch 2012).

mannoside with the side chain of the Q98 residue of the protein (fig. 8b). Regarding the specific spot at which the carbohydrate binds, the Flo5A domain comprises two important regions, namely, the carbohydrate binding loops (CBL) 1 and 2. The CBL1 is linked to β 11 and β 12 strands and includes the Asp-Asp motif or *DcisD* motif, which is a rare *cis* peptide occurring between two non-proline residues (aspartate residues). From these two residues, D160 and D161, D160 is the one that directly binds the Ca^{2+} ion, and any mutation on either of the two residues culminates in complete lack of flocculation. CBL2 is linked to β 15 and β 16 strands and its contribution effect to calcium binding it's originated by the

side chain of the N224 residue and the two carbonyl groups of V226 and W228 residues. This observation completely settles the lectin-like theory present in the flocculation phenomena (Miki et al. 1982).

The reason why flocculins preferentially bind sugar residues in *trans* (other cells) instead of in *cis* (sugar residues in their own origin cell) is also hypothesized. At the back of the Flo5A domain exists a secondary binding site, which recognizes hexoses in a non-specific and Ca²⁺ independent manner, driven by hydrogen bonds in β 3 and β 4 strands. Accordingly, this secondary binding site may play a role in the preferentiality of Flo adhesins to bind sugar residues in *trans*, since this region could bind sugar residues present in the cell wall (*cis* interaction), in this way exposing the primary binding site to interaction with an outer cell wall.

Lg-Flo1A and Flo1A domains: After the successful protein structure prediction for the N-terminal domain of Flo5 protein, two later papers reported the structures of the N-terminal domains of Flo1 and Lg-Flo1, which also showed to be highly useful for the understanding of the interactions among the different yeast strains (Sim et al. 2013; Goossens et al. 2015).

As for N-Flo5p, the N-Flo1p also contains a the Flo5 subdomain at one end of the protein, close to the carbohydrate binding site, which is also stabilized by two disulphide bridges. However, in N-Lg-Flo1p, this subdomain is absent, as seen in the predicted protein structure in figure 9, being replaced by a highly flexible loop, the flexible loop 2 (L2) (Sim et al. 2013; Goossens et al. 2015). For all the three proteins, a flexible loop 3 (L3) is present, which presents great importance regarding the sugar residue recognition. It's possible to see in figure 9 that L3 is much closer to the binding site in N-Flo1p protein, than in N-Flo5p. Moreover, the lysine residue at position 194 of L3 appears to directly interact with the sugar residue, which does not happen in Flo5 N-terminal domain – in fact, this might explain the higher affinity of Flo1p to mannose, compared to Flo5p. N-Flo1p also has an higher affinity for disaccharides than for monosaccharides, as it happen in its homologue N-Flo5p . As for N-Flo5p as well, N-Flo1p also contains the CBL1 and CBL2 domains, which directly impact the sugar binding and Ca²⁺ coordination. Moreover, the residues D160, D161 and N224 are highly conserved among these proteins, which explains their mandatory role in the Ca²⁺ binding phenomena (Veelders et al. 2010). Furthermore, the analysis of N-Lg-Flo1p revealed that its carbohydrate binding pocket is much more enclosed than for N-Flo1p, which might explain its higher affinity for mannose, comparing with the Flo1 protein. Moreover, it was also reported that Lg-Flo1p does not interact with longer oligosaccharides, probably due to a steric hindrance present in the protein binding site (Sim et al. 2013; Goossens et al. 2015).

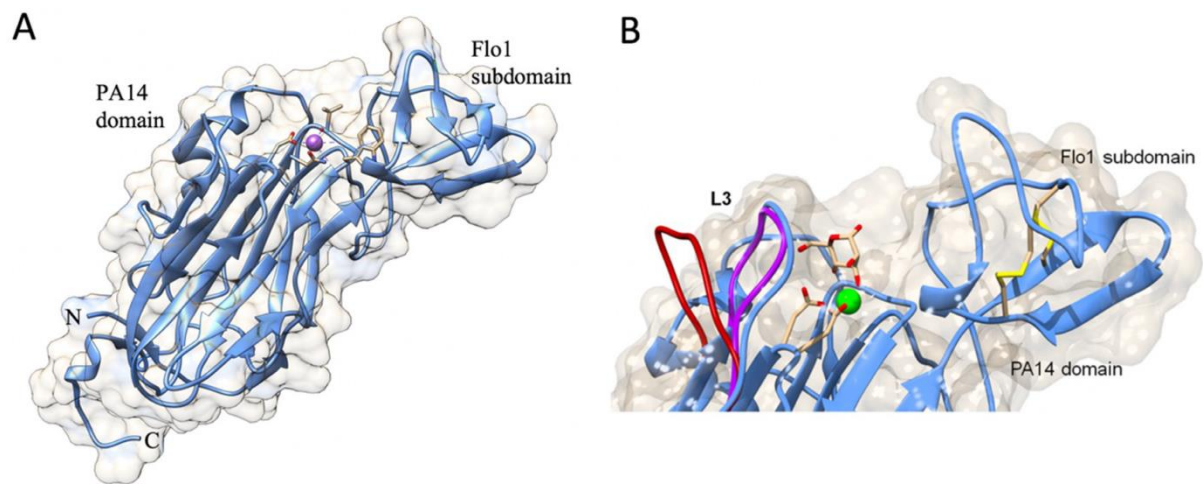


Figure 9 - N-terminal domain of Flo1p in *Saccharomyces cerevisiae* (Willaert 2018). Three-dimensional structure of N-Flo1p protein is depicted in A. In B, the N-Flo1p binding pocket (light blue ribbon close to the carbohydrate) is presented in complex with calcium and mannose. Additionally, the L3 loop of N-Lg-Flo1 is represented in purple and loop of N-Flo5p represented in crimson.

The way by which N-Flo1p proteins interact was uncovered, permitting answering why do yeast cell flocculins prefer to bind to other cell walls. Flo1 protein is highly *O*- and *N*-glycosylated at three specific sites (Goossens et al. 2015). This protein has the capacity of interacting homophilically with glycans that are present in other N-Flo1p of other cell walls. Since on flocculating cells Flo proteins dominate the yeast cell wall (Bony et al. 1997), N-Flo1p interactions – instead of heterophilic interactions of N-Flo1p and glycans present on the other cell wall – will be the main type of interaction occurring. Moreover, the fact that N-Flo1p has a lower affinity for mannose than for other Flo proteins on the same cell wall enhances the idea that binding to the Flo1 protein to another cell wall is always preferred. Finally, from this same study it was also reported that a two-step process is involved in the cell-cell adhesion phenomena (Goossens et al. 2015). In a first moment, interactions between glycans of the two cell walls are dominant, which serve as a stabilizing factor for the overall flocculation process. Again, calcium plays an important role, by interacting with the negatively charged phosphate groups present in the glycans bound to the nitrogen groups of the N-terminals of Flo1 proteins. Only after this process, the correct binding of the glycans to the N-Flo1p binding pockets is assured. Again, the lectin-like plus the “Ca²⁺-bridge” hypothesis for being the main processes in flocculation are also settled (Miki et al. 1982).

1.4.4. FLO genes regulation

A considerable number of papers were published regarding the genetic regulation of *FLO11* gene. Conversely, much less is known about the other *FLO* genes, as *FLO1*, *FLO5*, *FLO9* and *FLO10* (Brückner and Mösch 2012). Since *FLO11* is mostly associated with pseudohyphal growth and adhesion properties, it shall not be considered in the next section.

Since the discover of *FLO8* gene, it was already reported its influence as a transcriptional regulator of other *FLO* genes. Indeed, it is reported that this gene is implicated on the regulation of *FLO1*, and the absence of an active *FLO8* in the non-flocculating *S. cerevisiae* S288C strain was also reported (Liu et al. 1996; Kobayashi et al. 1996; Kobayashi et al. 1999). Later on, it was found that the replacement of

the defective *FLO8* for an active one (or its overexpression) could induce flocculation capacity on the abovementioned yeast strain, testifying the role of *FLO8* as a genetic regulator of *FLO1* and, additionally, *FLO11* (Bester et al. 2006). Additionally, the way by which *FLO8* acts as a transcriptional activator appears to be unlighted: Flo8p inactivates the TUP1-SSN6-encoded cascade, which acts as a negative regulator of flocculation in certain strains (Liu et al. 1996; Kobayashi et al. 1996). Tup1-Ssn6 complex is a widely spread corepressor in the budding yeast, being characterized as an intervenient in many transcriptional de-activation cascades (Malavé and Dent 2006). Upon *FLO8*, another transcriptional regulator was reported as having influence on *FLO* genes expression, the Mss11p (Bester et al. 2006; Fichtner et al. 2007). This transcriptional regulator is shown to be intervenient in starch metabolism (Webber et al. 1997) and hyphal growth in *Candida albicans* (Su et al. 2009). Its presence in the activation of *FLO* genes was also unravelled, being that it appears to activate the transcription of *FLO1*, *FLO10* and *FLO11*, besides other cell wall mannoproteins (Bester et al. 2012).

Besides transcriptional regulation, *FLO* genes also seem to be regulated by epigenetic mechanisms. Because of their position near the ends of chromosomal telomeres, they are prone to be affected by telomeric silencing phenomena (Halme et al. 2004). Strength of silencing seems to be variable among different yeast strains (Pryde and Louis 1999) or different telomeres, probably due to the different composition in the number of repeats in each chromosome end (Loney et al. 2009). Specifically, the complex proteins associated with Set1 (COMPASS) methylation complex seem to have high influence on *FLO* genes expression. Namely, it was observed that the deletion of this complex seems to enhance the flocculation capacity of yeast cells (earlier onset of flocculation and larger aggregates formed), by increasing the transcription of *FLO1*, *FLO5* and *FLO9* genes. All in all, it appears that the COMPASS complex has a preponderant action in the silencing of those genes, in high gravity brewing conditions (Dietvorst and Brandt 2008). Upon this protein complex, the histone deacetylase Hda1 and the histone acetyltransferase Gcn5 also appear to have influence on *FLO* genes expression. These histone modifier proteins are reported to be transcriptional repressors, since their action on chromatin creates gene-silenced areas on the DNA. Further on, the deletion of Hda1 derepressed the transcription of *FLO1*, whereas the deletion of Gcn5 seemed to have a similar action, but on the genes *FLO5* and *FLO9* (Dietvorst and Brandt 2010).

2. Aim and approach of work

Although lager brewing yeast *S. pastorianus* is used in the brewing industry since long ago, a variety of flocculation phenotypes exists within this species. The demand for innovative products and higher productivity levels result in novel wort compositions being applied. An example is the substitution of full malted barley with different adjuncts, as rice or sorghum. The different wort compositions could impact flocculation phenotypes, but this has been poorly investigated. Therefore, the aim of the present work is to get more insight in the flocculation process and how this is affected by changing conditions and wort compositions.

One of the challenges is to measure flocculation in a stable reproducible way. Therefore, the first goal was to further develop and validate a novel flocculation assay developed by Heineken. With this new flocculation measurement platform, three strains with different flocculation characteristics according to the Helm's test (D'Hautcourt and Smart 1999) were cultivated on two different wort compositions to study the impact of wort type on their flocculation characteristics. A thorough approach was taken, to take all the many factors affecting flocculation into account. Genetic influences were studied by RNA-seq, chemical influences by careful monitoring of many wort compounds and physical aspects by using stable and well controlled conditions in bioreactors. The data were used to highlight factors that have a major impact on the expressed flocculation phenotypes.

3. Materials and Methods

3.1. Yeast strains and media

Lager brewing yeast strains of *Saccharomyces pastorianus* species used in this study include strains A, B and C (HEINEKEN's property).

Heineken standard wort – Full Malt wort: full malt wort with an extract content of 16.8 °P, produced at the Heineken brewery of Zoeterwoude, The Netherlands, directly collected from the coolers at the brewery. The collected wort was afterwards supplemented with 0.6mg.L⁻¹ of ZnSO₄.7H₂O (Merck KGaA, Germany) and 1mL.L⁻¹ of antifoam (Snapsil antifoam FD10, Brunschwig Chemie). It was then autoclaved for 15 min at 121°C.

50% Adjunct wort: full malt wort mixed with sucrose solution, with a final mass/mass ratio of 1:1 and a final extract content of 16.8 °P. The prepared Adjunct wort was afterwards supplemented with 0.6mg.L⁻¹ of ZnSO₄.7H₂O (Merck KGaA, Germany), 1mL.L⁻¹ of antifoam (Snapsil antifoam FD10, Brunschwig Chemie) and 20mg.L⁻¹ of CaCl₂ (Merck KGaA, Germany), in order to achieve a final concentration of Ca²⁺ in the final wort superior to 30mg.L⁻¹. It was then autoclaved for 15 min at 121°C.

3.2. Fermentation setups

Pre-cultures: Original pure cultures stored at -80°C were directly pitched in 50 mL of Heineken standard wort in a 100mL shake flask and left growing at 21°C under continuous shaking at 150rpm, for 48h (wake-up flasks). Afterwards, 1 mL of the 50 mL growing culture was pitched in 50 mL of Full malt wort in 100 mL shake flasks. This new culture was left to grow at 21°C under continuous shaking at 150rpm, for 48h (1st propagation step). The full 50 ml flask was transferred to 240 mL of Heineken standard wort in 500 mL Erlenmeyer flasks, which were left to grow at 21°C under continuous shaking at 150rpm, for 72h (2nd propagation step).

Fermentations settings: The controlled fermentations were carried out at the Pilot Brewery facilities, which belong to the Global Innovation and Research of the Heineken Supply Chain department, located in Zoeterwoude, The Netherlands. At the Pilot Brewery, bioreactors were used for the controlled fermentations. The bioreactors, with a working volume of 7L, allowed the online measurement, monitoring and control (if specified) of temperature, aeration, rotation speed, pressure and pH. Additionally, the optical density probe allowed for the online monitoring and measurement of the total cell density during the ongoing fermentation. Cleaning and sterilization of the bioreactor are done in place (CIP and SIP).

All the different fermentation setups were performed in duplicate. The applied temperature profile consisted of pitching at 9°C and controlled linear temperature rise to 16°C in 72h and kept at 16°C until the end of the fermentation. Pitching was done with full volume of the 2nd propagation step in 6.50 L of fermentation medium in the bioreactor. pH was not adjusted during the fermentation, unless stated otherwise. Offline samples were taken two times per day (unless stated otherwise), for analysis of fermentation parameters as apparent extract, ethanol content, pH, cell count and viability – performed at Heineken Pilot Brewery facilities. Upon this general parameters, additional analysis of the fermenting

wort (2 times per day, unless stated otherwise) included: glucose, fructose, sucrose, maltose, maltotriose, acetaldehyde, dimethyl sulphide (DMS), acetone, ethylformiate, ethylacetate, methanol, ethylpropionate, propanol, isobutanol, isoamylacetate, amyl alcohols, ethylcapronate, total higher alcohols, diacetyl and 2,3-Pentanedione. All these analyses were performed by the Heineken Quality Assurance Laboratory (QAL).

Samples for RNA seq analysis and Cell Surface Hydrophobicity analysis were also performed. The times at which the samples were performed during the fermentations are depicted in table 1. During the ongoing fermentations, four samples for RNA sequencing analysis were taken, at previously defined time points. RNA and CSH samples were performed at the same times.

Fermentations for volume impact analysis: On this experiment, no samples were taken during the ongoing fermentations, in order to evaluate the impact of sampling volume on the OD profile and flocculation profile of the strains (table 2).

Fermentations for pH impact analysis: These fermentations were carried out in 50% Adjunct wort with pH controlled with automated addition of 2 M NaOH, in order to evaluate the impact of a higher pH on the OD profile and flocculation profile of the used strains (table 3).

Fermentations for increased nitrogen content impact analysis: These fermentations were carried out in 50% Adjunct wort with increased nitrogen content, in order to evaluate the impact of a higher initial nitrogen value in the OD and flocculation profile of the yeast strains (table 4). Fully prepared Adjunct wort was supplemented with 0.3 g.L⁻¹ of (NH₄)₂HPO₄ (VWR chemicals, Belgium).

Fermentations for different temperatures impact analysis: These fermentations were carried out in Heineken standard wort and the temperature was increased to 24°C or decreased to 12°C between the 118h and 198h of fermentation, and then set again to 16°C, in order to evaluate the impact of temperature on the OD and flocculation profile of the yeast strains (table 5).

Table 1 - RNA seq fermentations overview. Each fermentation setup was carried out in two bioreactors (in duplicate). Experiments ID, strains name, fermentation media, bioreactors names and time sample points (1st to 4th) are respectively depicted on the table.

| Experiment ID | Strain | Fermentation Media | Bioreactors names | 1 st sample | 2 nd sample | 3 rd sample | 4 th sample |
|---------------|--------|--------------------|-------------------|------------------------|------------------------|------------------------|------------------------|
| F19F | A | Full malt wort | R12 and R20 | 72 | 96 | 125 | 144 |
| F19F | B | Full malt wort | R21 and R31 | 67 | 91 | 120 | 144 |
| F19G | A | 50% Adjunct | R32 and R40 | 72.5 | 91.5 | 119 | 143 |
| F19G | B | 50% Adjunct | R41 and R10 | 67.5 | 96 | 119.5 | 144 |
| F19H | C | Full malt wort | R20 and R21 | 67.5 | 92 | 166 | 190.5 |
| F19I | C | 50% Adjunct | R10 and R11 | 73 | 98 | 123 | 170 |

Table 2 - Volume impact fermentations overview. Each fermentation setup was carried out in two bioreactors (in duplicate). Experiments ID, strains, fermentations media and bioreactors names are respectively depicted on the table.

| Experiment ID | Strain | Fermentation Media | Bioreactors names |
|---------------|--------|--------------------|-------------------|
| F19L | C | Full malt wort | R21 and R31 |
| F19L | C | 50% Adjunct | R40 and R41 |
| F19L | B | Full malt wort | R12 and R20 |

Table 3 - pH impact fermentations overview. Each fermentation setup was carried out in two bioreactors (in duplicate). Experiments ID, strains, fermentations media and bioreactors names are respectively depicted in the table.

| Experiment ID | Strain | Fermentation Media | Bioreactors names |
|---------------|--------|--------------------------|-------------------|
| F19K1 | C | 50% Adjunct pH corrected | R20 and R21 |
| F19K1 | B | 50% Adjunct pH corrected | R11 and R12 |

Table 4 - Nitrogen impact fermentations overview. Each fermentation setup was carried out in two bioreactors (in duplicate). Experiments ID, strains, fermentations media and bioreactors names are respectively depicted in the table.

| Experiment ID | Strain | Fermentation Media | Bioreactors names |
|---------------|--------|--------------------------------------|-------------------|
| F19K2 | C | 50% Adjunct with increased N content | R40 and R41 |
| F19K2 | B | 50% Adjunct with increased N content | R31 and R32 |

Table 5 - Temperature impact fermentations overview. Each fermentation setup was carried out in two bioreactors (in duplicate). The temperature profile applied to the bioreactor is depicted in the last column. Experiments ID, strains, fermentations media and bioreactors names are respectively depicted in the table.

| Experiment ID | Strain | Fermentation Media | Bioreactors names | Applied temperature at 118h-198h |
|---------------|--------|--------------------|-------------------|----------------------------------|
| F19L1 | B | Heineken standard | R11 and R12 | 12°C |
| F19L1 | B | Heineken standard | R20 and R21 | 24°C |
| F19L2 | C | Heineken standard | R31 and R32 | 24°C |
| F19L2 | C | Heineken standard | R40 and R41 | 12°C |

3.3. RNA sequencing analysis

The fermentation samples intended for RNA seq analysis were taken according to the protocol *P1: Cell sampling for micro arrays analysis from chemostat cultures* (M. Almering, 2003, TU-Delft) (Supplemental material) was followed. The sample volume was adapted to the actual study, according to the following equation: (Maarten and Verhoeven, 2013):

$$\text{Equation 4: } A = 9.32 \times 10^7 B - 3.77 \times 10^6$$

in which A represents cell concentration (cells/mL) and B the absorbance detected by the OD probe.

Equation 5 was applied to determine the required volume corresponding to 240 mg of biomass.

$$\text{Equation 5: } V = \frac{1.1 \times 10^{10} \times 0.24}{[C]}$$

The samples for RNA-seq analysis were immediately quenched in liquid nitrogen to avoid impact of sampling on the transcriptome. Samples were subsequently processed as depicted in *P1* protocol (Supplemental material). Due to the lower biomass content, the protocol was scaled down.

The RNA isolation and sequencing procedures were performed at BaseClear (Leiden, The Netherlands) and RNA was sequenced using the Illumina HiSeq sequencing platform (Illumina, San Diego, CA). Paired-end sequence reads were generated using the Illumina NovaSeq 6000. FASTQ read sequence files were generated using bcl2fastq2 version 2.18. Initial quality assessment was based on data passing the Illumina Chastity filtering. Subsequently, reads containing PhiX control signal were removed using an in-house filtering protocol. In addition, reads containing (partial) adapters were clipped (up to a minimum read length of 50 bp). The second quality assessment was based on the remaining reads using the FASTQC quality control tool, version 0.11.5. RNA sequences were statistically analysed by the service provider, including quality controls and reads quantification, which were mapped against the reference genome (A_v4). Effect of media and sampling times on the reads count was performed for all the three strains, as well as the differences between strains.

3.4. Cell Surface Hydrophobicity analysis

The samples for Cell Surface Hydrophobicity (CSH) analysis were taken from the fermentations for RNA sequencing analysis, at the same time points (table 1). Knowing the cell concentration at the sample time point (equation 3), the volume of sample was calculated, aiming for a total cell count of 1.00×10^9 cells per sample. Calculation is depicted on equation 6, in which V accounts for the sample volume in mL and $[C]$ accounts for the cell concentration in cells.mL⁻¹.

$$\text{Equation 6: } V = \frac{1 \times 10^9}{[C]}$$

The sampling procedure and afterwards sample processing was performed as described in protocol P2: *Cell Surface Hydrophobicity Measurement Protocol* (Supplemental material). Samples were kept in the freezer (-20°C) and stored in a 30% glycerol solution until subsequent CSH measurement, for a time no longer than 3 months. The CSH measurement applied is already described elsewhere (Kopecká and Němec 2015). The used technique is based on the MATH (microbial adhesion to hydrocarbons) (Grivet et al. 2000). Stored samples were thawed, and 1 mL of the total sample was washed with phosphate buffer (0.05M, pH 7), resuspended and diluted in phosphate buffer to an absorbance of 0.85 (I value) at 550nm. Forwardly, 400 µL of n-Hexadecane were added to 3 mL of the resultant cell suspension. Samples were vortexed for 30s, left standing for 5s and vortexed again for 30s. The phases were allowed to separate for 30 min, after which a 1mL sample (aqueous phase) was taken from under the meniscus. Its absorbance was measured (F value) at 550nm. The percentage of adhesion or the CSH was calculated as depicted in equation 7:

$$\text{Equation 7: } CSH(\%) = \left(1 - \frac{F}{I}\right) \times 100$$

Each sample was analysed in triplicate and a control was performed by measuring the OD at 550nm for a sample without n-Hexadecane.

3.5. Quality Analysis

Optical density, OD600, of the samples taken was measured directly through the glass surface using the BugLab's OD Scanner for shake flasks (BugLab LLC, Concord, CA). The pH was measured using the bench pH meter (inoLab® - WTW series). The Anton Paar density meter (Anton Paar GmbH,

Oosterhout, NL) was used to measure the alcohol content, density, original gravity (OG), real extract (RE) and apparent extract (AE), where the latest were expressed in Plato degrees (°P).

The analysis of total fermentable sugars – glucose, fructose, sucrose, maltose and maltotriose – was performed within the Sensory and Analytical Service and Research (SASR) of the Heineken Supply Chain, Zoeterwoude, The Netherlands. The sugars were analysed using the Ultra Performance Liquid Chromatography (UPLC) containing an Acquity UPLC BEH Amide 1.7 μm (2.1x150 mm) column, operating at 65 °C with a mobile phase made by 75% Acetonitrile / 25% milli Q H₂O and a flexible amount of TEA (average 0.05) at a flow rate of 0.2 mL/min.

4. Results

4.1. Flocculation Measurement Method

4.1.1. Non-volume changed fermentations: the proof of concept

In order to get a good comparison between the different fermentations, several tests were performed with a constant working volume. This was achieved by not taking samples during the fermentations. In this way, the position of the probe relative to the surface of the culture remained constant. Strains B and C were cultivated in Full malt wort and the OD was measured over time. The RS interval data points (fig. 10) were obtained and processed according to the formulations presented in section 2 of the Confidential Annex. This data was afterwards converged to averaged lines, which enabled an easier comparison between different fermentations (fig. 11).

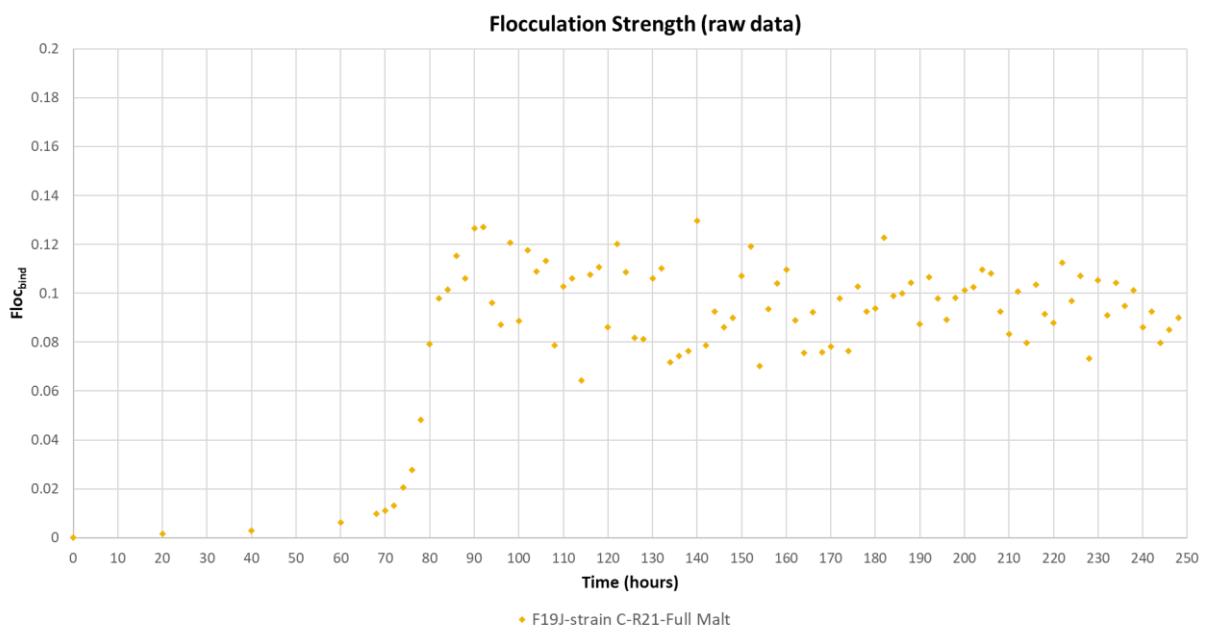


Figure 10 - Raw data points representative of the flocculation strength parameter, for the fermentation carried with strain C in Full malt wort without volume change (F19J series). Each point of the graph represents the calculated $Floc_{Cbind}$ value (equation C1) for each RS interval during the fermentation (phase 1) – Confidential annex, section 2.

Two important characteristics can be taken from the averaged plots (fig. 11): 1 – the onset of flocculation, time at which the $Floc_{Cbind}$ values sharply increase during the fermentations, and which correspond to the first inflexion point in the plots; 2 – the maximum flocculation strength, time at which the curves show a stable maximum value, which permits the comparison of the binding strength between the cells of the different strains. The data shows for both strains C and B a similar flocculation onset time at 75h of fermentation. Furthermore, the maximum flocculation strength value is also similar between both strains.

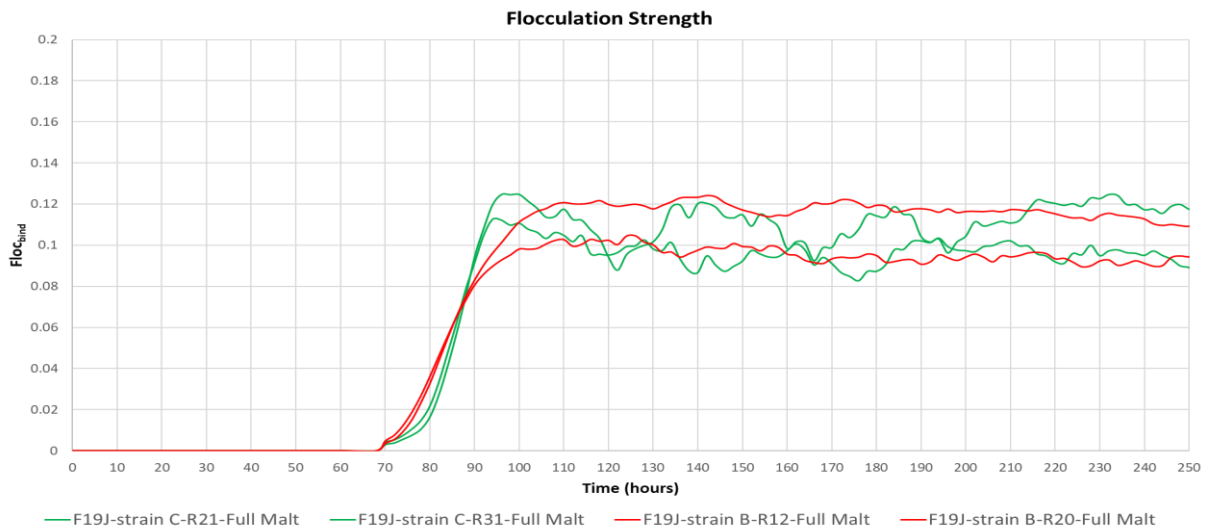


Figure 11 - Flocculation strength for the two tested strains B and C in Full malt wort composition. Fermentations carried out without volume change (F19J series). Each duplicate is represented with the same colour, but in two separate lines. Lines are derived from moving averages (period = 11) of each scatter plot (fig.10).

The second analysed parameter, linked to floc morphology, is shown on figure 12 for both C and B strains. Both strains show the same trend for the values obtained in the 2nd phase of the RS interval. An increase in the values is observed at the onset of flocculation for both strains. This increase reaches a plateau between 120-130 hours of fermentation, and the $Floc_{behav}$ values progressively decrease afterwards, until the end of the fermentation time. The connection of the obtained values to floc morphology points to more loose flocs formed by strain C cells in comparison to strain B cells. Towards the end of the fermentation, both strains cell flocs become progressively more compact.

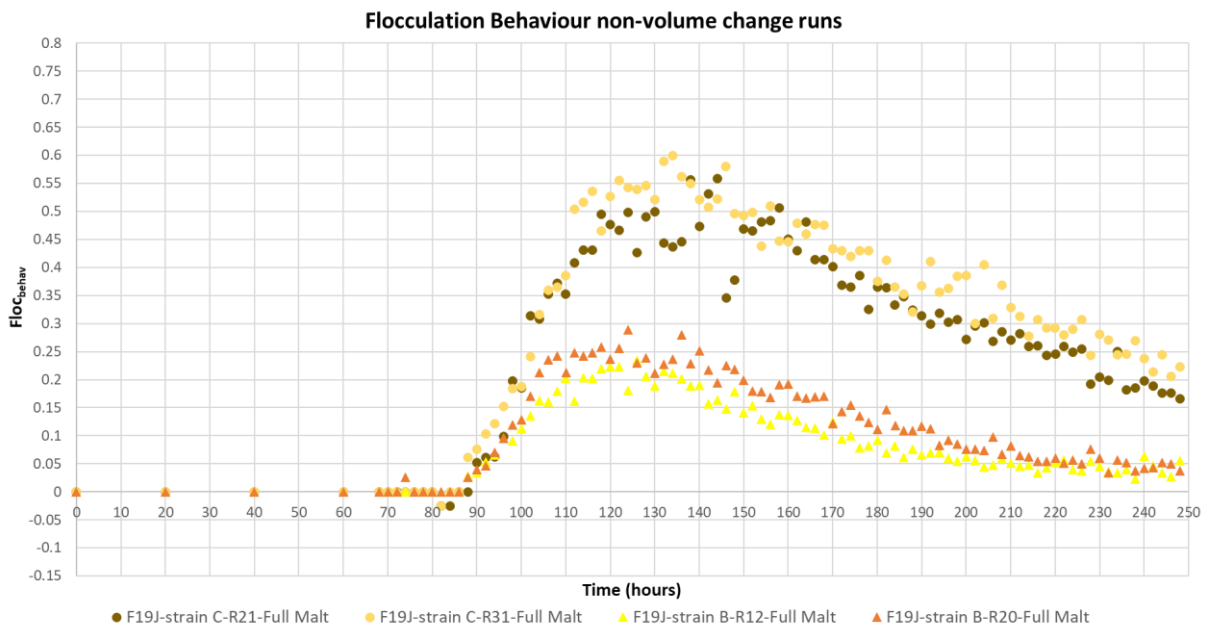


Figure 12 - Flocculation Behaviour graph for the non-volume change runs (F19J series). In the graph are represented strains B and C in Full malt wort. Each point of the graph represents the calculated $Floc_{behav}$ value (equation C2) for each RS interval during the fermentation (phase 2) – Confidential annex, section2.

4.2. – Temperature impact on flocculation

In order to understand the impact of temperature on the flocculation phenotype, different temperature profiles were applied. This set of fermentations was carried out in Full malt wort, and flocculent strains C and B were tested. The normal temperature profile applied for all the fermentations included a pitching temperature of 9°C, constant increase to 16°C for three days and maintenance of 16°C until the end of the fermentation. In the present section, the normal temperature profile was applied from the pitching phase until 118h of fermentation. At this time, temperature was either increased or decreased from 16°C to 24°C or 12°C, respectively. Those temperatures were maintained for 80 hours, and after this time the temperature was set to 16°C again. Close to 240h of fermentation, the bioreactors were cooled to 2°C, temperature that was maintained until the end of the fermentation.

No significant differences were found for the flocculation strength parameter for both strains, in response to the increased or decreased media temperatures (fig. S5). Flocculation onset and maximum flocculation strength remained almost unaltered, in response to the different temperature profiles. For strain C (fig. S5 b), it's observable a slight increase in the $Floc_{bind}$ values, as the temperature is increased to 24°C. The $Floc_{bind}$ values stop increasing as the temperature is normalized to 16°C.

The flocculation behaviour of both strains' cells was not significantly altered by changes in temperature applied to the fermentation media (fig. S6). For strain B, $Floc_{behav}$ values do not present significant differences in response to increase or decrease of the temperature (fig. S6 b). For strain C, no significant differences are observable as well (fig. S6 a), and a duplicates variation is observed. No conclusions regarding the shape of the flocs can be taken, regarding the temperature differences on the media.

Figure 13 depicts the OD trends of C and B strains in the temperature increased and decreased fermentations, as well for the normal temperature setups (Full malt wort, section 3). In all the performed fermentations (see next sections), as the cell populations achieved the stationary phase, different OD values were observed, in relation to the normal temperature profiles. For both B (fig. 13 a) and C (fig. 13 b) strains, the increase in temperature resulted in a more pronounced decrease in the measured OD. The decrease in temperature imparted the completely opposite scenario: as the temperature was decreased, a less pronounced decrease in OD is observed in relation to the normal and increased temperature setups. Finally, at 240h of fermentation, the bioreactors were cooled down to 2°C, which clearly imparted an increase in OD values, for both strains.

4.3. – Full malt wort vs Adjunct wort: different media impact on flocculation

The use of Adjunct wort formulations in breweries is already a practice worldwide. However, a deeper understanding of its impact on the flocculation characteristics of the different strains is emergent. Better prediction of the flocculation onset and characteristics might be achieved by its investigation. To do so, A, B and C strains were tested in two different wort types – full malt wort and 50% Adjunct wort. Zinc and Calcium levels were corrected for the 50% Adjunct wort solution, but calcium levels were still lower in 50% Adjunct (33mg.L⁻¹) than in full malt wort (45mg.L⁻¹). The flocculation characteristics of the three strains were followed during such experiments. In addition, genetic and physical state analysis of the

cells was also performed, by following gene expression and evolution of the cell surface hydrophobicity of the cell populations.

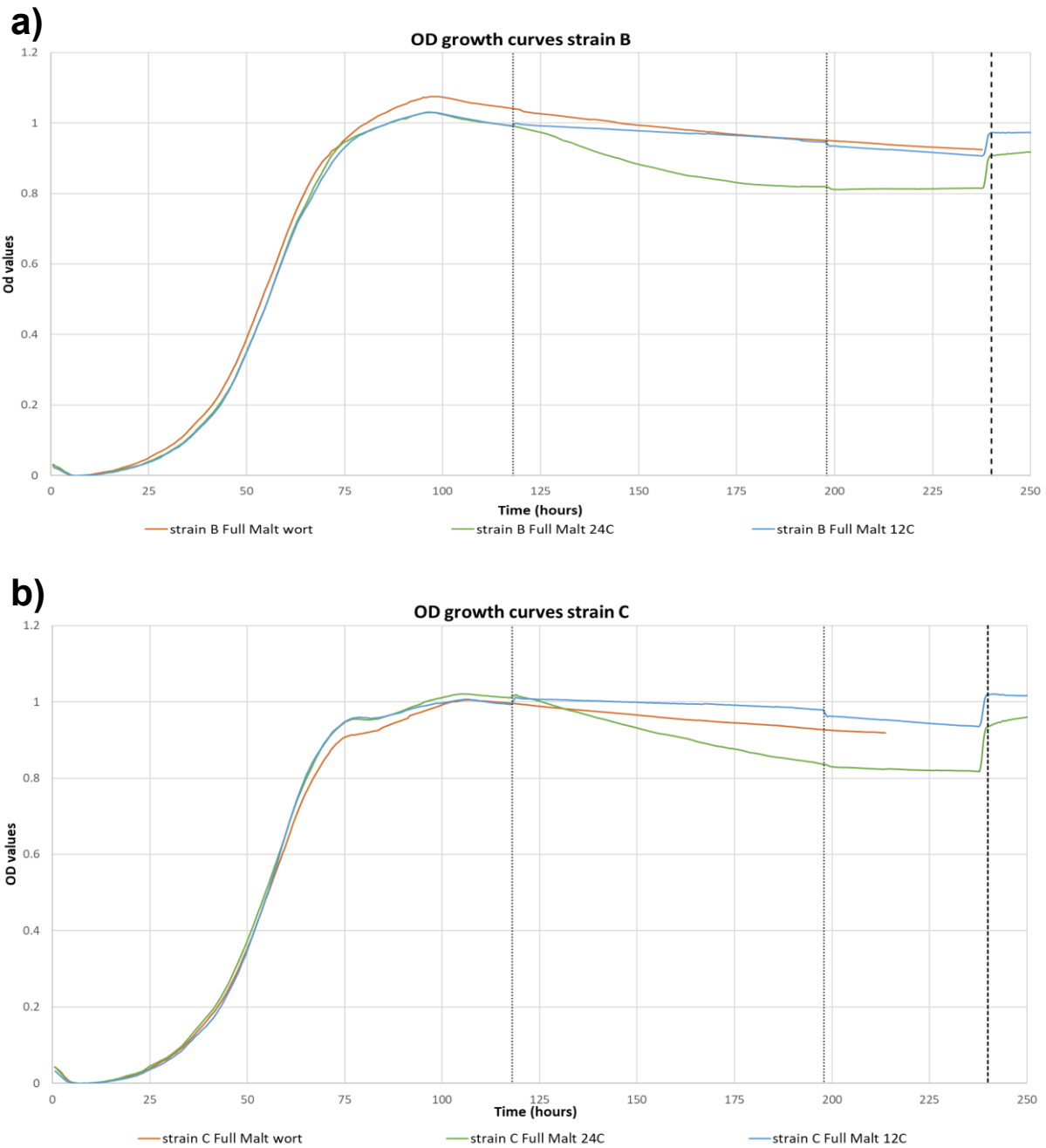


Figure 13 - OD growth curves of the tested B (a) and C (b) strains in Full malt wort, for the temperature changed fermentations (F19L series). The two dotted vertical lines represent the times in the fermentations at which the temperatures were either increased or decreased. The last stringed vertical line represents the time in the fermentation at which the temperature was decreased to 2°C, in all fermentations. Only one curve per duplicates fermentation is presented, since duplicates presented similar curves. Values were normalized.

The analysis of the flocculation strength and flocculation behaviour – flocculation phenotype parameters determined and mathematically developed in section 1 of the results – permitted to achieve better insights regarding the impact of different wort compositions in flocculation. Fermentations using

A, B and C strains were performed in full malt wort and 50% adjunct wort formulations. On these fermentations, multiple samples were performed. Such samples were subject to analysis of sugars consumption and ethanol production, gene expression profiles and evolution of cell surface hydrophobicity. For gene expression analysis, four samples at different cell population growth phases were performed by cell quenching in liquid nitrogen and subsequent storage for further processing (section 7). For the analysis of the cell surface hydrophobicity, samples were taken and immediately stored at -20°C, aiming to later processing (section 6).

In figure 14 is depicted the flocculation strength of each strain in each fermentation media, with the duplicates also discriminated. Strain A, the least flocculent strain, showed almost no flocculation in both wort compositions. In the flocculation strength graphs (fig. 14) the $Floc_{bind}$ values of strain A cells never surpasses 0.02. This value was set as the threshold flocculation value, below which no real flocculation is ongoing, but only single cell sedimentation is taking place.

Both strains B and C present maximum strength values higher in 50% Adjunct wort than in full malt wort. In the full malt wort media, both B and C strains present higher duplicate variation, than in 50% Adjunct wort. Strain B always presents a slightly lower flocculation strength than strain, in each wort type (fig. 14). The flocculation onset of strain C in Adjunct wort is the latest of all the experiments (between 100-110h), presenting a 30h delay in comparison with Full malt wort (75h). It also presents the highest maximum flocculation strength of all the strains as well. Strain B starts to flocculate earlier (65h) in 50% Adjunct wort, in comparison to Full malt wort (75h) (fig. 14). Strikingly, an opposite behaviour is presented by C and B strains: strain C cells start to flocculate earlier in Full malt wort than in 50% Adjunct wort, while B strain cells flocculate earlier in 50% Adjunct wort than in Full malt wort.

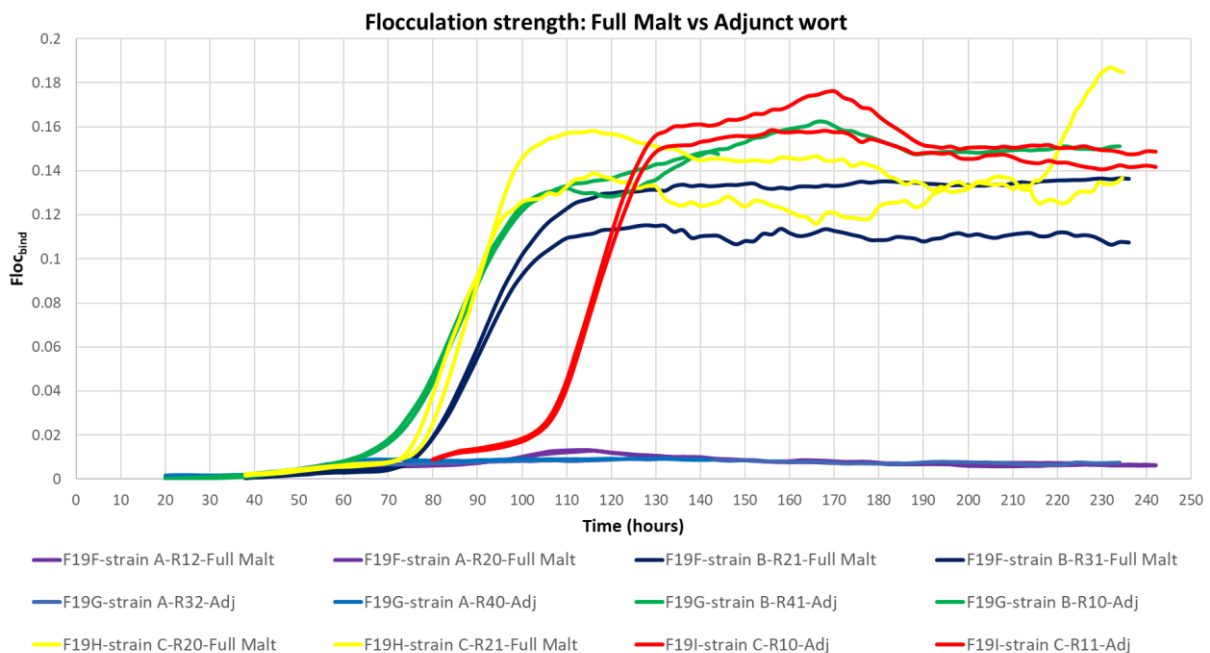


Figure 14 - Flocculation strength graph for the three tested strains – A, B and C – in the two different wort compositions – Full malt wort and 50% Adjunct wort (F19F, F19G, F19H and F19I series). Each duplicate is represented with the same colour, but in two separate lines.

The flocculation behaviour of the two flocculent strains B and C also presents evident differences between each other, and among the two different wort compositions (fig. 15). For this parameter,

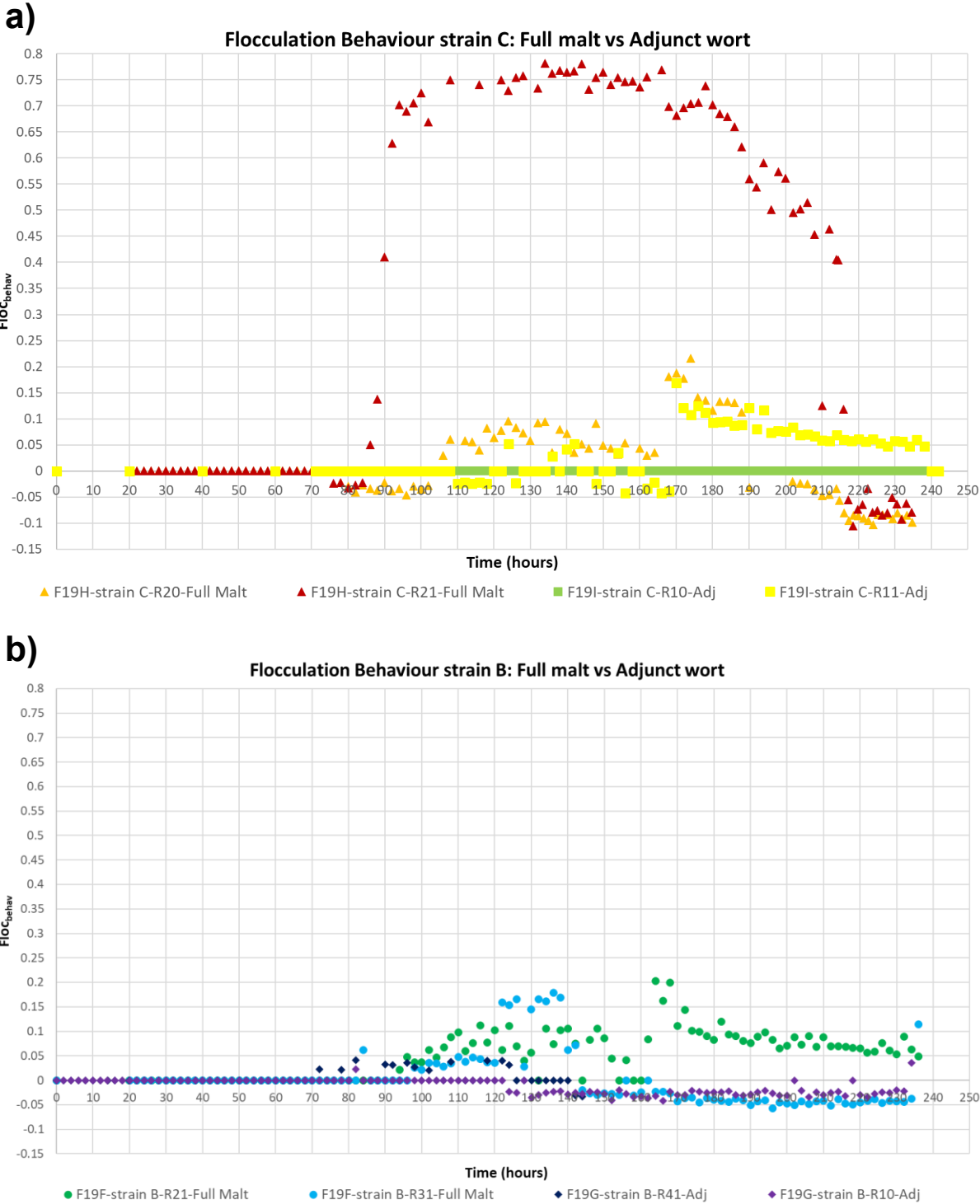


Figure 15 - Flocculation Behaviour of strains C (a) and B (b) in each fermentation media, Full malt wort and 50% Adjunct wort (F19F, F19G, F19H and F19I series). Strain A values are not depicted, since it represents the negative control (Flocculation Behaviour values = 0).

significant duplicates variation is observed for strain C in Full malt wort: extremely high values for $Floc_{behav}$ observed in reactor 21, but lower values in reactor 20. Besides it, and using the F19J series

results as template (section 4.1.1.), the evolution of the flocculation behaviour parameter is similar throughout the fermentation: an increase in $Floc_{behav}$ values as the flocculation onset occurs, the achievement of maximum values between 100-140h of fermentation, and $Floc_{behav}$ values decrease afterwards, towards the end of the fermentation. Higher values for this parameter are achieved by C strain in Full malt wort, than B strain in the same wort composition (fig. 15). C strain presents a great difference of flocculation behaviour values, regarding the different wort compositions. In 50% Adjunct wort, much lower $Floc_{behav}$ values are observed, than in Full malt wort for this strain. Both strains present similar flocculation behaviour results, for the 50% Adjunct wort type (fig. 15). For B strain, differences between the duplicates in Full malt wort composition are also visible. Strain B in reactor 21 presents positive values – but never as high as C strain – and in reactor 31 presents negative values (fig. 15 b). In the overall, the confidence of the non-volume change runs for this parameter is higher, with more consistent results between the duplicates.

Sugars and ethanol in media are known to have impacts on the flocculation capacity of yeast cells (Miki et al. 1982; Claro et al. 2007), as well as environmental pH (Stratford 1996). Sugars consumption (fig. 16), pH evolution and alcohol production (fig. 17) present differences among the different strains and media. Due to the similar trends in each fermentation duplicate, results were averaged for the two independent fermentations of each fermentation setup (strain + wort type). Sugar consumption for the 3 strains in both wort compositions are described in figure 16. Sucrose initial values for the 50% Adjunct wort compositions are similar among the 3 strains fermentations (fig. 16 c). An abrupt decline in its concentration is observed, due to its conversion to glucose and fructose, which can be seen by the increase of the concentration of both sugars between the beginning of the fermentations and 70h of running experiments. In the 50% Adjunct wort composition, different glucose and fructose concentrations are observed at the second sample point for C, B and A strain (ordered by decreasing concentrations). Those different concentrations, regarding the similar concentrations of initial sucrose, suggest that the consumption of fructose and glucose seems to be faster for A strain, followed by B and C strains with a slower consumption of both sugars. C strain also totally consumes fructose and glucose later than B and A strains, in 50% Adjunct wort composition (fig. 16 a and b).

In Full malt wort, similar trends for the three strains are visible, in relation to glucose, fructose and sucrose evolution. The difference depicted in the graphs must be an artefact of the lack of sample points for A and B strains (fig. 16 a, b and c). Maltose and Maltotriose initial concentrations are very similar in Full malt and 50% Adjunct wort fermentations, for all the three strains (fig. 16 d and e). Half of the concentrations of those sugars are found in Adjunct wort, in comparison with Full malt wort, due to the 50% dilution of Full malt wort with sucrose solution. The sugar consumption of maltose and maltotriose seems to be similar for the three strains, in Full malt wort composition. An evident difference is found in maltose and maltotriose consumption in 50% Adjunct wort, comparing strain C with B and A strains (fig. 16 d and e). Strain C presents a faster and higher consumption of both sugars, reaching the end of the fermentation with lower concentrations than the other two strains. The difference is more evident for maltose final concentrations (fig. 16 d) than for maltotriose final concentrations (fig. 16 e). Finally, the total fermentable sugars follow similar trends in Full malt wort for all the three strains, and the final concentrations in Adjunct wort reflect the different maltose and maltotriose consumptions of strain C and

both A and B strains (fig. 16 f). Strain C presents a lower concentration of final total fermentable sugars than A and B, correlating with the lower maltose and maltotriose concentrations as well.

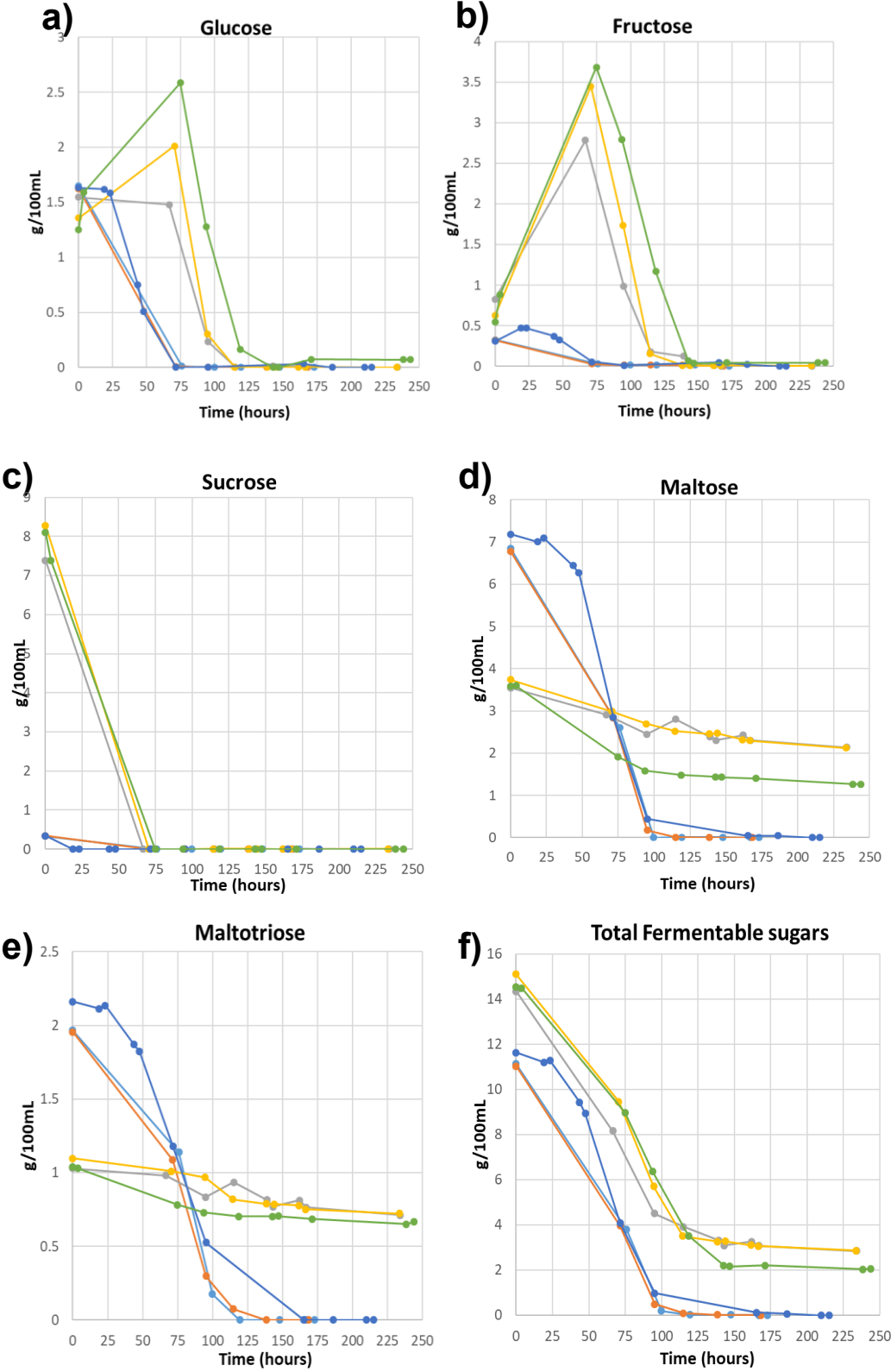


Figure 16 - Sugars (glucose, fructose, sucrose, maltose, maltotriose and total fermentable sugars) consumption trends correspondent to the Full malt and 50% Adjunct wort fermentations (F19F, F19G, F19H and F19I series). Each line corresponds to the average values of two independent fermentations. Legend: — strain A Full Malt — strain B full Malt — strain A Adj — strain B Adj — strain C Full Malt — strain C Adj

The different sugar consumption profiles presented by the three strains in Adjunct wort composition is reflected on the alcohol production profiles in this fermentation media (fig. 17 b). Strain C presents the highest production of ethanol in Adjunct wort, by comparison with strains A and B in the same wort. In full malt wort, the three strains all produce similar amounts of ethanol. pH trends are very similar for the three strains in each wort type, with lower pH being achieved in Adjunct wort fermentations (around 3.5) comparing with full malt wort (around 4). In both wort types, after pH achieves a minimum at approximately 100 hours of fermentations, a slow increase is depicted for both wort compositions and all the three strains (fig. 17 a).

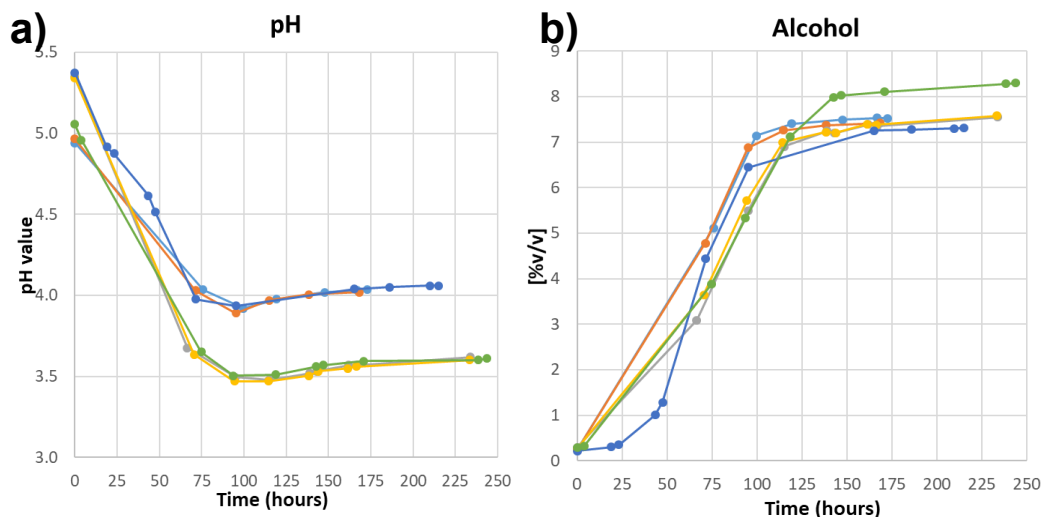


Figure 17 - pH evolution and alcohol production trends in Full malt and 50% Adjunct wort fermentations (F19F, F19G, F19H and F19I fermentations). Each line represents the averaged values of two independent fermentations. Legend: —●— strain A Full Malt —●— strain B full Malt —●— strain A Adj —●— strain B Adj —●— strain C Full Malt —●— strain C Adj

The OD growth profiles of each strain in each fermentation media are depicted in figure 18. Since the OD probes measure the cell density inside the bioreactors, correlations between the OD values and biomass inside the bioreactors might be possible. For both wort types, strain A always presents the higher OD values, with longer exponential phases than strains C and B. However, a decrease in exponential growth slope is visible in Adjunct wort composition for strain A, and a lower maximum OD value is reached. Strain C, conversely, presents a longer growth in OD, reaching the stationary phase later in Adjunct wort than in full malt wort. However, the maximum OD does not significantly differ for this strain, for both wort types. Finally, strain B presents a higher increase in OD in full malt wort than in Adjunct wort, with a longer deceleration phase occurring in Adjunct wort fermentation media.

4.4. – Adjunct wort pH-controlled fermentations

The goal of this set of fermentations was to know whether a change in the pH value throughout the fermentation would impart differences in the flocculation phenotype showed by the strains. Since the pH in normal Adjunct wort always declines for values around 3.5, the pH was controlled to pH 4.0, by addition of NaOH. The alkaline agent was added in a way that a pH pattern similar to a full malt wort fermentation would be observed in the Adjunct wort composition. The calcium levels on these fermentations were similar to the normal Adjunct wort fermentations (Table S1).

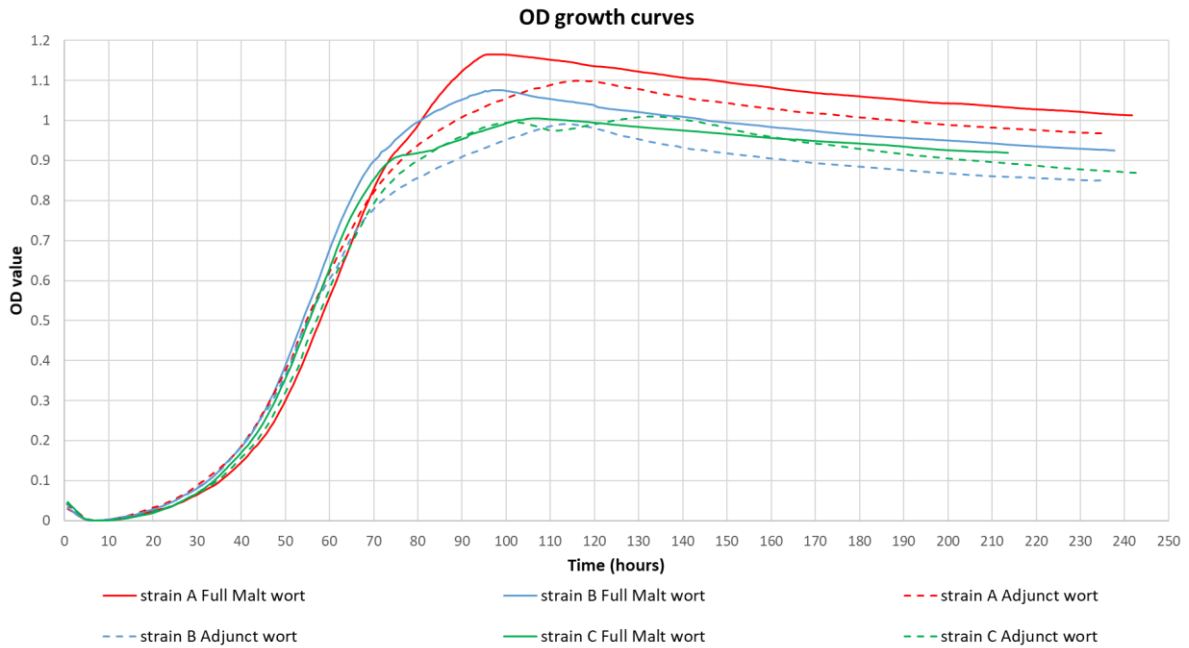


Figure 18 - OD growth curves of the tested strains in Full malt and 50% Adjunct wort fermentations (F19F, F19G, F19H and F19I fermentations). Only one curve per duplicate fermentation is presented, since the duplicates presented similar curves. Values were normalized.

The increased pH value of the fermentation media incremented the flocculation strength values of both B and C strains (fig. 19), and imparted profound changes on the phase 2 measurements of the RS intervals, which are associated with floc morphology (fig. 20).

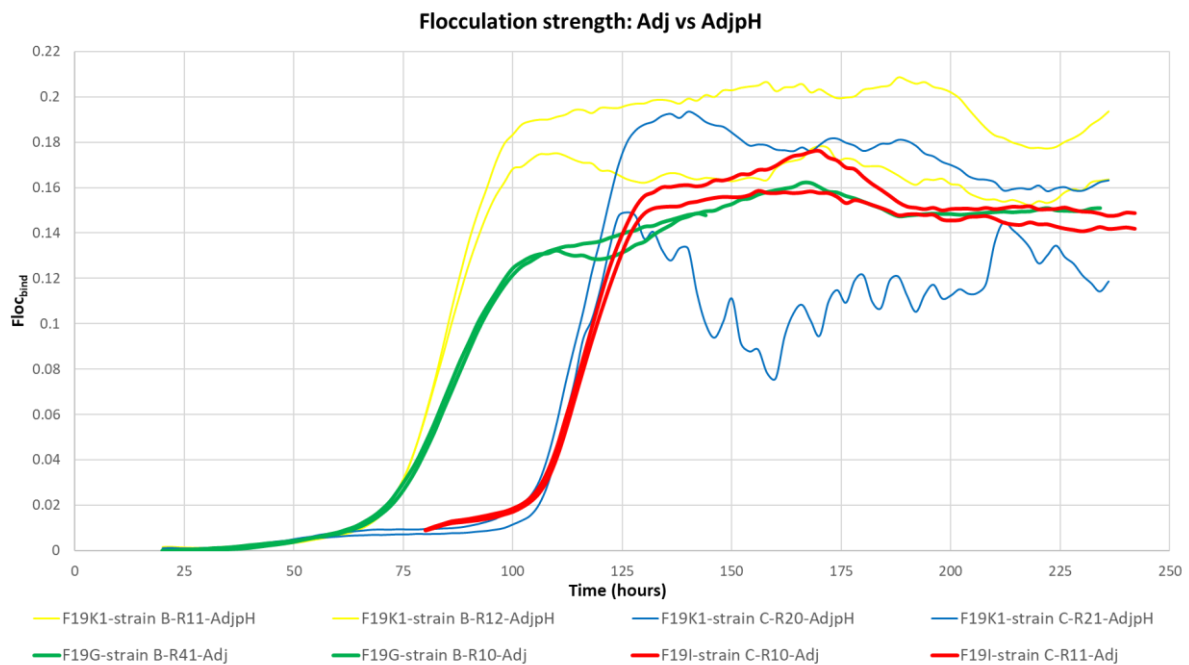


Figure 19 - Flocculation strength graphs for strains C and B in 50% Adjunct wort and 50% Adjunct wort pH corrected. Each duplicate fermentation is represented with the same colour, in two separate lines.

Regarding the flocculation onset of both strains, the changes in the pH value did not impart any difference. Both C and B strains started to flocculate at the same times as they would in non-pH controlled Adjunct wort fermentations. For the B strain, the increased pH values imparted interesting differences on the maximum flocculation strength of this strain. The maximum $Floc_{bind}$ values were higher in pH-controlled adjunct wort fermentations, in comparison with the normal adjunct wort formulations. For strain C, a striking difference in the flocculation strength is observed between both duplicates for the pH - controlled fermentations (fig. 20). However, focusing on the duplicate which achieved the higher values for the flocculation strength, it is possible to see that the increase in pH also imparted an increased maximum flocculation strength for the C strain. In section 3, results showed higher flocculation strength values in Adjunct wort in comparison to Full malt wort. In the present section, results show that flocculation extent values are even more incremented in relation to the two previous wort formulations, by increasing the pH value in Adjunct wort (fig. 20). This observation loses validity for strain C due to low quality of the duplicates.

pH - increase of Adjunct wort imparted striking differences on the flocculation behaviour parameter values. For both strains, a duplicate variation is observed (fig. 20). For B strain, an increase in positive values is observed, a few hours after the flocculation onset (fig. 20 a). Comparing with the non-volume change fermentations (F19J series, section 1.3), a similar trend is observed, with a sharp increase of the $Floc_{behav}$ values after the flocculation onset until 120-130h of fermentation, and a progressive decrease afterwards. It seems that B strain in pH increased adjunct wort adopts a similar floc morphology trend, as the one observed in Full malt wort composition: flocs get looser in the first 40h of active flocculation, becoming afterwards more compact towards the end of the fermentation.

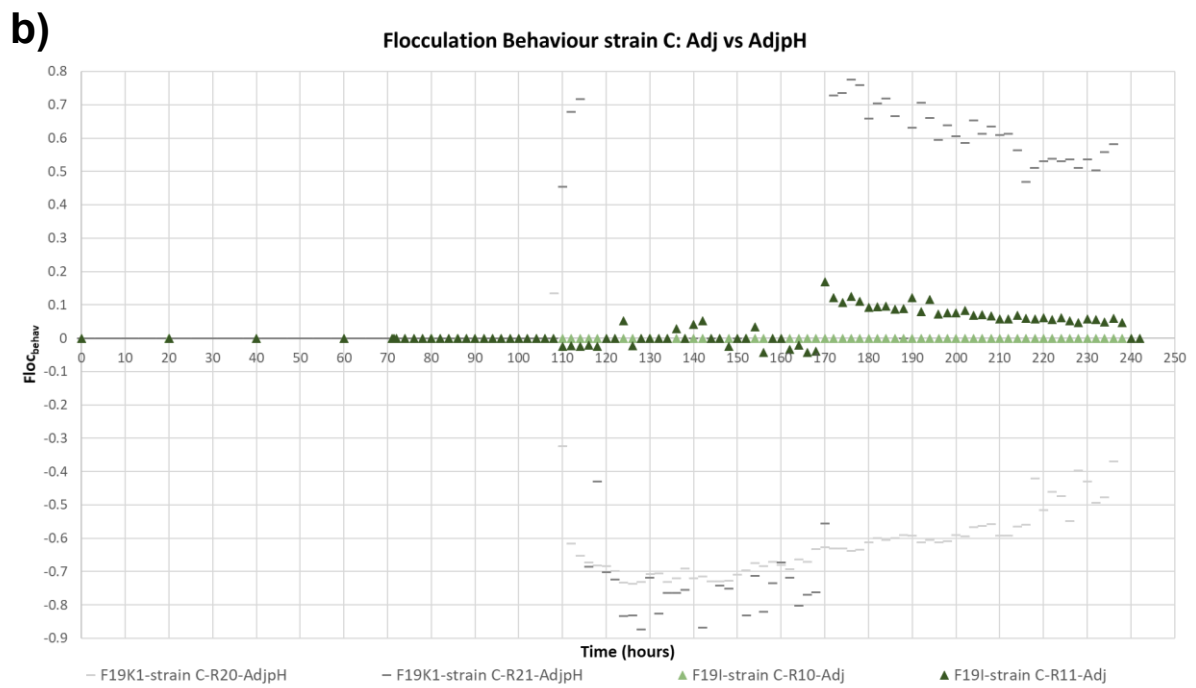
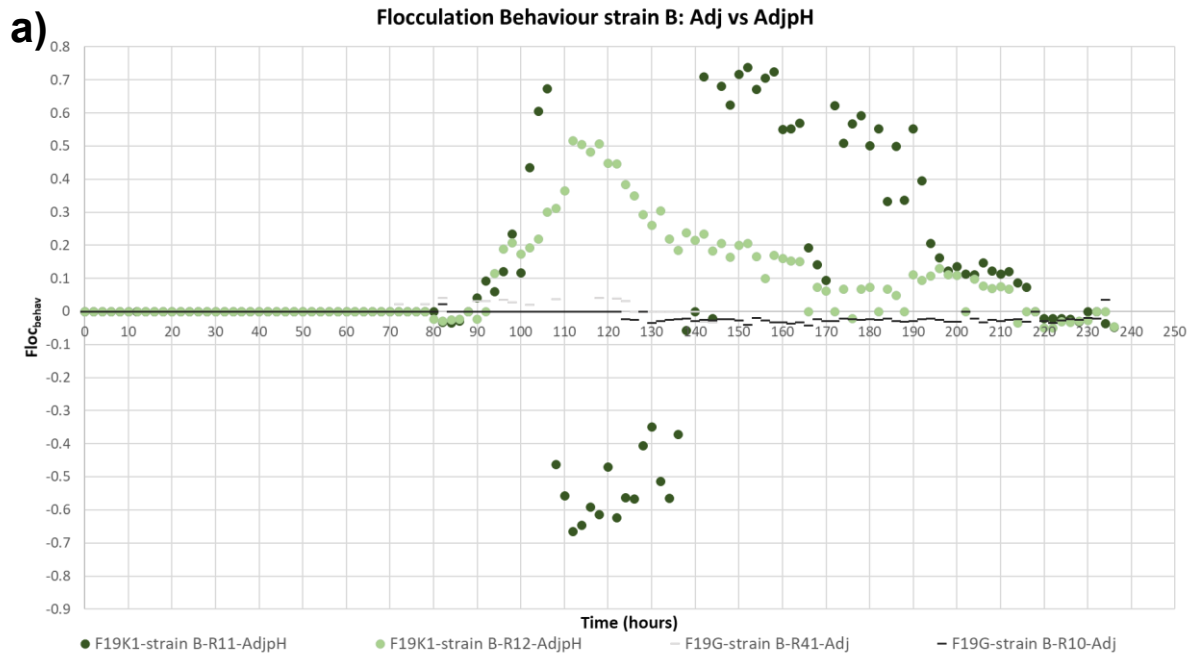


Figure 20 - Flocculation Behaviour graphs for B (a) and C (b) strains in 50% Adjunct wort (F19G and F19I series) and 50% Adjunct wort pH corrected (F19K1 series).

Strain C presented a great variation between duplicates (fig. 20 b). In reactor 20 shows highly negative values during all the fermentation. In reactor 21, opposite values are observed, unless between 110-170h of fermentation, in which negative values like the other duplicate are observed. Hypothesis regarding this experiment are consequently difficult to derive, since the quality of the data is not good.

In the Adjunct wort pH-controlled fermentations, the results for the sugar consumption and alcohol production were very similar to the trends observed for the RNA-seq fermentations (fig. S7). The growth curves presented also small differences on this fermentation sets, in comparison with the fermentations in normal Adjunct wort composition (fig. 21).

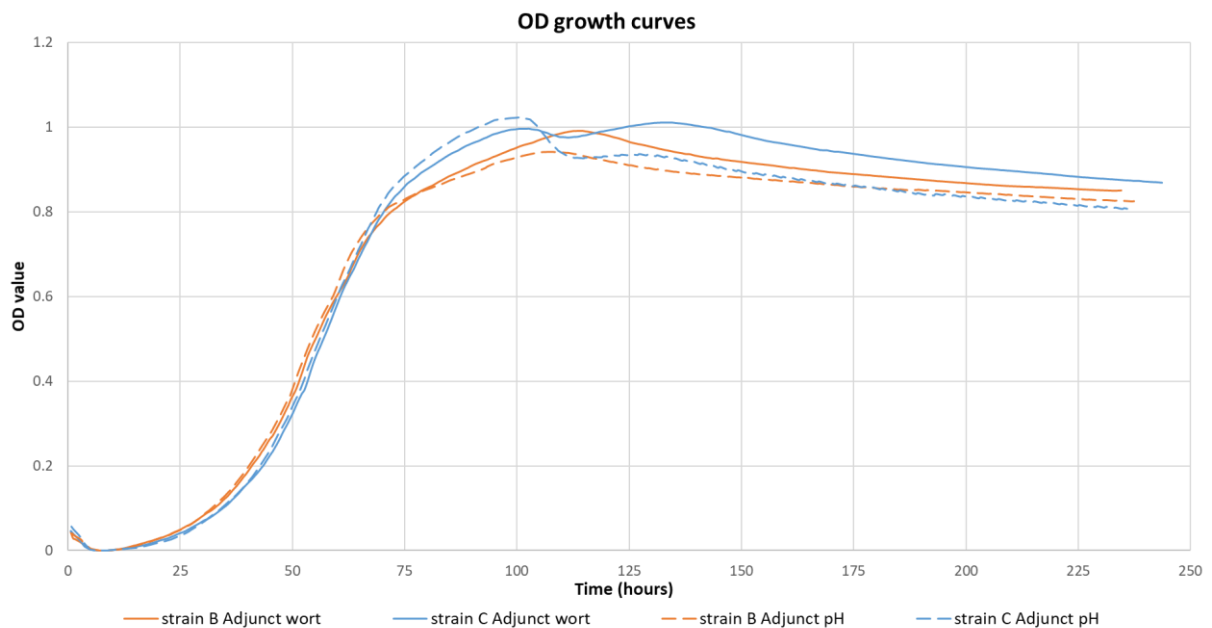


Figure 21 - OD curves for both C and B strains in normal Adjunct wort (F19G and F19I fermentations) and in Adjunct wort pH corrected (F19K1 fermentations). Only one curve per duplicate fermentation is presented, since duplicates presented similar curves. Values were normalized.

The pH profiles in the Adjunct wort pH-controlled fermentations are depicted in figure 22. Adjunct wort pH-controlled fermentations were successfully controlled, taking in mind the objective of ensuring a similar pH pattern as the one observed for the Full malt wort fermentations.

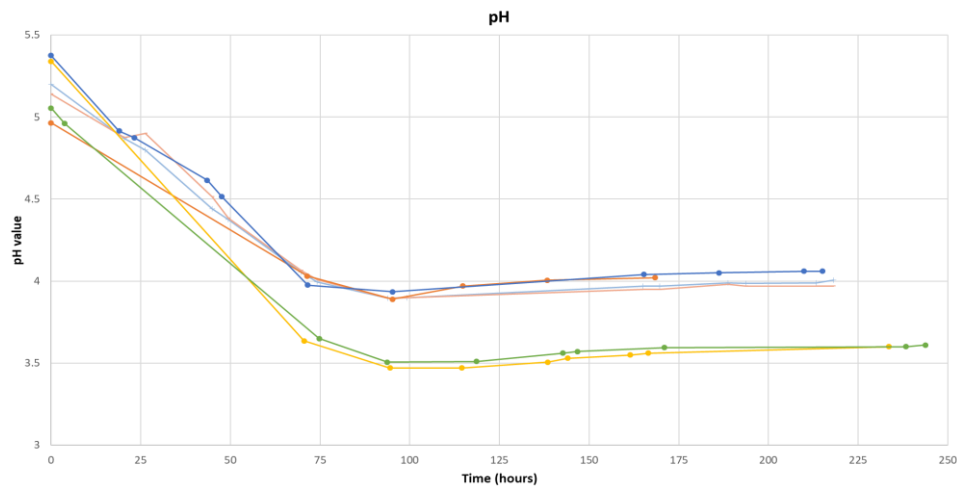


Figure 22 - pH profiles comparison for the Full malt wort (F19F and F19H series), 50% Adjunct wort (F19G and F19I series) and 50% Adjunct wort pH controlled (F19K1 series) for the strains C and B. Legend: — strain B Adj pH — strain C Adj pH — strain B Full Malt — strain B Adj — strain C Full Malt — strain C Adj

4.5. Adjunct-wort fermentations with higher initial nitrogen content

As influence of the 50% dilution of Full malt wort with a sucrose solution, to make a 50% adjunct wort, a 50% decrease in the Total Nitrogen and Free Amino Nitrogen is observed in the Adjunct wort configurations (Table S1). In this way, the goal of this fermentation sets was to evaluate the impact of nitrogen supplementation of normal Adjunct wort with Di-ammonium phosphate, which functions as an ammonia nitrogen source for the growing yeast. The results showed profound effects, not only regarding the flocculation phenotype showed by C and B strains, but as well on the sugar consumption and alcohol production. The calcium levels of the nitrogen supplemented Adjunct wort were lower than the normal full malt wort fermentations (Table S1).

Two important changes occurred in the flocculation strength of C and B strains, while the wort was supplemented with a nitrogen source: 1) the flocculation strength significantly reduced with the supplementation of DHAP for both strains and 2) the onset of flocculation was significantly delayed for B strain, with the supplementation of nitrogen (fig. 23). B strain cultivated in Adjunct wort with additional nitrogen content showed an increase in $Floc_{bind}$ values at the same time as in the normal Adjunct wort configuration. However, this small increase is followed by a decrease to base levels, and the actual flocculation onset is achieved at around 112h of fermentation. Not only the flocculation onset is later, but also the increase to the maximum flocculation strength is slower, and much lower $Floc_{bind}$ values for this parameter are achieved – around 0.1, contrarily to normal Adjunct wort, which achieves 0.16. In the case of strain C, the flocculation onset is not significantly altered, and the increase to its maximum value is not increased or decreased (fig. 23). However, a significant decrease in the maximum flocculation extent is observed, with a variation of around 0.16 in normal Adjunct wort, to 0.11 in Adjunct wort supplemented with nitrogen. Regarding the flocculation behaviour for both strains, no significant differences were found between the normal Adjunct wort configurations and Adjunct wort supplemented with nitrogen (fig. S8).

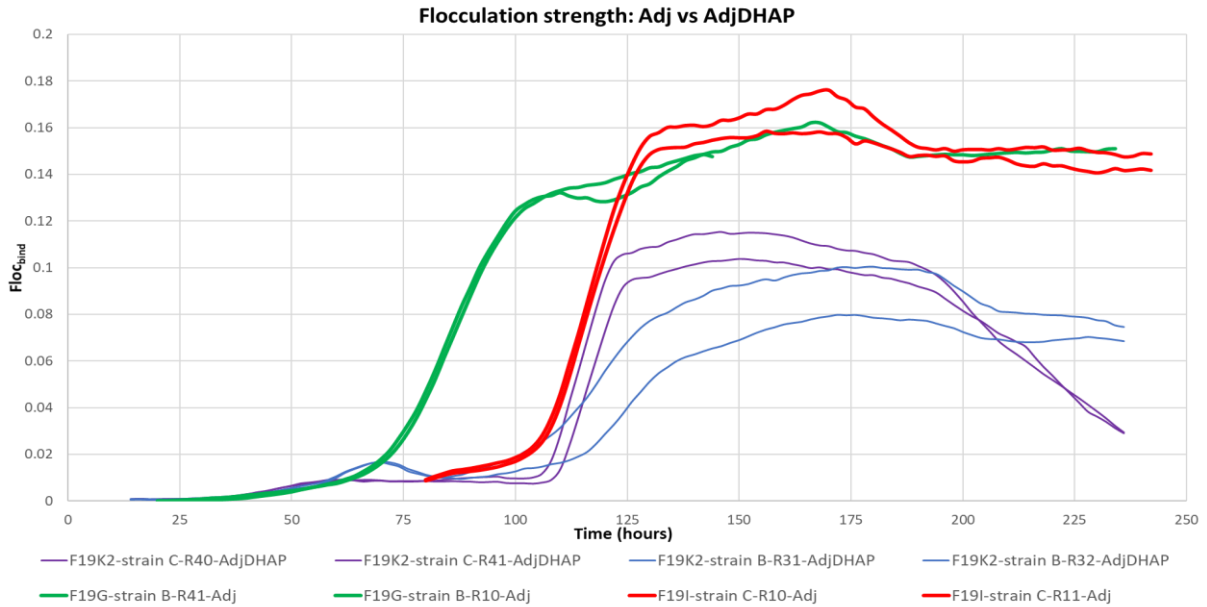


Figure 23 - Flocculation strength graphs of C and B strains for the normal Adjunct wort fermentations (F19G and F19I series) and nitrogen supplemented Adjunct wort fermentations (F19K2 series).

The analysis of the sugar consumption profiles did not show a significant difference regarding the sugar concentration patterns of sucrose, glucose and fructose, presenting similar patterns to the normal Adjunct wort configuration (fig. S9). However, the consumption of maltose and maltotriose – and, consequently, the Total fermentable sugars concentration – presented a shift between both wort types.

Regarding strain B, an increased consumption of maltose and maltotriose was observed (fig. 24 a and b). The analysis of the initial concentrations of both sugars also shows a decreased value for the nitrogen supplemented Adjunct wort. However, before the wort is pitched, it is analysed for the sugars present. The values for the sugars concentrations before pitching are similar to the initial sugar concentrations for the normal Adjunct wort fermentations (Table S1). In this way, the lower values for maltose and maltotriose concentrations for strain B fermentations are a result of a higher consumption of those sugars. The final values for maltose concentrations are 12.5 g/L in the nitrogen supplemented Adjunct wort, much lower than the above 20g/L values in normal Adjunct wort (fig. 24 a).

In the same way, the final values for maltotriose concentrations are 6g/L in nitrogen supplemented Adjunct wort, lower than the 7.5 g/L concentration in the normal Adjunct wort configuration (fig. 24 b). Subsequently, the values for the final total fermentable sugars differ from 2 g/L in nitrogen supplemented Adjunct wort, to almost 3 g/L in normal Adjunct wort (fig. 24c).

Strain C presented similar results to strain B for sugars consumption, but the differences from Adjunct wort to nitrogen supplemented wort are not as dramatic as for strain B. The total fermentable sugars graph presents only a slightly lower concentration for the final sample, in comparison with normal Adjunct wort (fig. 24 c).

As result from the different sugar consumption patterns and extents at the different wort compositions, different alcohol production and pH trends are also observable (fig. 24 d and e). In fact, the decrease in pH for the nitrogen supplemented wort is higher, probably result of a higher sugar consumption and so higher fermentation rate. The pH values in normal Adjunct wort never dropped below 3.5 value, whereas for nitrogen supplemented wort, a 3.3 value was achieved (fig. 24 d). Regarding the alcohol production, no great difference is observed from nitrogen supplement wort to the normal Adjunct wort, for strain C. However, more alcohol is produced by B strain, in the nitrogen supplemented Adjunct wort configuration (fig. 24 e).

Finally, the OD trends also present differences among both strains and wort types (fig. 25). For both C and B strains, increased OD values are achieved in the nitrogen supplemented wort configuration. Deceleration phases of both strains in nitrogen supplemented Adjunct wort depict higher slope. Strain B achieves the higher OD values of all the fermentations, in nitrogen supplemented Adjunct wort.

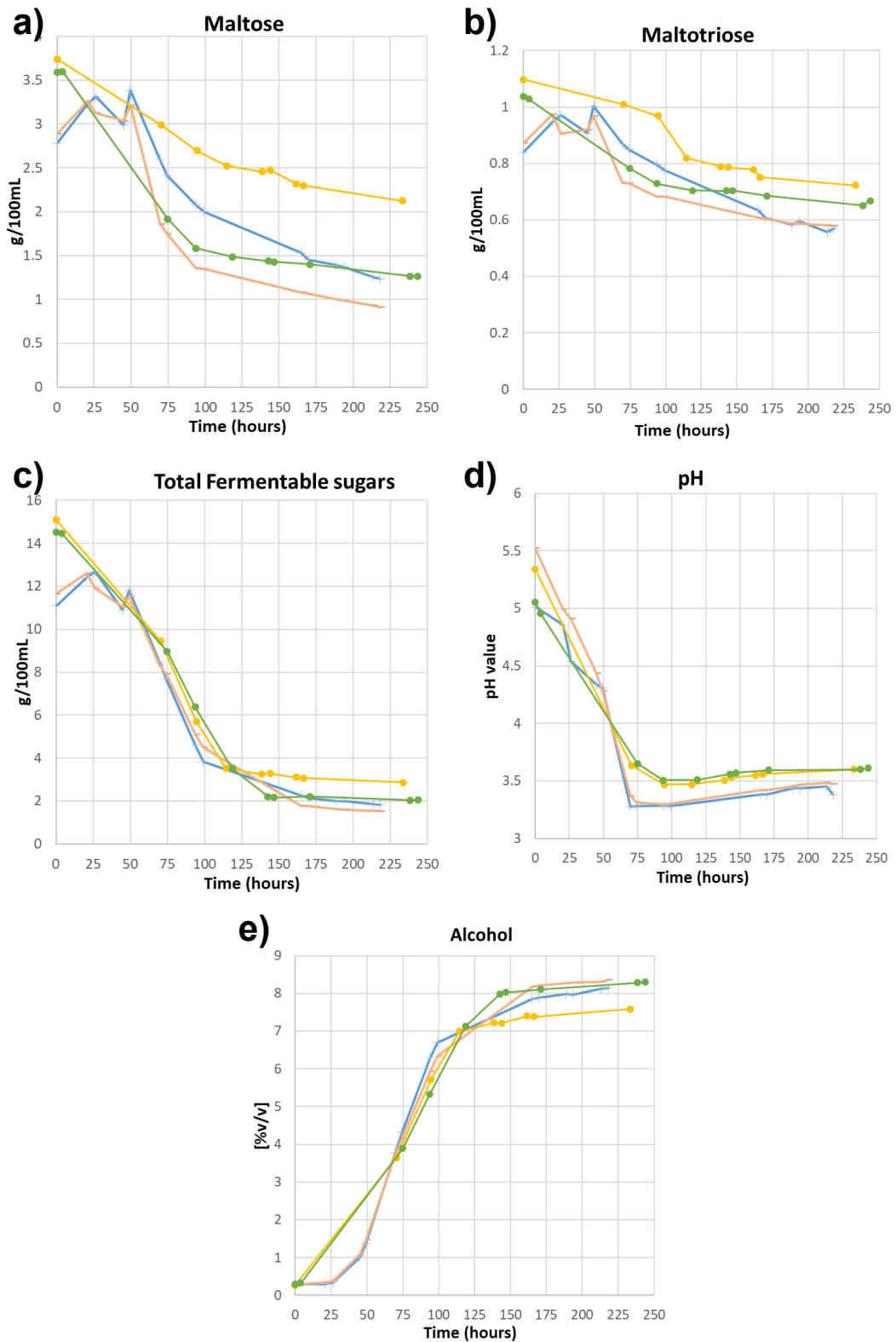


Figure 24 - Sugars (maltose, maltotriose and total fermentable sugars) consumption, ethanol production and pH profiles on normal Adjunct wort (F19G and F19I series) and nitrogen supplemented Adjunct wort (F19K2 series) for B and C strains. Legend: — strain B AdjDHAP — strain C AdjDHAP — strain B Adj — strain C Adj

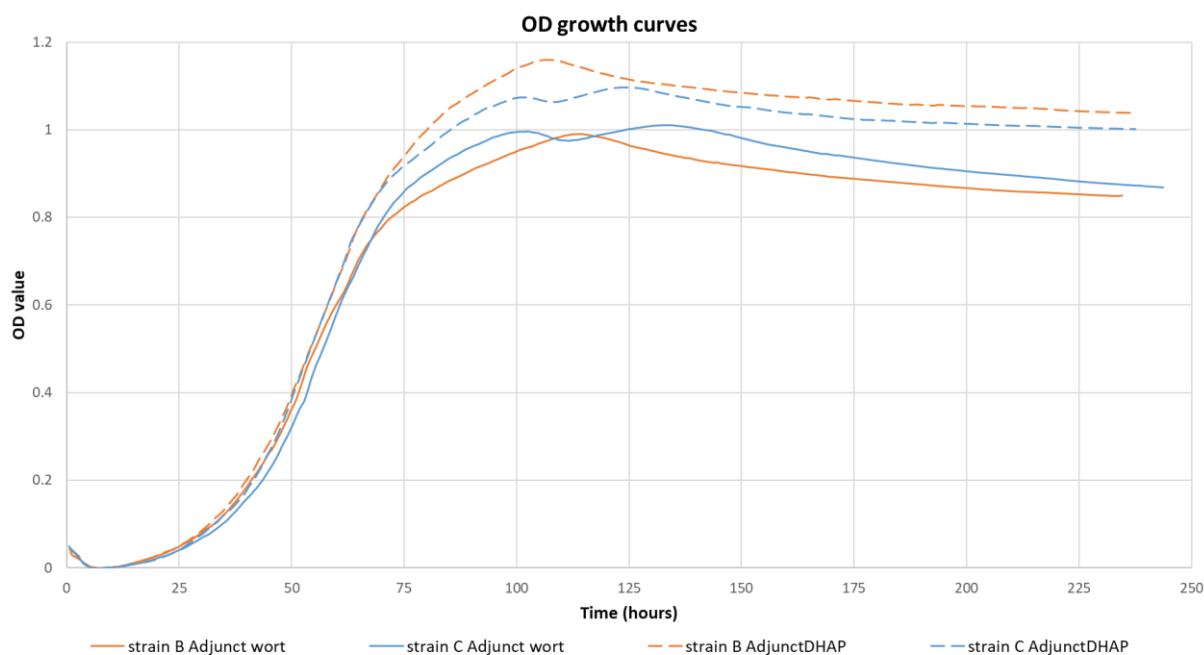


Figure 25 - OD growth curves for C and B strains. Fermentations in normal Adjunct wort (F19G and F19I fermentations) and nitrogen supplemented Adjunct wort (F19K2 fermentations) are represented. Only one curve per duplicate fermentation is presented, since duplicates presented similar curves. Values were normalized.

4.6. Cell Surface Hydrophobicity evolution during the fermentations

Cell surface hydrophobicity is a cell physical state parameter, which is strongly correlated with the flocculation ability of yeast cells (Kopecká and Němec 2015). In order to evaluate the hydrophobicity of yeast cells in suspension, samples from the running bioreactors were taken throughout the running fermentations. Four samples per fermentation were taken, at the same sampling times as the RNA-seq samples (Materials and Methods, F19F, F19G, F19H and F19I fermentation runs). The sample times in relation to each growth curve of each strain are represented in fig. S10. The CSH measuring method was adapted from the MATH test (Kopecká and Němec 2015), and is expressed in % of cells that adhered to the organic solvent (n-hexadecane) layer.

Figure 26 depicts the changes of CSH value for the three strains, in full malt wort (fig. 26 a) and Adjunct wort (fig. 26 b). Generally, an increase in the CSH value is observed with increased fermentation time. It appears that cells achieve greater CSH values in Adjunct wort than in full malt wort, especially for the 3rd and 4th samples, which are coincident with the maximum flocculation extents achieved at the stationary phase of growth for B and C strains. The non-flocculent A strain also presents variation throughout the fermentation time, and higher CSH values in the Adjunct wort composition. In the full malt wort configuration, strain A presents a small variation of the CSH value from the 1st to the 4th sample. However, a great increase is observed from the 1st to the 2nd sample in Adjunct wort configuration, presenting higher CSH at the 2nd sample time than the B strain. It also presents a higher value than C strain, at the 3rd sample time in Adjunct wort. C strain in Full malt wort presents a higher CSH value at the 1st sample than at the 2nd sample time, increasing greatly on the two subsequent samples (fig. 26 a). However, no relevant variation is found for its 4 samples values in Adjunct wort,

remaining always in values around 80% at the four sample times (fig. 26 b). In Adjunct wort, the data available for C strain lacks quality, and further tests should be conducted. For the B strain, a continuous CSH value increase is observed from the 1st to the 4th sample in Full malt wort, and the highest value for CSH of all the 3 strains is achieved in the Adjunct wort, at the 3rd sample (fig. 26 b). Interestingly, an almost 20% decrease in the CSH value from this 3rd sample to the 4th sample is observable as well. In general, C strain always presents higher values of CSH than B strain, except for the 2nd sample, in Full malt wort (fig. 26 a).

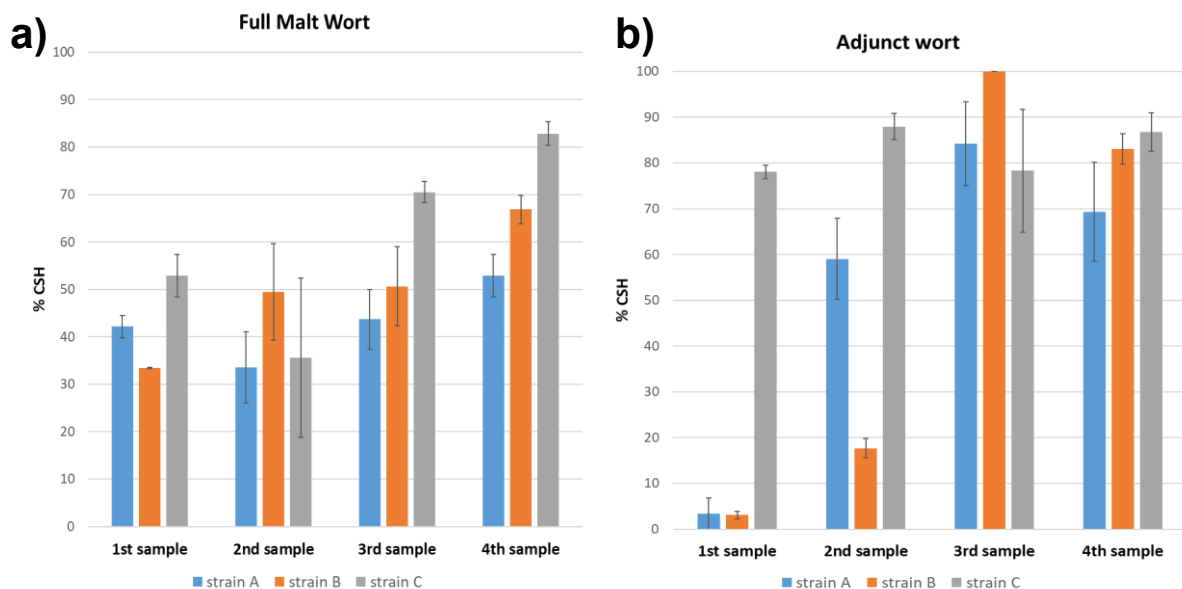


Figure 26 - Cell Surface Hydrophobicity evolution during the fermentations in Full malt and 50% Adjunct wort, for all the three tested strains A, B and C (F19F, F19G, F19H and F19I fermentations). Each of the bars represent an averaged value of two independent fermentations. On each fermentation time point, samples were analysed in triplicate.

4.7. RNA-seq data results

In order to know the influence of different fermentation conditions on the FLO genes expression, RNA-seq analysis was performed. The collection of RNA samples was done at 4 different time points per strain (A, B and C), in each wort type (Full malt and 50% Adjunct wort). In fig. S10 the growth curves of each strain with the sampling times are given. Sample times were chosen in such way that samples were representing the same growth stages for each strain. The four samples for RNA-seq analysis were performed at the end of the exponential phase, deceleration phase and twice on the stationary phase of growth.

4.7.1. Quality assessment of the RNA samples

After total isolation of RNA took place, the resultant reads were sequenced in Illumina platform for library preparation. The data was analysed for its quality, and the RNA reads were normalized, to afford a reliable comparison of transcripts level. At the 5' region of the reads, normal typical unequal distribution of bases was detected. This problem was solved by trimmomatic treatment, which culminated in good quality of the RNA reads in the end of all the quality assessment. All the reads were mapped against

their correspondent reference genome, revealing a 93.4% mapping overall, for the three strains. In order to be possible to compare different expression of transcripts among the different samples, the data was normalized. This analysis showed a similar median value and distribution for all the 48 samples analysed.

A Principal Component Analysis (PCA) was also performed, in order to check whether the replicates for each fermentation setup would cluster together. This procedure is important to check for batch to batch variations, among the samples performed. Figure 22 depicts the PCA, in which is possible to see that no obvious outliers are present, with the replicates clustering well together (fig. 27 a). Relatively to the variation of the two principal components, the variance shows that the principal component 1 variation is mainly due to the medium and strain variation (fig. 27 b) and the second principal component variance is due to the different times of the samples (fig. 27 c).

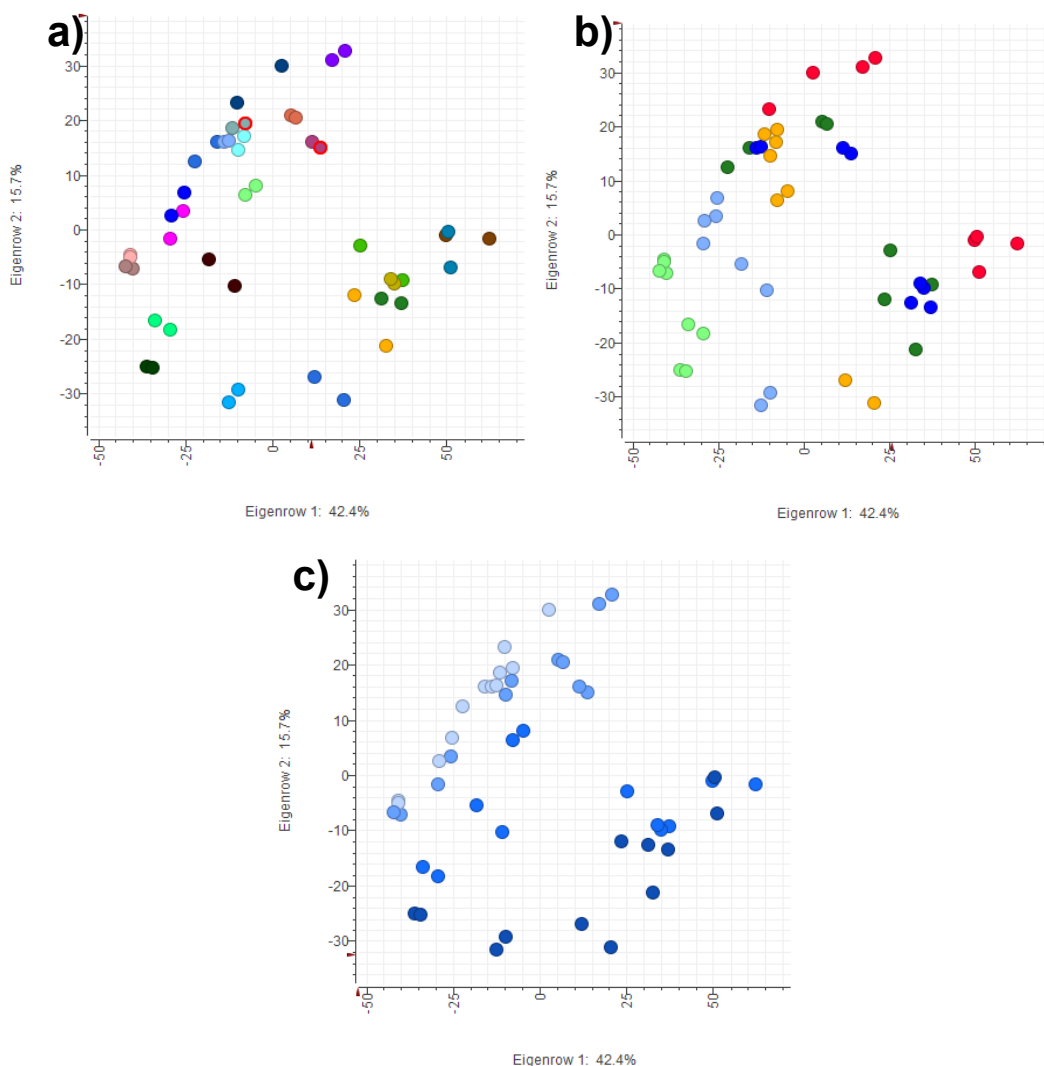


Figure 27 - PCA analysis of the 48 analysed RNA samples. On figure a), all individual samples are represented, with each two replicates represented by the same colour. On figure b), replicates are represented according to the strain and media (Legend: ■ C Adjunct wort; ■ C Full malt wort; ■ A Adjunct wort; ■ A Full malt wort; ■ B Adjunct wort; ■ B Full malt wort). On figure c), replicates are represented according to the sample number/time (Legend: 1st sample ■; 2nd sample ■; 3rd sample ■; 4th sample ■).

4.7.2. Evolution of the transcript levels among the different strains

The analysis of the different transcripts and their quantity showed differences on the expression level, throughout the different sample times, strains and media composition. Some of the transcripts identified include most of the known FLO genes: genes X, Y, Z, W and gene O (O') were identified, showing differences in expression for the tested strains, media and sample times (data not shown). Among these different genes, paralogs for each gene were also identified. However, due to their relative higher expression levels, three transcripts were categorized as the potential effectors of the observed flocculation differences among the strains, all of them paralogs of Y gene. The paralogs found were nominated Y, Y1 and Y2, all located at chromosomes R1, R2 and R3, respectively. The RNA transcript levels are depicted in figure C5 (Confidential Annex, section 3). From the figure, the higher transcript levels are found for the Y1 paralog (fig. C5 B). Both strains C and A show high transcript levels, with B strain showing the lower values of transcripts of this gene. However, for all the three strains, a variation in the mRNA quantity of this paralog is found throughout the four samples, and differences are also found among different wort compositions. For strain C in Adjunct wort, an increase from the first to the third sample is observed, declining at the fourth sample time. A different pattern is found for the same strain in Full malt wort, in which the maximum transcript level is found at the second sample time, and with overall lower expression values. Strain A shows similar trends, with increase in expression from the first to the third sample in Adjunct wort, and only from the first to the second sample in Full malt wort. Strain B shows the lower expression values, and the variations in expression with the time of sampling are very subtle for both wort compositions.

The second more expressed paralog is Y2 (fig. C5 C). For strain C, this gene showed a similar expression trend to Y1 (fig. C5 B) and Y (fig. C5 A) paralogs. Y2 paralog was barely expressed by A and B strains, in both wort compositions (fig. C5 C). Finally, Y paralog, the least expressed one, shows similar trends to all the other paralogs for C strain, and its absent for A strain. Strain B shows similar expression trends of this paralog, to C strain (fig. C5 A).

4.7.3. The gene structure of the Y1 homologues

In order to see potential DNA level differences among the Y1 homologues on the different strains, a whole genome comparison of this gene and protein level predictions were performed, using the reference genomes of each strain, which were already previously sequenced. The analysis of the gene in three different strains show evident differences in terms of size, with Y1 homologue on strain C genome assembly presenting a longer gene than for the other two strains, A and B (data not shown). Regarding the protein level prediction, it was predicted that the PA14 domain, which is present on the N-terminal domain of all known yeast flocculins (Brückner and Mösch 2012), is absent on the Y1 homologues of A and B strains, but present on C strain Y1 gene (fig. 28).

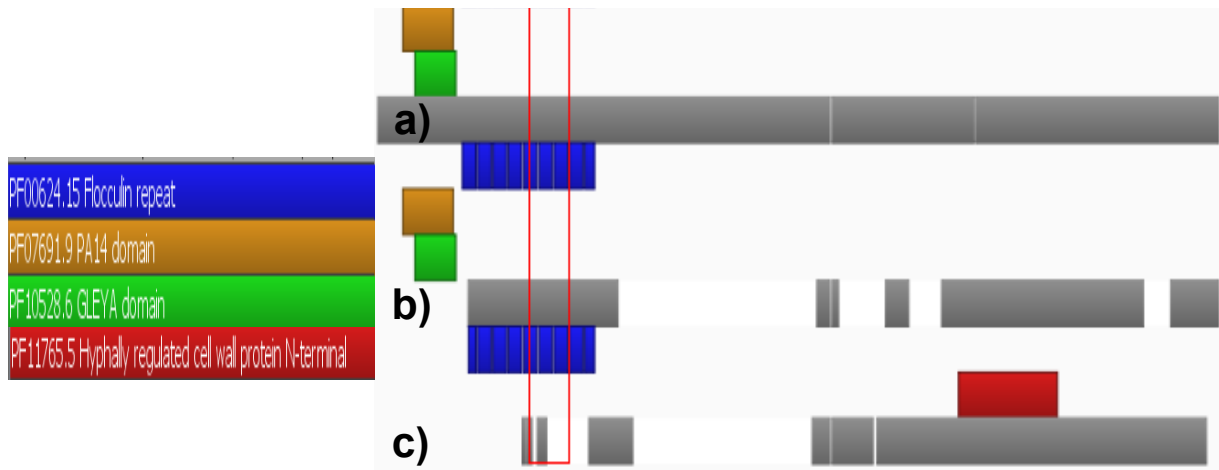


Figure 28 - Protein level comparison of the Y1 homologue for each of the studied strains C (fig. a)), A (fig. b)) and B (fig. c)), with the sequence of each strain's homologue represented in grey. The coloured blocks represent known protein domains being them flocculin repeats (blue), PA14 domain (yellow), GLEYA domain (green) and the hyphally regulated cell wall protein N-terminal (red).

5. Discussion

The present work aimed to have new insights regarding the complex flocculation phenomena. Flocculation is highly dependent on the flocculins, proteins encoded by the sub telomeric regions-located *FLO* genes. The testing and development of a new flocculation measurement was crucial, to enable the correct comparison of flocculation phenotypes among the strains A, B and C. This method not only sought to give online results, by which better correlations between fermentation conditions and different yeast phenotypes could be achieved, but also showed to unravel a new parameter, regarding the cell flocs morphology characteristics of different yeast strains. Since strain C is reported to show some incoherence in respect to the flocculation times, different fermentation conditions and wort compositions were tested. A transcriptomic comparison was tried by RNA-seq analysis during different fermentations, for the above-mentioned strains.

In previous investigations (D'Hautcourt and Smart 1999; Speers et al. 2006; Claro et al. 2007), higher ethanol concentrations are related with increased flocculation efficiency. In Adjunct wort fermentations, strain C produces more ethanol than in Full malt wort fermentations, correlating with previous findings. For both B and C strains cultivated in Adjunct wort, maltose and maltotriose are not fully consumed. Several are the studies that correlate sugars presence to flocculation inhibition (Soares et al. 2004), even more for brewing yeast strains, which normally start to flocculate at the end of the fermentation, when all the sugars in wort are almost depleted (Verstrepen et al. 2003). However, results for flocculation strength of B and C strains show $FloC_{bind}$ values are higher in Adjunct wort, where more sugars are still present in solution, than in Full malt wort, where all sugars in wort are totally consumed. Besides this, it should be considered that different flocculins have different binding affinities towards different types of sugars (Van Mulders et al. 2009; Willaert 2018). It could be that the flocculins expressed by C and B strains do not have a broad specificity towards maltose and maltotriose, enabling flocculation even with some of these sugars still present in the wort.

The pH controlled Adjunct wort fermentations showed, for B strain, an increase in cell binding strength and higher fluffiness of the flocs. For the C strain, the great duplicates variation disables a clear comparison, and the fermentations should be repeated. The fact that a higher cell binding strength is followed by an increase in fluffiness totally correlates with the relocation phenomena (see Introduction – Cells are particles – colloids science vs flocculation) (Stratford 1992). However, it could be asked why the cell binding strength increases in response to the increase of 0.5 value in pH. Previous research (Dengis et al. 1995) showed that lager yeast shows an optimal pH range-value for flocculation between 4-4.5. However, at the time of this paper, no structure of the flocculins was solved. Veelders et al. (Veelders et al. 2010) showed, for the first time, the sub-atomic structure of the N-terminal part of the Flo5 protein. At the sugar binding site, two aspartic acid residues are highly preserved among N-terminal domains of different flocculins. These two residues are known to be responsible for calcium binding. With the increase in pH, these residues might be much less protonated, and more able to bind calcium, a preponderant requirement for flocculation to take place (Stratford 1989). Moreover, the isoelectric point of the aspartic acid aminoacid is between 3.9-4, below which the sidechains of the residue are highly protonated, and less able to bind other ions (like calcium). However, it should be noted that some

characteristics of the amino acids, as the isoelectric point, may vary when they are in a protein context (Urry et al. 1993).

The supplementation of Adjunct wort with nitrogen showed severe implications on the flocculation strength of the cells. Both B and C strains show lower flocculation strength values, in comparison with normal adjunct wort, and the flocculation onset of strain B is delayed in response to a higher initial nitrogen content. The nitrogen was already reported as being correlated with the flocculation onset in *S. cerevisiae* strains (Sampermans et al. 2005). Coincidentally, the shortage in nitrogen leads to earlier flocculation onsets, which agrees with what was observed for the B strain. Strain B lacks a correlation for its flocculation onset and the amount of sugars in solution. For the nitrogen supplemented fermentation, strain B consumes more sugars, but presents lower $Floc_{bind}$ values than in normal Adjunct wort, in which leaves more sugars in solution. Same can be said about the ethanol concentrations. Strain B produces more ethanol if it has more nitrogen at the beginning of the fermentation, but the flocculation strength is lower. For the C strain, no correlation is found between nitrogen concentration and flocculation onset. In fact, this strain flocculates later in normal Adjunct wort than in full malt wort, but no shift was found in the nitrogen supplemented Adjunct wort. Conversely, it seems from the analysis of sugars in all fermentations that C strain starts to flocculate, as soon as the sugars concentrations in wort drop below 4g/100mL. For Adjunct wort supplemented with nitrogen, higher cell densities were achieved, as shown by the normalized OD curves, for both strains C and B. Previous papers (Verstrepen et al. 2003) reported that higher cell densities are correlated with higher flocculation efficiencies. However, it seems that it's not the case for the nitrogen supplemented fermentation runs. An interesting correlation between state of growth and flocculation onset is found for both strains. For B strain, the flocculation onset in Full malt wort and normal Adjunct wort happens to coincide with the beginning of the deceleration phase of the cell population. However, when Adjunct wort is supplemented with nitrogen, the flocculation onset is delayed to the end of the same phase. For C strain, the same difference is visible by comparing the flocculation onset of this strain in Full malt (earlier onset) and Adjunct wort (later onset). Finally, for both strains, the pH values dropped slightly more than for normal Adjunct wort fermentations. From the pH-controlled fermentations, it was seen that an increase of 0.5 induced a higher flocculation efficiency. In the same way, it might be the case that those slightly lower pH values imparted an extreme decrease in the flocculation efficiency in nitrogen supplemented Adjunct wort.

Since the cell surface hydrophobicity is a known important parameter influencing the flocculation ability of flocculent cells (Van Holle et al. 2012), samples were taken throughout Full malt and Adjunct wort fermentations for all the three studied strains. The values from the Full malt wort fermentations show the better correlation with flocculation efficiency, since for all the strains, an increase from the 1st to the 4th samples are observed, which is also in line with the increase in flocculation efficiency. Besides it, C strain shows slightly higher CSH values for 3rd and 4th samples in Full malt wort, which goes in line with the higher flocculation efficiency of this strain, in comparison with B strain. For the Adjunct wort fermentations, the data set is poor in terms of significance. C strain CSH values never really change throughout the 4 samples. However, for B strain, there's an increase in hydrophobicity, and its values are higher in Adjunct wort than in Full malt wort (for the samples at which flocculation is already

occurring, 3rd and 4th samples), which correlates with the higher flocculation strength in that wort type. The values of strain A shows also that CSH is important for the flocculation efficiency, but by its own not enough to enable flocculation.

The results from RNA-seq analysis showed interesting transcript patterns. The most transcribed genes included gene Y and its paralogs, namely, Y1 and Y2. Among these three, Y1 showed the higher transcript levels, and differences in its expression throughout the fermentation time are observable for all the three tested strains. C strain showed for this gene a good correlation between level of transcription and onset of flocculation. In Adjunct wort, on which the higher transcript levels of Y1 are achieved, an increase from the 1st to the 3rd samples are observed. Interestingly, this increase in expression until the third sample time is coincident with the onset of flocculation for this strain in this wort composition. The 3rd sample was performed at 123 hours of fermentation, and the onset of flocculation was around 105 hours of fermentation time. Coincidentally, the same can be said for Full malt wort results. C strain started to flocculate at around 75 hours of fermentation in Full malt wort, and the maximum transcript level for Y1 gene is observed at the 2nd sample, which was performed at 92 hours of fermentation. In both wort compositions, the transcript levels declined after the flocculation onset was achieved. Besides not so evident, B strain also reveals a similar pattern, and the achievement of the flocculation onset is coincident with the higher transcript levels, which decline afterwards. Strain A also presented high transcription levels of Y1 gene, but its $FloC_{bind}$ values are almost null, in comparison with C and B strains. However, the protein level comparison revealed that Y1 homologue of A strain genome is lacking for the PA14 domain, which contains the binding site of the sugar residues (Brückner and Mösch 2012). Without this domain, no sugar binding can take place, and so the protein cannot be functional. B strain revealed the same result for the protein prediction, besides its flocculation phenotype. However, it should be noted that other *FLO* genes revealed expression for this strain, revealing that other gene or genes besides Y1 are responsible for the flocculation phenotype showed by this strain.

Besides the difference in transcription levels, the data coming from the RNA-seq analysis fails in confidence. The RNA samples showed a good quality, meaning that the sample and subsequent treatment were successful. However, the DNA sequencing assemblies are not 100% reliable for the chromosome regions in which the analysis was performed. *FLO* genes show zero coverage for some parts of their DNA sequence, meaning that assembly mistakes are present, which on their way make it difficult to draw solid conclusions about the transcript expression data. In fact, two great obstacles are found when analysing *FLO* genes in *Saccharomyces pastorianus* strains. First, *FLO* genes are presented in sub-telomeric regions, which by itself makes it difficult for reliable sequencing data, due to the high repetitive regions present (Van Mulders et al. 2010). Secondly, the fact that *S. pastorianus* is a hybrid of *S. cerevisiae* and *S. eubayanus* species makes it even harder for correct assembly procedure of their genomes, due to the high rates of aneuploidies present on this yeast species (Nakao et al. 2009).

6. Conclusions and future perspectives

The objective of following the relevant flocculation genes in the *Saccharomyces pastorianus* tested strains was revealed to be incomplete. Y gene and its paralogs were classified as the most relevant, due to their relative high expression, in relation to all the other gene transcripts. However, the lack of confidence on the reference genome doesn't enable to answer clearly to the raised questions. To answer them, upgrades regarding genome sequencing techniques must be done, since the highly repetitive zones of *Saccharomyces pastorianus* genome are still out of reach.

The flocculation measurement method, however, revealed potential in solving the question of how to characterize a flocculation phenotype of a strain. Besides being an online method, also permits the evaluation of two characteristics of yeast cells flocculation: binding strength and floc morphology. Further improvements must be performed, but all points for a new perspective regarding this so important parameter, which will might improve the prediction of flocculation capacity of certain yeast strains.

7. References

- Amory DE, Rouxhet PG. 1988. Surface properties of *Saccharomyces cerevisiae* and *Saccharomyces carlsbergensis*: chemical composition, electrostatic charge and hydrophobicity. *BBA - Biomembr.* doi:10.1016/0005-2736(88)90122-8.
- Andreasen AA, Stier TJB. 1953. Anaerobic nutrition of *Saccharomyces cerevisiae*. I. Ergosterol requirement for growth in a defined medium. *J Cell Comp Physiol.* 41(1):23–36. doi:10.1002/jcp.1030410103.
- Bauer FF, Govender P, Bester MC. 2010. Yeast flocculation and its biotechnological relevance. *Appl Microbiol Biotechnol.* doi:10.1007/s00253-010-2783-0.
- Bester MC, Jacobson D, Bauer FF. 2012. Many *Saccharomyces cerevisiae* Cell Wall Protein Encoding Genes Are Coregulated by Mss11, but Cellular Adhesion Phenotypes Appear Only Flo Protein Dependent. *G3 Genes, Genomes, Genet.* doi:10.1534/g3.111.001644.
- Bester MC, Pretorius IS, Bauer FF. 2006. The regulation of *Saccharomyces cerevisiae* FLO gene expression and Ca²⁺-dependent flocculation by Flo8p and Mss11p. *Curr Genet.* doi:10.1007/s00294-006-0068-z.
- Bony M, Thines-Sempoux D, Barre P, Blondin B. 1997. Localization and cell surface anchoring of the *Saccharomyces cerevisiae* flocculation protein Flo1p. *J Bacteriol.* doi:10.1128/jb.179.15.4929-4936.1997.
- Brown CA, Murray AW, Verstrepen KJ. 2010. Rapid expansion and functional divergence of subtelomeric gene families in yeasts. *Curr Biol.* 20(10):895–903. doi:10.1016/j.cub.2010.04.027. <http://www.ncbi.nlm.nih.gov/pubmed/20471265>.
- Brückner S, Mösch HU. 2012. Choosing the right lifestyle: Adhesion and development in *Saccharomyces cerevisiae*. *FEMS Microbiol Rev.* doi:10.1111/j.1574-6976.2011.00275.x.
- Chen EH, Grote E, Mohler W, Vignery A. 2007. Cell-cell fusion. *FEBS Lett.* doi:10.1016/j.febslet.2007.03.033.
- Claesson PM, Christenson HK. 1988. Very long range attractive forces between uncharged hydrocarbon and fluorocarbon surfaces in water. *J Phys Chem.* doi:10.1021/j100317a052.
- Claro FB, Rijsbrack K, Soares E V. 2007. Flocculation onset in *Saccharomyces cerevisiae*: Effect of ethanol, heat and osmotic stress. *J Appl Microbiol.* doi:10.1111/j.1365-2672.2006.03130.x.
- D'Hautcourt O, Smart KA. 1999. Measurement of Brewing Yeast Flocculation. *J Am Soc Brew Chem.* doi:10.1094/ASBCJ-57-0123.
- Davis RH, Hunt TP. 1986. Modeling and Measurement of Yeast Flocculation. *Biotechnol Prog.* doi:10.1002/btpr.5420020208.
- Dengis PB, Nelissen LR, Rouxhet PG. 1995. Mechanisms of yeast flocculation: Comparison of top- and bottom-fermenting strains. *Appl Environ Microbiol.* 61(2):718.
- Dietvorst J, Brandt A. 2008. Flocculation in *Saccharomyces cerevisiae* is repressed by the COMPASS methylation complex during high-gravity fermentation. *Yeast.* doi:10.1002/yea.1643.
- Dietvorst J, Brandt A. 2010. Histone modifying proteins Gcn5 and Hda1 affect flocculation in *Saccharomyces cerevisiae* during high-gravity fermentation. *Curr Genet.* doi:10.1007/s00294-009-0281-7.
- Dranginis AM, Rauceo JM, Coronado JE, Lipke PN. 2007. A Biochemical Guide to Yeast Adhesins: Glycoproteins for Social and Antisocial Occasions. *Microbiol Mol Biol Rev.* 71(2):282–294. doi:10.1128/mbr.00037-06.
- Dunn B, Sherlock G. 2008. Reconstruction of the genome origins and evolution of the hybrid lager yeast *Saccharomyces pastorianus*. *Genome Res.* 18(10):1610–1623. doi:10.1101/gr.076075.108.
- Duszyk M, Doroszewski J. 1986. Poiseuille flow method for measuring cell-to-cell adhesion. *Cell Biophys.* doi:10.1007/BF02788476.

- Elimelech M (Menachem). 1995. Particle deposition and aggregation : measurement, modelling, and simulation. Butterworth-Heinemann.
- Fichtner L, Schulze F, Braus GH. 2007. Differential Flo8p-dependent regulation of FLO1 and FLO11 for cell-cell and cell-substrate adherence of *S. cerevisiae* S288c. *Mol Microbiol*. doi:10.1111/j.1365-2958.2007.06014.x.
- Frieman MB, McCaffery JM, Cormack BP. 2002. Modular domain structure in the *Candida glabrata* adhesin Epa1p, a β 1,6 glucan-cross-linked cell wall protein. *Mol Microbiol*. 46(2):479–492. doi:10.1046/j.1365-2958.2002.03166.x.
- Gibson B, Liti G. 2015. *Saccharomyces pastorianus*: Genomic insights inspiring innovation for industry. *Yeast*. 32(1):17–27. doi:10.1002/yea.3033.
- Gibson BR, Storgårds E, Krogerus K, Vidgren V. 2013. Comparative physiology and fermentation performance of Saaz and Froberg lager yeast strains and the parental species *Saccharomyces eubayanus*. *Yeast*. 30(7):255–266. doi:10.1002/yea.2960.
- Gimeno CJ, Ljungdahl PO, Styles CA, Fink GR. 1992. Unipolar cell divisions in the yeast *S. cerevisiae* lead to filamentous growth: Regulation by starvation and RAS. *Cell*. doi:10.1016/0092-8674(92)90079-R.
- Goossens KVV, Ielasi FS, Nookaew I, Stals I, Alonso-Sarduy L, Daenen L, Van Mulders SE, Stassen C, Van Eijsden RGE, Siewers V, et al. 2015. Molecular mechanism of flocculation self-recognition in yeast and its role in mating and survival. *MBio*. 6(2):1–16. doi:10.1128/mBio.00427-15.
- Gouveia C, Soares E V. 2004. Pb²⁺ Inhibits Competitively Flocculation of *Saccharomyces cerevisiae*. *J Inst Brew*. 110(2):141–145. doi:10.1002/j.2050-0416.2004.tb00193.x.
- Govender P, Domingo JL, Bester MC, Pretorius IS, Bauer FF. 2008. Controlled expression of the dominant flocculation genes FLO1, FLO5, and FLO11 in *Saccharomyces cerevisiae*. *Appl Environ Microbiol*. doi:10.1128/AEM.00394-08.
- Gregory J. 1993. The role of colloid interactios in solid-liquid separation. *Water Sci Technol*. doi:10.2166/wst.1993.0195.
- Grivet M, Morrier JJ, Benay G, Barsotti O. 2000. Effect of hydrophobicity on in vitro streptococcal adhesion to dental alloys. *J Mater Sci Mater Med*. 11(10):637–642. doi:10.1023/A:1008913915399.
- Guilliermond A. 1920. The yeasts. New York, USA: John Wiley and Sons.
- Guo B, Styles CA, Feng Q, Fink GR. 2000. A *Saccharomyces* gene family involved in invasive growth, cell-cell adhesion, and mating. *Proc Natl Acad Sci U S A*. 97(22):12158–12163. doi:10.1073/pnas.220420397.
- Halme A, Bumgarner S, Styles C, Fink GR. 2004. Genetic and epigenetic regulation of the FLO gene family generates cell-surface variation in yeast. *Cell*. doi:10.1016/S0092-8674(04)00118-7.
- Hamaker HC. 1937. The London-van der Waals attraction between spherical particles. *Physica*. doi:10.1016/S0031-8914(37)80203-7.
- Van Holle A, MacHado MD, Soares E V. 2012. Flocculation in ale brewing strains of *Saccharomyces cerevisiae*: Re-evaluation of the role of cell surface charge and hydrophobicity. *Appl Microbiol Biotechnol*. 93(3):1221–1229. doi:10.1007/s00253-011-3502-1.
- Hsu JWC, Speers RA, Paulson AT. 2001. Modeling of orthokinetic flocculation of *Saccharomyces cerevisiae*. *Biophys Chem*. doi:10.1016/S0301-4622(01)00236-8.
- Jentoft N. 1990. Why are proteins O-glycosylated? *Trends Biochem Sci*. 15(8):291–294. doi:10.1016/0968-0004(90)90014-3.
- Jin Y-L, Ritcey LL, Speers RA, Dolphin PJ. 2001. Effect of Cell Surface Hydrophobicity, Charge, and Zymolectin Density on the Flocculation of *Saccharomyces cerevisiae*. *J Am Soc Brew Chem*. 59(1):1–9. doi:10.1094/asbcj-59-0001.
- Jin Y-L, Speers RA. 2000. Effect of Environmental Conditions on the Flocculation of *Saccharomyces cerevisiae*. *J Am Soc Brew Chem*. 58(3):108–16. doi:10.1094/asbcj-58-0108.
- Jones ST, Korus RA, Admassu W, Heimsch RC. 1984. Ethanol fermentation in a continuous tower fermentor. *Biotechnol Bioeng*.

doi:10.1002/bit.260260717.

Klis FM, Boorsma A, De Groot PWJ. 2006. Cell wall construction in *Saccharomyces cerevisiae*. *Yeast*. doi:10.1002/yea.1349.

Kobayashi O, Hayashi N, Kuroki R, Sone H. 1998. Region of Flo1 proteins responsible for sugar recognition. *J Bacteriol*. 180(24):6503–6510.

Kobayashi O, Suda H, Ohtani T, Sone H. 1996. Molecular cloning and analysis of the dominant flocculation gene FLO8 from *Saccharomyces cerevisiae*. *Mol Gen Genet*. doi:10.1007/s004380050220.

Kobayashi O, Yoshimoto H, Sone H. 1999. Analysis of the genes activated by the FLO8 gene in *Saccharomyces cerevisiae*. *Curr Genet*. doi:10.1007/s002940050498.

Kock JLF, Venter P, Smith DP, Van Wyk PWJ, Botes PJ, Coetzee DJ, Pohl CH, Botha A, Riedel KH, Nigam S. 2000. A novel oxylipin-associated “ghosting” phenomenon in yeast flocculation. *Antonie van Leeuwenhoek, Int J Gen Mol Microbiol*. doi:10.1023/A:1002735216303.

Kopecká J, Němec M. 2015. Effect of Growth Conditions on Flocculation and Cell Surface Hydrophobicity of Brewing Yeast. *J Am Soc Brew Chem*. doi:10.1094/asbcj-2015-0324-01.

Lawrence SJ, Smart KA. 2007. Impact of CO₂-induced anaerobiosis on the assessment of brewing yeast flocculation. *J Am Soc Brew Chem*. 65(4):208–213. doi:10.1094/ASBCJ-2007-0817-01.

Lehle L, Strahl S, Tanner W. 2006. Protein glycosylation, conserved from yeast to man: a model organism helps elucidate congenital human diseases. *Angew Chem Int Ed Engl*. 45(41):6802–18. doi:10.1002/anie.200601645. <http://www.ncbi.nlm.nih.gov/pubmed/17024709>.

Li E, Yue F, Chang Q, Guo X, He X, Zhang B. 2013. Deletion of Intragenic Tandem Repeats in Unit C of FLO1 of *Saccharomyces cerevisiae* Increases the Conformational Stability of Flocculin under Acidic and Alkaline Conditions. *PLoS One*. doi:10.1371/journal.pone.0053428.

Libkind D, Hittinger CT, Valefio E, Gonçalves C, Dover J, Johnston M, Gonçalves P, Sampaio JP. 2011. Microbe domestication and the identification of the wild genetic stock of lager-brewing yeast. *Proc Natl Acad Sci U S A*. 108(35):14539–14544. doi:10.1073/pnas.1105430108.

Liti G, Peruffo A, James SA, Roberts IN, Louis EJ. 2005. Inferences of evolutionary relationships from a population survey of LTR-retrotransposons and telomeric-associated sequences in the *Saccharomyces sensu stricto* complex. *Yeast*. 22(3):177–192. doi:10.1002/yea.1200.

Liu H, Stylest CA, Finkt GR, Rudolph AA. 1996. S288C has a mutation in FLO8, a gen required for filamentous growth. *Growth (Lakeland)*. 144(3):967–978.

Liu N, Wang D, Wang Z, He X, Zhang B. 2009. Deletion of tandem repeats causes flocculation phenotype conversion from Flo1 to NewFlo in *Saccharomyces cerevisiae*. *J Mol Microbiol Biotechnol*. 16(3–4):137–45. doi:10.1159/000112318. <http://www.ncbi.nlm.nih.gov/pubmed/18057865>.

Liu N, Wang D, Wang ZY, He XP, Zhang B. 2007. Genetic basis of flocculation phenotype conversion in *Saccharomyces cerevisiae*. *FEMS Yeast Res*. doi:10.1111/j.1567-1364.2007.00294.x.

Lo WS, Dranginis AM. 1996. FLO11, a yeast gene related to the STA genes, encodes a novel cell surface flocculin. *J Bacteriol*. 178(24):7144–7151. doi:10.1128/jb.178.24.7144-7151.1996.

Lommel M, Strahl S. 2009. Protein O-mannosylation: Conserved from bacteria to humans. *Glycobiology*. 19(8):816–828. doi:10.1093/glycob/cwp066.

Loney ER, Inglis PW, Sharp S, Pryde FE, Kent NA, Mellor J, Louis EJ. 2009. Repressive and non-repressive chromatin at native

telomeres in *Saccharomyces cerevisiae*. *Epigenetics Chromatin*. 2(1):18. doi:10.1186/1756-8935-2-18. <http://www.ncbi.nlm.nih.gov/pubmed/19954519>.

Long M, Goldsmith HL, Tees DFJ, Zhu C. 1999. Probabilistic modeling of shear-induced formation and breakage of doublets cross-linked by receptor-ligand bonds. *Biophys J*. doi:10.1016/S0006-3495(99)77276-0.

Lorenz RT, Parks LW. 1991. Involvement of heme components in sterol metabolism of *Saccharomyces cerevisiae*. *Lipids*. 26(8):598–603. <http://www.ncbi.nlm.nih.gov/pubmed/1779707>.

Machado MD, Soares E V., Soares HMVM. 2010. Removal of heavy metals using a brewer's yeast strain of *Saccharomyces cerevisiae*: Application to the treatment of real electroplating effluents containing multielements. *J Chem Technol Biotechnol*. doi:10.1002/jctb.2440.

Malavé TM, Dent SYR. 2006. Transcriptional repression by Tup1-Ssn6. *Biochem Cell Biol*. 84(4):437–443. doi:10.1139/O06-073.

Masuoka J, Hazen KC. 2004. Cell wall mannan and cell surface hydrophobicity in *Candida albicans* serotype A and B strains. *Infect Immun*. 72(11):6230–6236. doi:10.1128/IAI.72.11.6230-6236.2004.

Masy CL, Henquinet A, Mestdagh MM. 2010. Flocculation of *Saccharomyces cerevisiae*: inhibition by sugars. *Can J Microbiol*. doi:10.1139/m92-214.

Meakin P. 1987. Fractal aggregates. *Adv Colloid Interface Sci*. doi:10.1016/0001-8686(87)80016-7.

Mercier-Bonin M, Ouazzani K, Schmitz P, Lorthois S. 2004. Study of bioadhesion on a flat plate with a yeast/glass model system. *J Colloid Interface Sci*. 271(2):342–350. doi:10.1016/j.jcis.2003.11.045.

Meussdoerffer FG. 2009. A Comprehensive History of Beer Brewing. In: *Handbook of Brewing: Processes, Technology, Markets*. Wiley-VCH Verlag GmbH & Co. KGaA. p. 1–42.

Miki BL, Poon NH, James AP, Seligy VL. 1982. Possible mechanism for flocculation interactions governed by gene FLO1 in *Saccharomyces cerevisiae*. *J Bacteriol*. 150(2):878–89. <http://www.ncbi.nlm.nih.gov/pubmed/7040343>.

Monds RD, O'Toole GA. 2009. The developmental model of microbial biofilms: ten years of a paradigm up for review. *Trends Microbiol*. doi:10.1016/j.tim.2008.11.001.

Van Mulders SE, Christianen E, Saerens SMG, Daenen L, Verbelen PJ, Willaert R, Verstrepen KJ, Delvaux FR. 2009. Phenotypic diversity of Flo protein family-mediated adhesion in *Saccharomyces cerevisiae*. *FEMS Yeast Res*. doi:10.1111/j.1567-1364.2008.00462.x.

Van Mulders SE, Ghequire M, Daenen L, Verbelen PJ, Verstrepen KJ, Delvaux FR. 2010. Flocculation gene variability in industrial brewer's yeast strains. *Appl Microbiol Biotechnol*. doi:10.1007/s00253-010-2843-5.

Nakao Y, Kanamori T, Itoh T, Kodama Y, Rainieri S, Nakamura N, Shimonaga T, Hattori M, Ashikari T. 2009. Genome sequence of the lager brewing yeast, an interspecies hybrid. *DNA Res*. 16(2):115–129. doi:10.1093/dnares/dsp003.

Nishihara H, Toraya T, Fukui S. 1982. Flocculation of cell walls of brewer's yeast and effects of metal ions, protein-denaturants and enzyme treatments. *Arch Microbiol*. doi:10.1007/BF01053991.

Ogata T, Izumikawa M, Kohno K, Shibata K. 2008. Chromosomal location of Lg-FLO1 in bottom-fermenting yeast and the FLO5 locus of industrial yeast. *J Appl Microbiol*. doi:10.1111/j.1365-2672.2008.03852.x.

Pasteur Louis ML. 1876. Pasteur ML (1876). *Études sur la bière ses Mal causes qui les Provoquent, procédé pour la rendre Ina avec une Theor Nouv la Ferment Gauthier-Villars, Paris*.

Pham T, Wimalasena T, Box WG, Koivuranta K, Storgårds E, Smart KA, Gibson BR. 2011. Evaluation of ITS PCR and RFLP for

differentiation and identification of brewing yeast and brewery "wild" yeast contaminants. *J Inst Brew.* 117(4):556–568. doi:10.1002/j.2050-0416.2011.tb00504.x.

Phillips R, Kondev J, Theriot J, Garcia HG, Orme N. 2012. *Physical biology of the cell.* Garland Science.

Powell CD, Quain DE, Smart KA. 2003. The impact of brewing yeast cell age on fermentation performance, attenuation and flocculation. *FEMS Yeast Res.* doi:10.1016/S1567-1356(03)00002-3.

Pryde FE, Gorham HC, Louis EJ. 1997. Chromosome ends: All the same under their caps. *Curr Opin Genet Dev.* 7(6):822–828. doi:10.1016/S0959-437X(97)80046-9.

Pryde FE, Louis EJ. 1997. *Saccharomyces cerevisiae* telomeres. A review. *Biochemistry (Mosc).* 62(11):1232–41. <http://www.ncbi.nlm.nih.gov/pubmed/9467847>.

Pryde FE, Louis EJ. 1999. Limitations of silencing at native yeast telomeres. *EMBO J.* 18(9):2538–2550. doi:10.1093/emboj/18.9.2538.

Ramsook CB, Tan C, Garcia MC, Fung R, Soybelman G, Henry R, Litewka A, O'Meally S, Otoo HN, Khalaf RA, et al. 2010. Yeast cell adhesion molecules have functional amyloid-forming sequences. *Eukaryot Cell.* 9(3):393–404. doi:10.1128/EC.00068-09.

Salazar AN, Gorter de Vries AR, van den Broek M, Brouwers N, de la Torre Cortés P, Kuijpers NG, Daran J-MG, Abeel T. 2019. Nanopore sequencing and comparative genome analysis confirm lager-brewing yeasts originated from a single hybridization. Unpublished. doi:10.1101/603480.

Sampermans S, Mortier J, Soares E V. 2005. Flocculation onset in *Saccharomyces cerevisiae*: The role of nutrients. *J Appl Microbiol.* doi:10.1111/j.1365-2672.2004.02486.x.

Sato M, Maeba H, Watari J, Takashio M. 2002. Analysis of an inactivated Lg-FLO1 gene present in bottom-fermenting yeast. *J Biosci Bioeng.* 93(4):395–398. doi:10.1016/S1389-1723(02)80073-1.

Sato M, Watari J, Shinotsuka K. 2001. Genetic Instability in Flocculation of Bottom-Fermenting Yeast. *J Am Soc Brew Chem.* 59(3):130–134. doi:10.1094/ASBCJ-59-0130. <https://www.tandfonline.com/doi/full/10.1094/ASBCJ-59-0130>.

Sim L, Groes M, Olesen K, Henriksen A. 2013. Structural and biochemical characterization of the N-terminal domain of flocculin Lg-Flo1p from *Saccharomyces pastorianus* reveals a unique specificity for phosphorylated mannose. *FEBS J.* 280(4):1073–1083. doi:10.1111/febs.12102.

Smit G, Straver MH, Lugtenberg BJ, Kijne JW. 1992. Flocculence of *Saccharomyces cerevisiae* cells is induced by nutrient limitation, with cell surface hydrophobicity as a major determinant. *Appl Environ Microbiol.* 58(11):3709–14. <http://www.ncbi.nlm.nih.gov/pubmed/1482191>.

Smukalla S, Caldara M, Pochet N, Beauvais A, Guadagnini S, Yan C, Vinces MD, Jansen A, Prevost MC, Latgé JP, et al. 2008. FLO1 Is a Variable Green Beard Gene that Drives Biofilm-like Cooperation in Budding Yeast. *Cell.* doi:10.1016/j.cell.2008.09.037.

Soares E V. 2011. Flocculation in *Saccharomyces cerevisiae*: A review. *J Appl Microbiol.* doi:10.1111/j.1365-2672.2010.04897.x.

Soares E V., De Coninck G, Duarte F, Soares HMVM. 2002. Use of *Saccharomyces cerevisiae* for Cu²⁺ removal from solution: The advantages of using a flocculent strain. *Biotechnol Lett.* 24(8):663–666. doi:10.1023/A:1015062925570.

Soares E V., Seynaeve J. 2000. Induction of flocculation of brewer's yeast strains of *Saccharomyces cerevisiae* by changing the calcium concentration and pH of culture medium. *Biotechnol Lett.* doi:10.1023/A:1005665427163.

Soares E V., Teixeira JA, Mota M. 1994. Effect of cultural and nutritional conditions on the control of flocculation expression in *Saccharomyces cerevisiae*. *Can J Microbiol.* 40(10):851–857. doi:10.1139/m94-135.

Soares E V., Vroman A, Mortier J, Rijsbrack K, Mota M. 2004. Carbohydrate carbon sources induce loss of flocculation of an ale-brewing yeast strain. *J Appl Microbiol.* 96(5):1117–1123. doi:10.1111/j.1365-2672.2004.02240.x.

Speers RA, Durance TD, Tung MA, Tou J. 1993. Colloidal Properties of Flocculent and Nonflocculent Brewing Yeast Suspensions.

Biotechnol Prog. doi:10.1021/bp00021a005.

Speers RA, Tung MA, Durance TD, Stewart GG. 1992. COLLOIDAL ASPECTS OF YEAST FLOCCULATION: A REVIEW. *J Inst Brew*. doi:10.1002/j.2050-0416.1992.tb01139.x.

Speers RA, Wan YQ, Jin YL, Stewart RJ. 2006. Effects of fermentation parameters and cell wall properties on yeast flocculation. *J Inst Brew*. 112(3):246–54. doi:10.1002/j.2050-0416.2006.tb00720.x.

Stewart G. 2018. Yeast Flocculation—Sedimentation and Flotation. *Fermentation*. doi:10.3390/fermentation4020028.

Stewart GG. 2009. The Horace Brown Medal lecture: Forty years of brewing research. *J Inst Brew*. doi:10.1002/j.2050-0416.2009.tb00340.x.

Stewart GG, Russell I, Garrison IF. 1975. SOME CONSIDERATIONS OF THE FLOCCULATION CHARACTERISTICS OF ALE AND LAGER YEAST STRAINS. *J Inst Brew*. doi:10.1002/j.2050-0416.1975.tb03686.x.

Stratford M. 1989. Yeast flocculation: Calcium specificity. *Yeast*. 5(6):487–496. doi:10.1002/yea.320050608.

Stratford M. 1992. Yeast flocculation: A new perspective. *Adv Microb Physiol*. 33:1–71. doi:10.1016/s0065-2911(08)60215-5.

Stratford M. 1996. Induction of flocculation in brewing yeasts by change in pH value. *FEMS Microbiol Lett*. 136:13–18. doi:10.1016/0378-1097(95)00456-4.

Stratford M, Assinder S. 1991. Yeast flocculation: Flo1 and NewFlo phenotypes and receptor structure. *Yeast*. doi:10.1002/yea.320070604.

Strauss CJ, Kock JLF, Van Wyk PWJ, Lodolo EJ, Pohl CH, Botes PJ. 2005. Bioactive oxylipins in *saccharomyces cerevisiae*. *J Inst Brew*. doi:10.1002/j.2050-0416.2005.tb00688.x.

Straver MH, Aar PCVD, Smit G, Kijne JW. 1993. Determinants of flocculence of brewer's yeast during fermentation in wort. *Yeast*. doi:10.1002/yea.320090509.

Su C, Li Y, Lu Y, Chen J. 2009. Mss11, a transcriptional activator, is required for hyphal development in *Candida albicans*. *Eukaryot Cell*. 8(11):1780–1791. doi:10.1128/EC.00190-09.

Taylor NW, Orton WL. 1975. CALCIUM IN FLOCCULENCE OF SACCHAROMYCES CEREVISIAE. *J Inst Brew*. 81(1):53–57. doi:10.1002/j.2050-0416.1975.tb03661.x.

Teunissen AWRH, Van Den Berg JA, Steensma HY. 1993. Physical localization of the flocculation gene FLO1 on chromosome I of *Saccharomyces cerevisiae*. *Yeast*. 9(1):1–10. doi:10.1002/yea.320090102.

Teunissen AWRH, Steensma HY. 1995. The dominant flocculation genes of *Saccharomyces cerevisiae* constitute a new subtelomeric gene family. *Yeast*. doi:10.1002/yea.320111102.

Urry DW, Peng SQ, Parker TM, Gowda DC, Harris RD. 1993. Relative Significance of Electrostatic- and Hydrophobic-Induced pKa Shifts in a Model Protein: The Aspartic Acid Residue. *Angew Chemie Int Ed English*. 32(10):1440–1442. doi:10.1002/anie.199314401.

Veelders M, Bruckner S, Ott D, Unverzagt C, Mosch H-U, Essen L-O. 2010. Structural basis of flocculin-mediated social behavior in yeast. *Proc Natl Acad Sci*. doi:10.1073/pnas.1013210108.

van de Ven TGM, Mason SG. 1977. The microrheology of colloidal dispersions VII. Orthokinetic doublet formation of spheres. *Colloid Polym Sci Kolloid Zeitschrift Zeitschrift für Polym*. doi:10.1007/BF01536463.

Verstrepen KJ, Derdelinckx G, Verachtert H, Delvaux FR. 2003. Yeast flocculation: What brewers should know. *Appl Microbiol Biotechnol*. doi:10.1007/s00253-002-1200-8.

- Verstrepen KJ, Jansen A, Lewitter F, Fink GR. 2005. Intragenic tandem repeats generate functional variability. *Nat Genet.* 37(9):986–90. doi:10.1038/ng1618. <http://www.ncbi.nlm.nih.gov/pubmed/16086015>.
- Verstrepen KJ, Klis FM. 2006. Flocculation, adhesion and biofilm formation in yeasts. *Mol Microbiol.* doi:10.1111/j.1365-2958.2006.05072.x.
- Verstrepen KJ, Reynolds TB, Fink GR. 2004. Origins of variation in the fungal cell surface. *Nat Rev Microbiol.* 2(7):533–540. doi:10.1038/nrmicro927.
- Vidgren V, Londesborough J. 2011. 125th anniversary review: Yeast flocculation and sedimentation in brewing. *J Inst Brew.* doi:10.1002/j.2050-0416.2011.tb00495.x.
- VOLKIN, V. D. 1989. Minimizing protein inactivation. *Protein Funct A Pract Approach.*:1–24.
- Walstra P. 2003. *Physical Chemistry of Foods.* Marcel Dekker Inc.
- Watari J, Takata Y, Ogawa M, Sahara H, Koshino S, Onnela M -L, Airaksinen U, Jaatinen R, Penttilä M, Keränen S. 1994. Molecular cloning and analysis of the yeast flocculation gene FLO1. *Yeast.* 10(2):211–225. doi:10.1002/yea.320100208.
- Webber AL, Lambrechts MG, Pretorius IS. 1997. MSS11, a novel yeast gene involved in the regulation of starch metabolism. *Curr Genet.* 32(4):260–266. doi:10.1007/s002940050275.
- Willaert R. 2018. Adhesins of Yeasts: Protein Structure and Interactions. *J Fungi.* doi:10.3390/jof4040119.
- Lo WS, Dranginis AM. 1998. The cell surface flocculin Flo11 is required for pseudohyphae formation and invasion by *Saccharomyces cerevisiae*. *Mol Biol Cell.* 9:161–171. <https://www.pubchase.com/article/9436998>.

Supplemental material

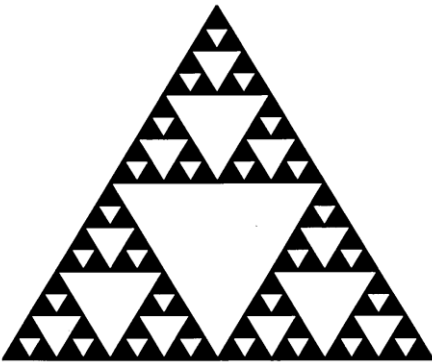


Figure S1 – Fractal triangle from clusters of clusters. The big triangle is formed from repetition of smaller triangles, following a well-defined pattern. As a result of the form size increase, the empty space within the particles increases, culminating in loss of density with particles size increase. In the same way, yeast flocs are observed to decrease in density, as larger the floc is, equally with a cluster/cluster fractal structure (Stratford 1992).

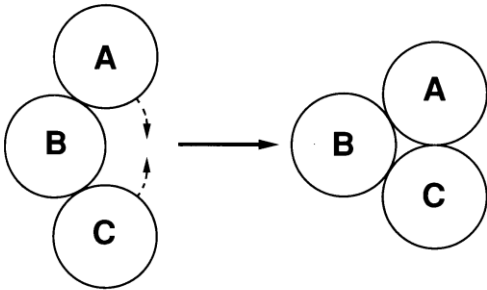


Figure S2 – Rolling movements of cells after initial contact, resulting in floc compaction and liquid exudation (syneresis). Strains forming too strong bonds between cells tend to resist to this process, remaining in open structures (Stratford 1992).

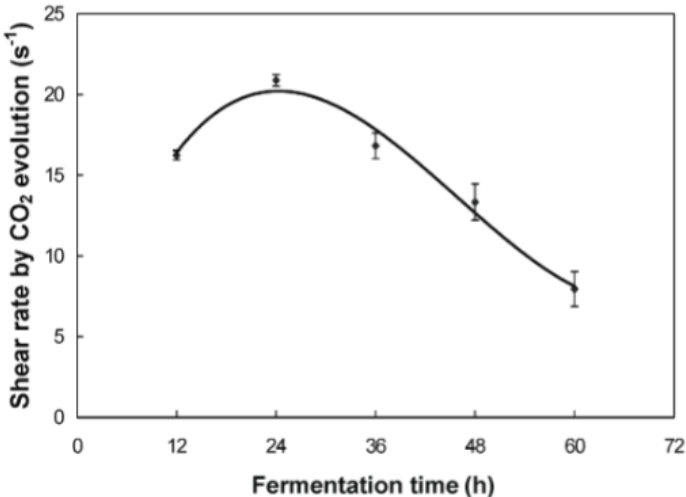


Figure S3 – Change of shear rates in fermentation media, calculated from CO₂ evolution (Speers et al. 2006).

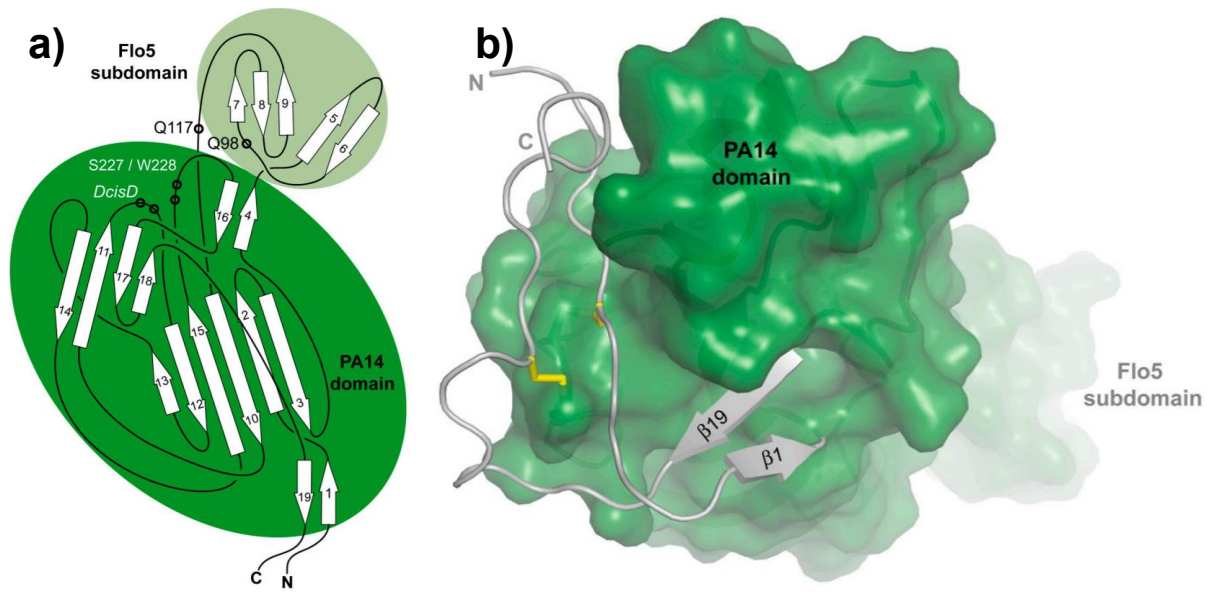


Figure S4 – Structural characteristics of Flo5A domain. In a) is depicted the topological diagram of Pa14 domain in dark green and the Flo5 subdomain in light green. In b) is depicted the L-shaped region formed by the N and C-termini regions of Flo5A in grey, and the disulphide bonds to β 12- β 13 loop of the PA14 core domain are highlighted in yellow.

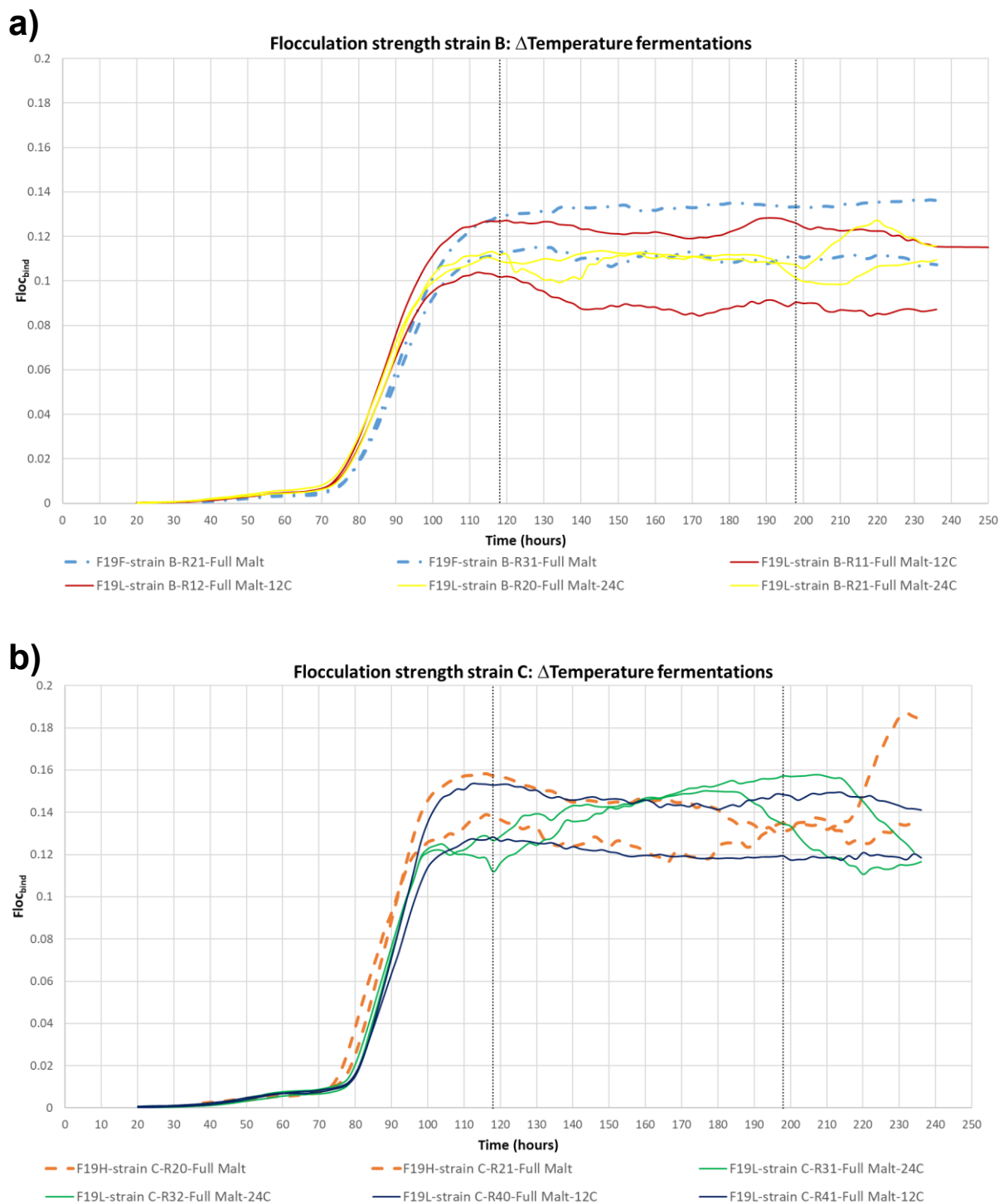


Figure S5 – Flocculation strength graphs of the temperature changed fermentations (F19L series). On the graphs are represented the tested B (a) and C (b) strains, in the fermentations with temperatures increased or decreased. For comparison, is also represented for both strains F19F (full malt wort, strain B) and F19H (full malt wort, strain C), fermentations carried in temperature unchanged fermentations. The vertical dotted lines delimitate the times in the fermentations at which the temperature was either increased or decreased (for F19L series).

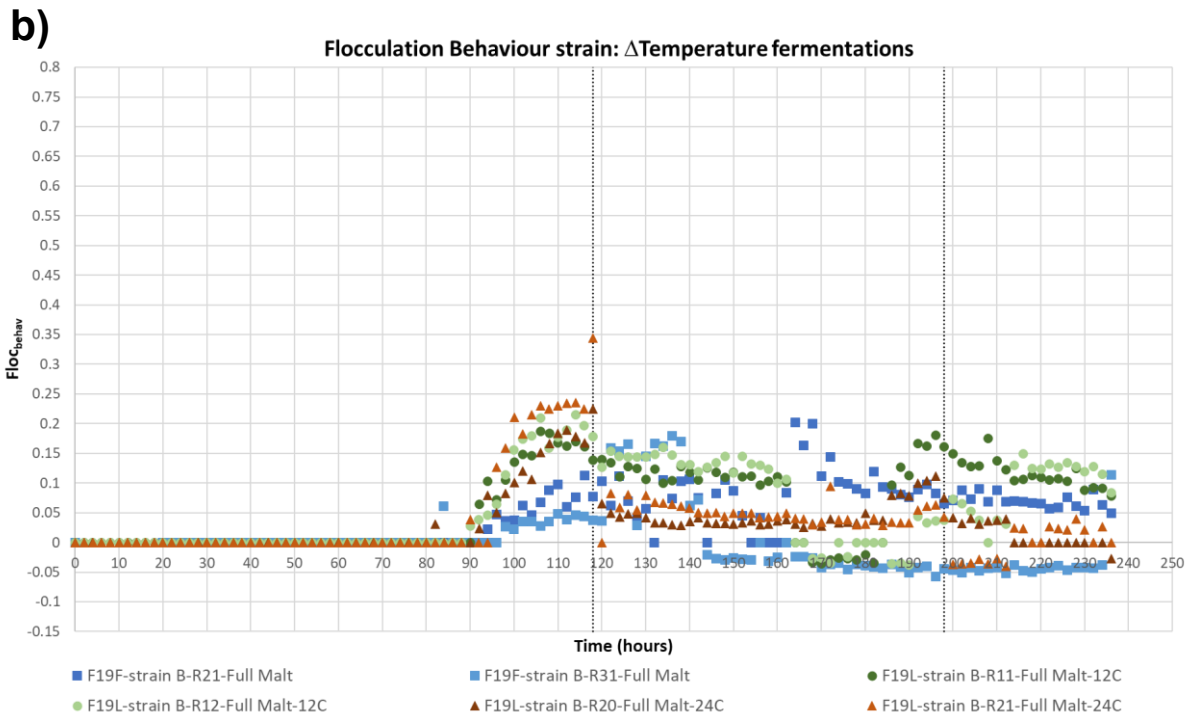
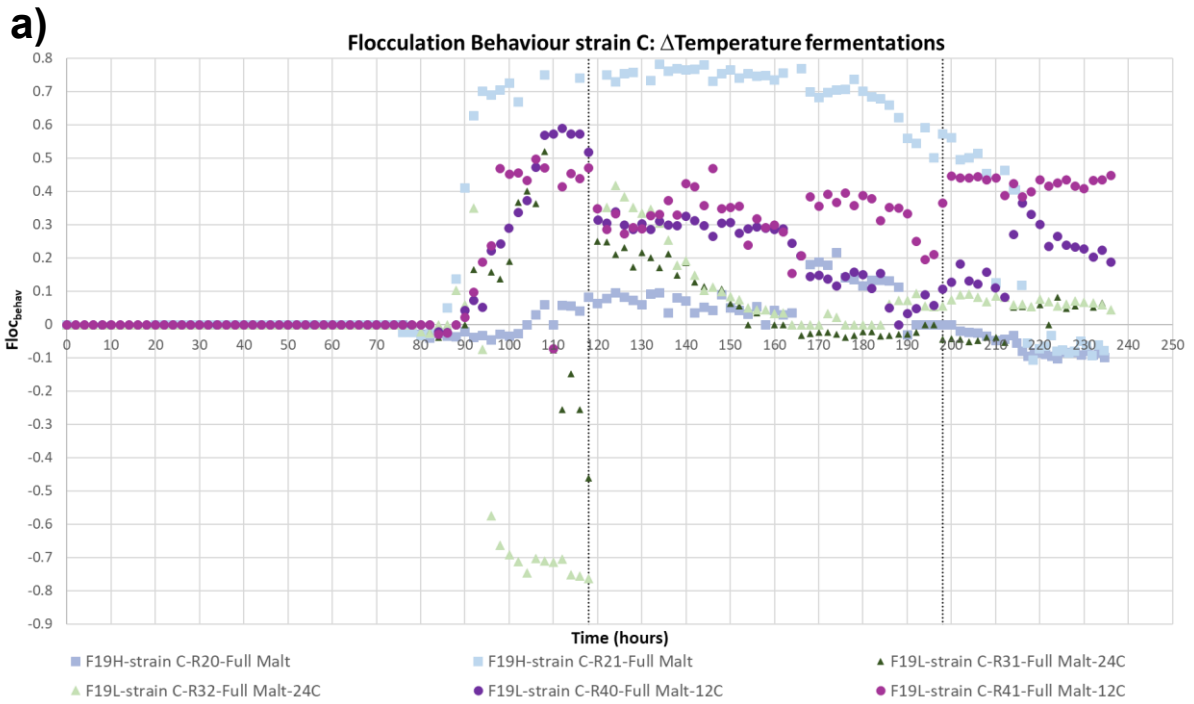
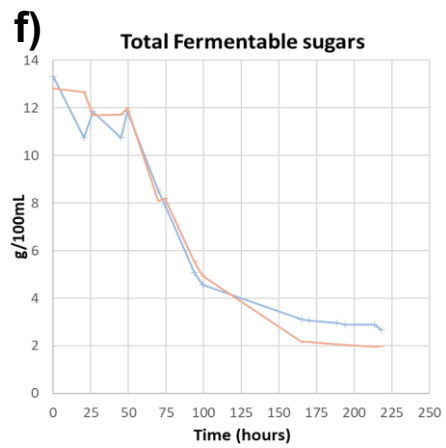
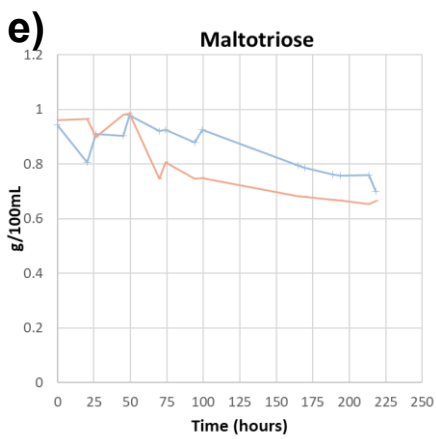
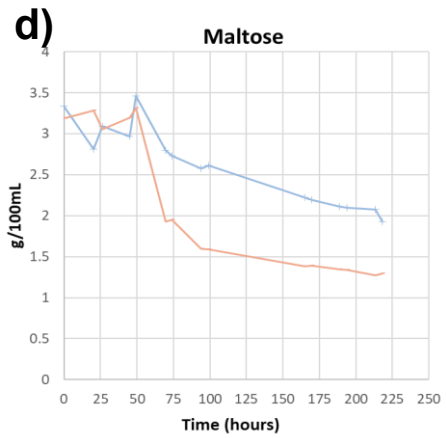
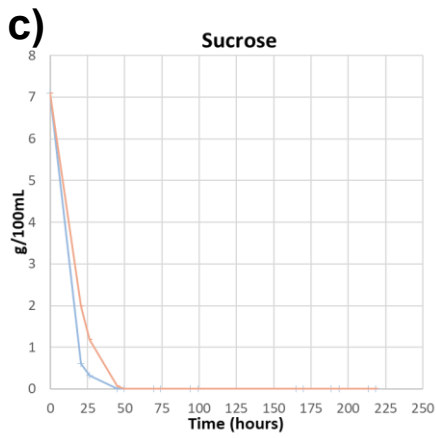
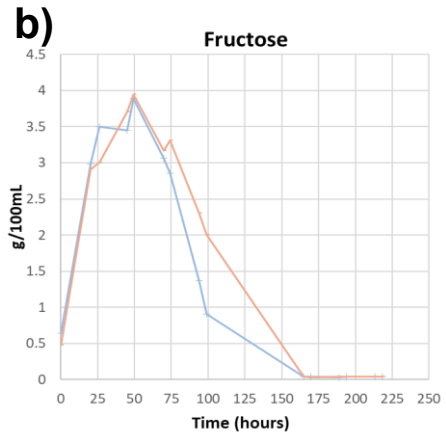
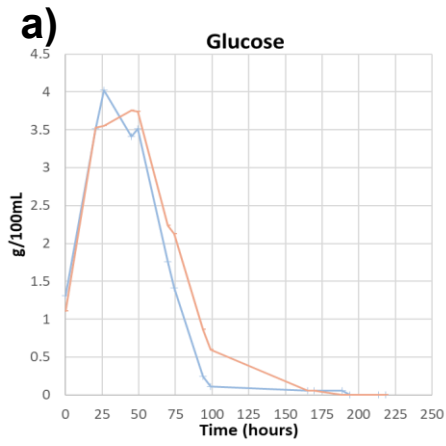


Figure S6 – Flocculation behaviour graphs for the temperature changed fermentations (F19L series). On the graphs are represented the tested C (a) and B (b) strains, in the fermentations with temperatures increased or decreased. For comparison, is also represented for both strains F19F (full malt wort, strain B) and F19H (full malt wort, strain C), fermentations carried in temperature unchanged fermentations. The vertical dotted lines delimitate the times in the fermentations at which the temperature was either increased or decreased (for F19L series).



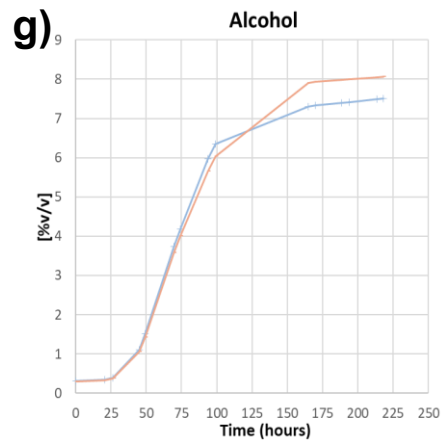


Figure S7 – Sugars consumption (glucose, fructose, sucrose, maltose, maltotriose and total fermentable sugars) and ethanol production graphs, representative of the fermentations in pH – corrected Adjunct wort (F19K1 series).
 Legend: — strain B AdjpH — strain C AdjpH



Figure S8 – Flocculation behaviour graphs, representative of the fermentations carried out in nitrogen supplemented Adjunct wort (F19K2 series). The tested strains B (a) and C (b) are represented, and each graph includes the graphs correspondent to normal Adjunct wort fermentations (B strain, F19G series and C strain, F19I series).

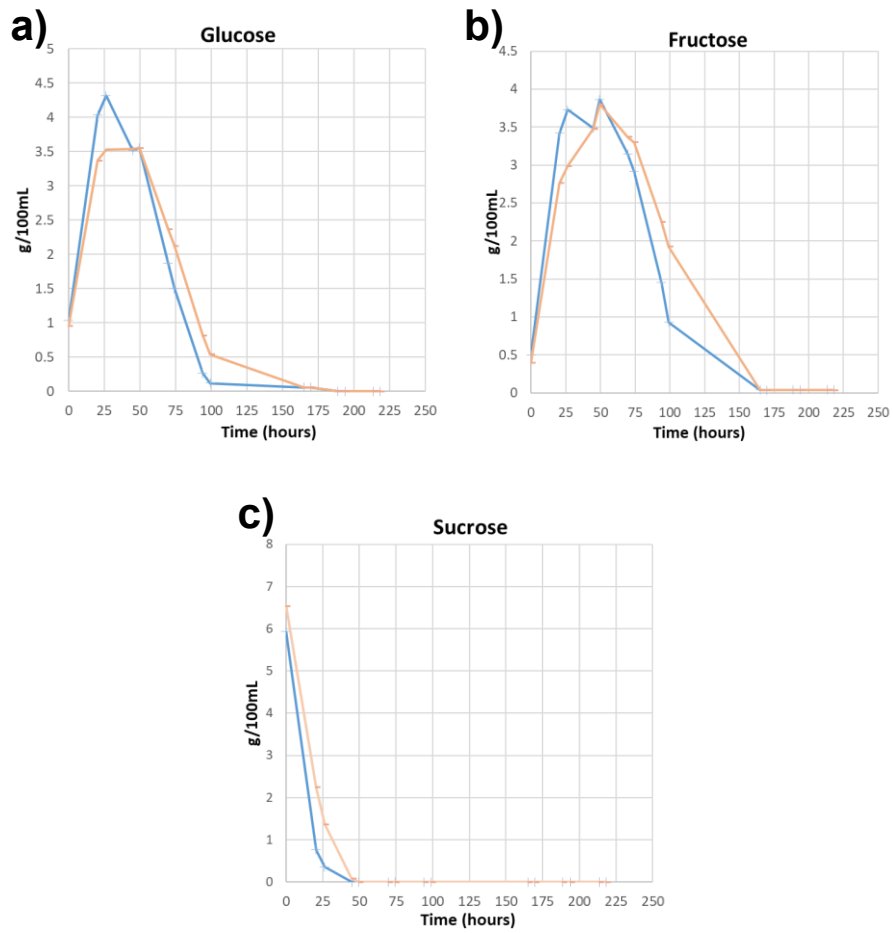


Figure S9 – Sugars consumption (glucose, fructose and sucrose) representative of the fermentations carried out in nitrogen supplemented Adjunct wort. Legend: —strain B AdjDHAP —strain C AdjDHAP

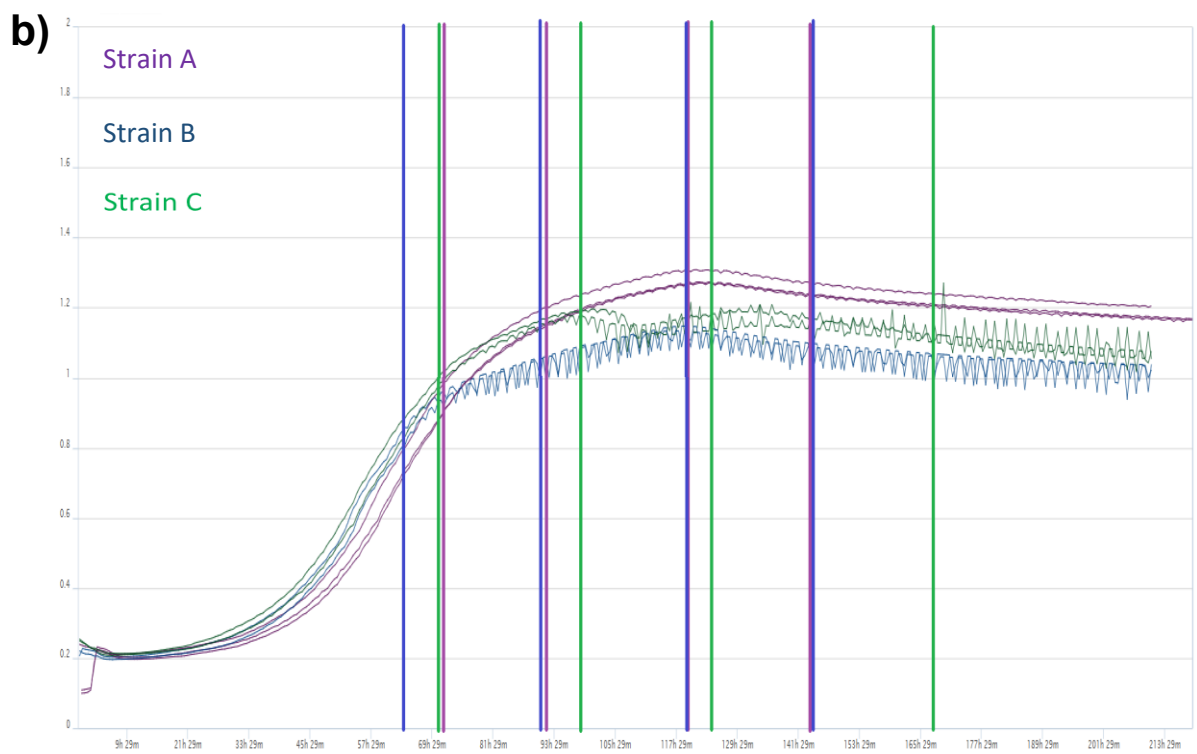
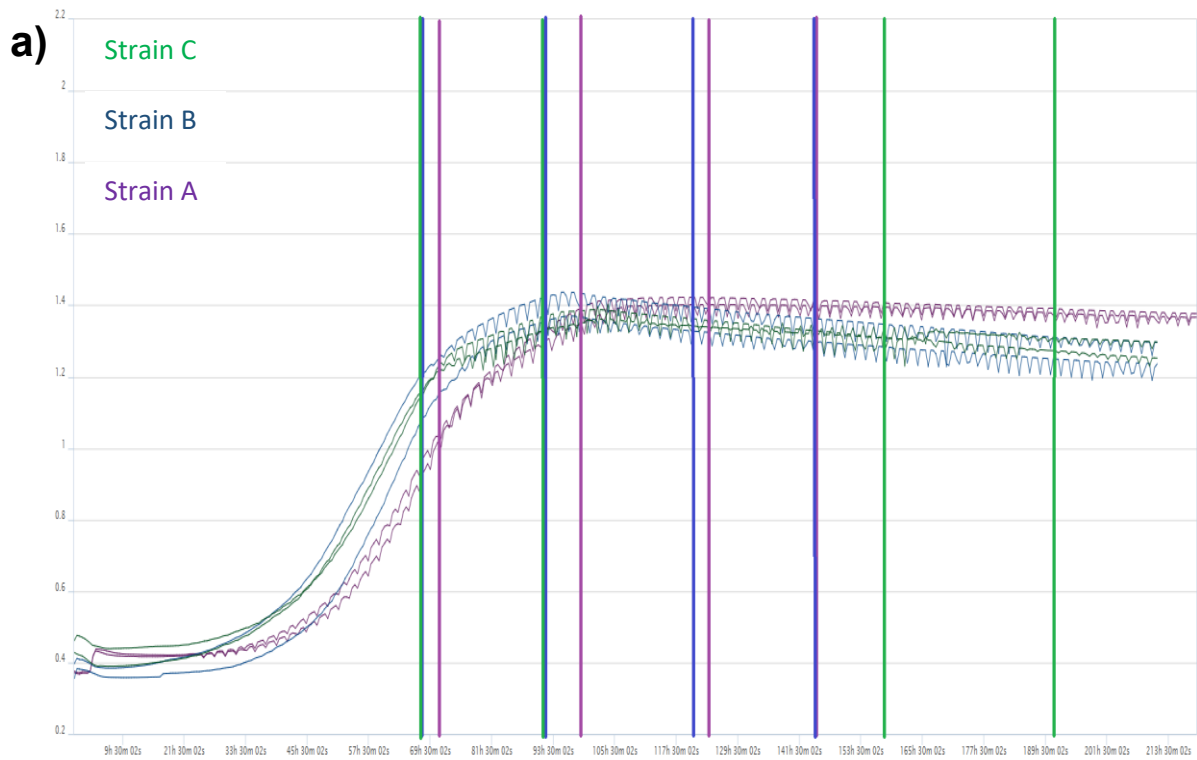


Figure S10 – OD graphs representative of the fermentations carried out in Full malt wort (a) and 50% Adjunct wort (b). The vertical lines represent the time in the fermentation at which samples for RNA-seq and CSH analysis were performed. Each line colour represents each strain sampling time, correspondent to the same OD curve colour. (legend on the graphs).

Protocol 1: Cell sampling for micro arrays analysis from chemostat cultures

Materials:

- Sterile 50mL falcons
- Liquid nitrogen
- Plastic beaker for sample collection in liquid nitrogen (1 L)
- Autoclave
- Screw cap microtubes of 1 mL (sterile and RNase free)
- Spatula or other instrument, that allows the crushing of the frozen sample
- Micro pipette tips (sterile and RNase free)
- Water bath

Used Chemicals:

- Sodium-acetate trihydrate (Sigma-Aldrich, USA)
- Acetic acid glacial (VWR Chemicals, Belgium)
- EDTA, Titriplex (MerckKGaA, Germany)
- Sodiumdodecylsulfate, SDS (VWR Chemicals, Belgium)
- Phenol-Chloroform-Isoamyl alcohol mixture, 125:24:1 (Sigma-Aldrich, USA)

Media, buffers and solutions:

- RNase free water: used UV-treated water, and autoclaved at 121C for 45 minutes;
- AE-buffer: Prepared 50mM Sodium-acetate trihydrate and 10mM-EDTA in UV-treated water, set pH at 5.0 with acetic acid glacial and autoclave for 45 minutes at 121C;
- SDS: 10% SDS (w/v) solution in RNase free water

Procedure:

- 1 - Sample a volume of culture corresponding to 240mg of cells in a plastic 1 L beaker half-full of liquid nitrogen (calculations for cell weight depicted in notes). Stir well sampling in order to assure instant freezing of cells;
- 2 - Crush the "iced yeast" in small bits using a clean big spatula. Pour the bits in 50mL falcons (2 to 3, depending on the cells quantity), and store them at -80C until former use;
- 3 - Thaw the samples by shaking tubes vigorously, putting them back on ice from time to time, to avoid warming - make sure that the temperature of the tubes remains close to 0C. During this time, set the centrifuge to 0C;

4 - When the culture is almost completely thawed (still small ice particles left), centrifuge 6 min at 0C (13500 rpm);

5 - Completely remove supernatant (keep cells on ice!) and re-suspend the pellet in 0.015mL/mg cells of ice cold AE-buffer in each tube.

6 - In fume hood, immediately add 0.015mL/mg cells of the acid phenol/chloroform/IAA mix and 0.015uL/mg cells of SDS 10% solution to each, and vortex each tube for, at least, 30 sec.

7 - Immediately place tubes in water bath for 5 min at 65C.

8 - After removal from water bath, place tubes in the fume hood and reduce pressure inside by opening the lids.

9 - Close the lids and vortex the tubes for 30 sec to homogenise. Rapidly distribute 800 µL aliquots in screw-cap RNase free tubes for each condition.

10 - Store the tubes at -80C or at least 15 min in the case the sample is processed immediately.

Protocol 2: Cell Surface Hydrophobicity Measurement Protocol

Materials:

Spectrophotometer (SPECTROstar Nano, BMG LABTECH)

Chemicals:

Sodium phosphate dibasic dihydrate (MerckKGaA, Germany)

Sodium phosphate monobasic monohydrate (MerckKGaA, Germany)

Deionized water (sterile)

Glycerol (Sigma-Aldrich, USA)

n-Hexadecane (Acros Organics, Germany)

Solutions:

Phosphate buffer (0.05M, pH 7): Do a solution of 0.0754 M of Sodium phosphate dibasic dihydrate and 0.0246 M of Sodium phosphate monobasic monohydrate with deionized water, and check the pH. If necessary, correct the pH either with NaOH or HCl. Autoclave it for 20 min, 121C.

Glycerol: Do a solution of 30% (v/v) of Glycerol, and autoclave for 20 min, 121C.

Procedure:

1 - Collect the sample, in order to have, at least, 1E9 cells/mL, and keep the cells in ice.

2 - Centrifuge the sample for 10 min, 13500 rpm, at 4C.

3 - Discard supernatant, and add 10 mL of sterile water to the pellet. Resuspend the pellet in the vortex, and centrifuge the solution at 13500rpm for 10 min (4C).

4 - Discard supernatant, and add 10 mL of 30% glycerol solution. Store cells at -20C.

5 - Thaw the samples by shaking, avoiding warming it too much. Keep cells on ice.

6 - Vortex to solubilize the pellet, and collect transfer 1 mL of the sample to 1.5 mL tube. Centrifuge at max speed, for 3 min.

7 - Discard supernatant, and add 1 mL of Phosphate buffer (0.05M, pH 7).

8 - Blank the spectrophotometer with phosphate buffer, at 550nm wavelength.

9 - Correct the sample to an OD of 0.85 (I value), in order to have a 15mL final solution of cells in phosphate buffer.

10 - Distribute 3 mL of the solution for 4 glass test tubes.

11 - In the fume hood, add 400uL of n-Hexadecane to the 3 mL solution (make a control without n-Hexadecane).

12 - Vortex the sample for 30 sec, let stand for 5 sec, and vortex again for 30 sec.

13 - Remove 1 mL of the resultant sample from under the meniscus.

14 - Measure OD at 550nm (F value).

The calculation for the CSH will be: $CSH (\%) = (1 - (F/I)) * 100$

The greater the value, the greater the hydrophobicity of the cells.

Table S1 – Initial concentrations of fermentable sugars, nitrogen composition and ions concentrations, for all the fermentation trials.

| Exp | Total Nitrogen (mg/L) | FAN (mg/L) | Glucose (g/L) | Fructose (g/L) | Sucrose (g/L) | Maltose (g/L) | Maltotriose (g/L) | Total Fermentable Sugars (g/L) | Ca ²⁺ (mg/L) | Zn ²⁺ (µg/L) |
|------|-----------------------|------------|---------------|----------------|---------------|---------------|-------------------|--------------------------------|-------------------------|-------------------------|
| F19F | 1454.6 | 325.41 | 17.4 | 3.1 | 4.1 | 73.7 | 22.1 | 120.5 | 45 | 730 |
| F19G | 796.1 | 177.54 | 8.5 | 1.6 | 87.3 | 35.3 | 10.1 | 142.8 | 33 | 680 |
| F19H | 1450.7 | 307.07 | 16 | 2.7 | 4 | 73.2 | 21.6 | 117.3 | 43 | 700 |
| F19I | 753.5 | 168.96 | 9.3 | 2.3 | 96.2 | 38.9 | 11.2 | 157.8 | 33 | 670 |
| F19K | 786 | 161 | 8.7 | 1.8 | 86.9 | 35.5 | 10.4 | 143 | - | - |
| F19L | - | - | 1.5 | 3.5 | 3.5 | 68 | 20 | 115 | - | - |